THE LINEAR CHANNEL AND ITS EFFECT ON THE GEOMORPHOLOGIC IUH

by
Diana M. Kirshen
and
Rafael L. Bras

RALPH M. PARSONS LABORATORY
Hydrology and Water Resource Systems

Report . No . 277

Prepared with the Support of
The Agency for International Development
The United States Department of State

June 1982

MIT

DEPARTMENT
OF
CIVIL
ENGINEERING

SCHOOL OF ENGINEERING
MASSACHUSETTS INSTITUTE OF TECHNOLOGY
Cambridge, Massachusetts 02139

R82-29 OSP 89965

THE LINEAR CHANNEL AND ITS EFFECT ON THE GEOMORPHOLOGIC IUH

by

DIANA M. KIRSHEN

and

RAFAEL L. BRAS

RALPH M. PARSONS LABORATORY
Hydrology and Water Resource Systems

Department of Civil Engineering
MASSACHUSETTS INSTITUTE OF TECHNOLOGY

Report No. 277

Prepared with the Support of

The Agency for International Development

The United States Department of State

June 1982

ABSTRACT

The Instantaneous Unit Hydrograph (IUH) is derived as a function of the basin's geomorphological and physiographic characteristics. Inherent in the basin IUH is the response of the individual channels composing the basin. The response of the individual channels is derived by solving the continuity and momentum equations for the boundary conditions defined by the IUH. Both the effects of upstream and lateral inflow to the channels is taken into account in the derivation of the basin's IUH. The time to peak and peak response are used as a basis for comparison between the results produced by this model and those produced by a model where the channel's response is assumed to be an exponential distribution. The comparisons indicate that if the approach taken in this paper is indeed accurate, for example, the assumptions used do not invalidate the model, then the type of channel response used for the basin's IUH is significant, and future efforts must be directed towards parameter estimation.

ACKNOWLEDGEMENTS

This work was sponsored by the U. S. Department of State, Agency of International Development, through the M. I. T. Technology Adaptation Program. The ideas and opinions are those of the authors and do not necessarily reflect those of the sponsors.

The authors would like to acknowledge the complete staff of the Technology Adaptation Program, which includes personnel at both M. I. T. and Cairo University. Their administrative support over the entire period of this study has been most helpful.

Elaine Healy deserves many special thanks for typing this work.

Work was performed at the Ralph M. Parsons Laboratory, Department of Civil Engineering, M. I. T.

PREFACE

This report is one of a series of publications which describe various studies undertaken under the sponsorship of the Technology Adaptation Program at the Massachusetts Institute of Technology.

The United States Department of State, through the Agency for International Development, awarded the Massachusetts Institute of Technology a contract to provide support at M. I. T. for the development, in conjunction with institutions in selected developing countries, of capabilities useful in the adaptation of technologies and problem-solving techniques to the needs of those countries. This particular study describes research conducted in conjunction with Cairo University, Cairo, Egypt.

In the process of making this TAP supported study some insight has been gained into how appropriate technologies can be identified and adapted to the needs of developing countries per se, and it is expected that the recommendations developed will serve as a guide to other developing countries for the solution of similar problems which may be encountered there.

Fred Moavenzadeh

Program Director

TABLE OF CONTENTS

LIST OF FIGURES

LIST OF TABLES

Chapter 1

INTRODUCTION

1.1 Motivation of Study

Many regions throughout the world lack the hydrologic data required for a detailed analysis of a basin's response to rainfall. Typical examples of this situation are the many wadis, or ephemeral streams, in Egypt. These basins respond to sporadic rainfall events, frequently causing considerable damage to villages and other developments in their surroundings. Effective planning and protection of these, and similar, sites require estimates of expected discharges from rainfall events of different magnitudes. Traditional estimation techniques are not feasible due to the lack of available hydrologic data. Limited watershed data is available from aerial photographs or survey maps.

Both climatic and physiographic factors influence runoff from a drainage basin. The climatic factors include the effects of various forms and types of precipitation, interception, evaporation and transpiration, all of which exhibit seasonal variations in accordance with the climatic environment. The physiographic factors include the basin's and channels' characteristics. Geometric factors such as size, shape, slope, orientation, elevation and stream density; and physical factors such as land use and cover, soil type and topographic conditions, characterize the basin. The channels are characterized by the channels' slope, roughness, length, and the size and shape of the channels' cross section.

Common practice in applied hydrology is the use of linear systems theory to determine the discharge from a river basin. The response of a continuous linear system to an arbitrary input, I(t), is the result of the familiar convolution equation,

$$Q(t) = \int_0^t I(\tau)h(t-\tau)d\tau$$

In hydrology, Q(t) is the discharge at time t and I(t) is the effective precipitation rate as a function of time. The function h(t) is the characteristic response of the river basin and is commonly called the Instantaneous Unit Hydrograph (IUH). If the IUH is known, it is then possible to obtain the discharge hydrograph corresponding to any arbitrary rainfall input. The functions I(t) and h(t) can be regarded, respectively, as the integral expressions of the climatic and physiographic factors that govern the discharge from the river basin.

Linear system theory, as represented by the convolution equation, has also been used to study the behavior of particular channels within a basin. In that case the input becomes upstream inflows and/or lateral flows from adjacent overland segments.

Various conceptual models have been proposed to delineate the IUH of channels and basins. One of the simplest conceptual channel IUHs

results from the assumption that a channel or basin behaves like a linear reservoir. A linear reservoir is defined by its storage discharge relationship which is given by

$$S(t) = KQ(t)$$

where S(t) is the storage in the reservoir at time t, K is a proportionality constant and Q(t) is the discharge from the reservoir. In essence, the storage in a linear reservoir is proportional to the discharge at all times. By solving the continuity equation for an instantaneous input of unit volume (Dirac Delta function) the resulting IUH is given by

$$h_c(t) = \frac{1}{K} e^{-t/K}$$

A popular conceptual model of a basin results by suggesting a configuration of n linear reservoirs operating in series. The output from each upstream reservoir being the input to the one immediately downstream. Such a model is shown in Figure 1.1. The functional form of the model is obtained by carrying out the convolution operation n times; the result of the first convolution being the input for the second convolution and so on. The results for an instantaneous input at the first channel is the Nash model which is given by

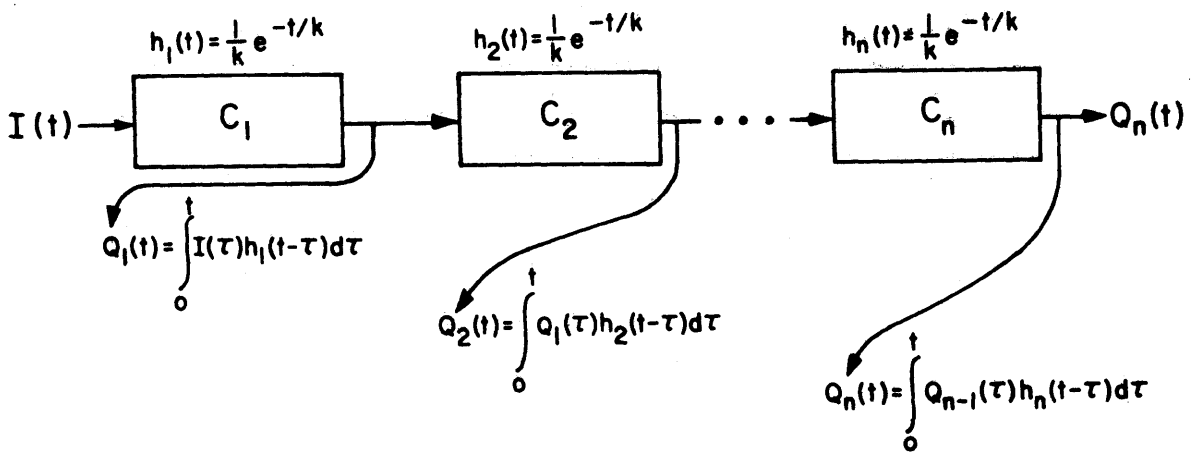

Figure 1.1: Schematic representation of a basin modeled as a series of n linear reservoirs.

$$h_B(t) = \frac{1}{K} \left(\frac{t}{K}\right)^{n-1} \frac{1}{\Gamma(n)} e^{-t/K}$$

where $\Gamma(\cdot)$ = Gamma function

K = time constant of the linear reservoirs

n = number of linear reservoirs added in series

In contrast to the previously stated conceptual model, recent studies by Rodriguez et al. (1979) and Gupta and Waymire (1980) demonstrate that the basin's hydrologic response can be determined from the basin's geomorphologic structure. The technique utilizes easily accessible geomorphologic and geometric basin parameters to obtain an analytical expression of basin response. These parameters relate to the several physiographic factors which affect discharge such as basin area and stream density. The model assumes that the individual channels behave as a linear reservoir, and using concepts from probability theory and geomorphology an expression is derived for the basin's response.

This work will study the importance of the linear reservoir assumption for channel response in the geomorphologic IUH theory. In doing so, use will be made of a general linear solution to the equations of motion in wide prismatic channels as suggested by Harley (1967). These results yield the theoretical linear response function (IUH) of a channel as a function of several physiographic factors (slope and Froude number, F) and the parameters required for linearization. The determination of the basin's response will be based on the recent work by Rodriquez et al., and Gupta and Waymire.

1.2 Scope of Study

A major focus of the forthcoming analysis is the relationship between runoff and the geomorphology of the basin, and thus Chapter 2 describes recent developments in hydrogeomorphology. The concept of the geomorphologic IUH is presented along with an analytical derivation of the basin IUH used to determine the discharge hydrograph. An example of the geomorphlogic basin IUH is presented using the assumption that the channels respond as linear reservoirs.

Chapter 3 presents a linearized solution to the continuity and momentum equations for the boundary conditions imposed by the definition of an IUH. The solution defines the upstream inflow IUH for the individual channels and is used to determine the lateral inflow IUH which accounts for an input occurring anywhere along the channel. A sensitivity analysis is performed on the input parameters and reference parameters used for linearization.

Chapter 4 presents the basin IUH obtained using the theory of the geomorphologic IUH presented in Chapter 2, where the channel response functions are as derived in Chapter 3. Both the upstream inflow and lateral inflow channel IUHs are used to enhance the hydrogeomorphology. A sensitivity analysis is performed on the input parameters.

Chapter 5 presents the discharge hydrograph determined in accordance with the IUH theory where the basin IUH is as derived in Chapter 4. Several hypothetical streams are used as input. Hydrographs for different basins are presented and compared to the time to peak and peak discharge determined by a rainfall-runoff model. The hydrographs are also compared to hydrographs determined using the assumption that the individual channels

respond as linear reservoirs, i.e., the channel IUH is given by the exponential distribution.

Finally Chapter 6 presents conclusions and recommendations for further research on the subject of determining runoff from ungaged river basins.

Chapter 2

THE GEOMORPHOLOGIC IUH

The ultimate aim of this study is to derive an analytic expression of the basin response in terms of the basin's geomorphological characteristics and channel properties which affect runoff. This chapter will outline the recent developments by Rodriguez et al. (1979) and Gupta and Waymire (1980) in hydrogeomorphology to estimate basin response. The technique presented utilizes easily accessible geomorphologic and geometric basin characteristics to obtain an analytical expression of basin response. Several concepts are utilized throughout, such as the quantitative analysis of a drainage network in terms of Horton's empirical laws and the idea of the IUH as the probability density function (pdf) for the travel time of a drop of water landing anywhere in the basin. Inherent in the expression is the response of the individual channel, the channel's IUH. This will be the subject of the subsequent chapter.

2.1 Quantitative Analysis of a Drainage Network

The quantitative analysis of channel networks began with Horton's (1945) method of classifying streams by order. Strahler (1957) revised Horton's classification scheme such that the ordering scheme is, unlike Horton's, purely topological, for it refers to only the interconnections and not to the lengths, shapes or orientation of the links comprising a network. A hypothetical channel network with Strahler's ordering scheme is presented in Figure 2.1. The ordering procedure is based on the following rules:

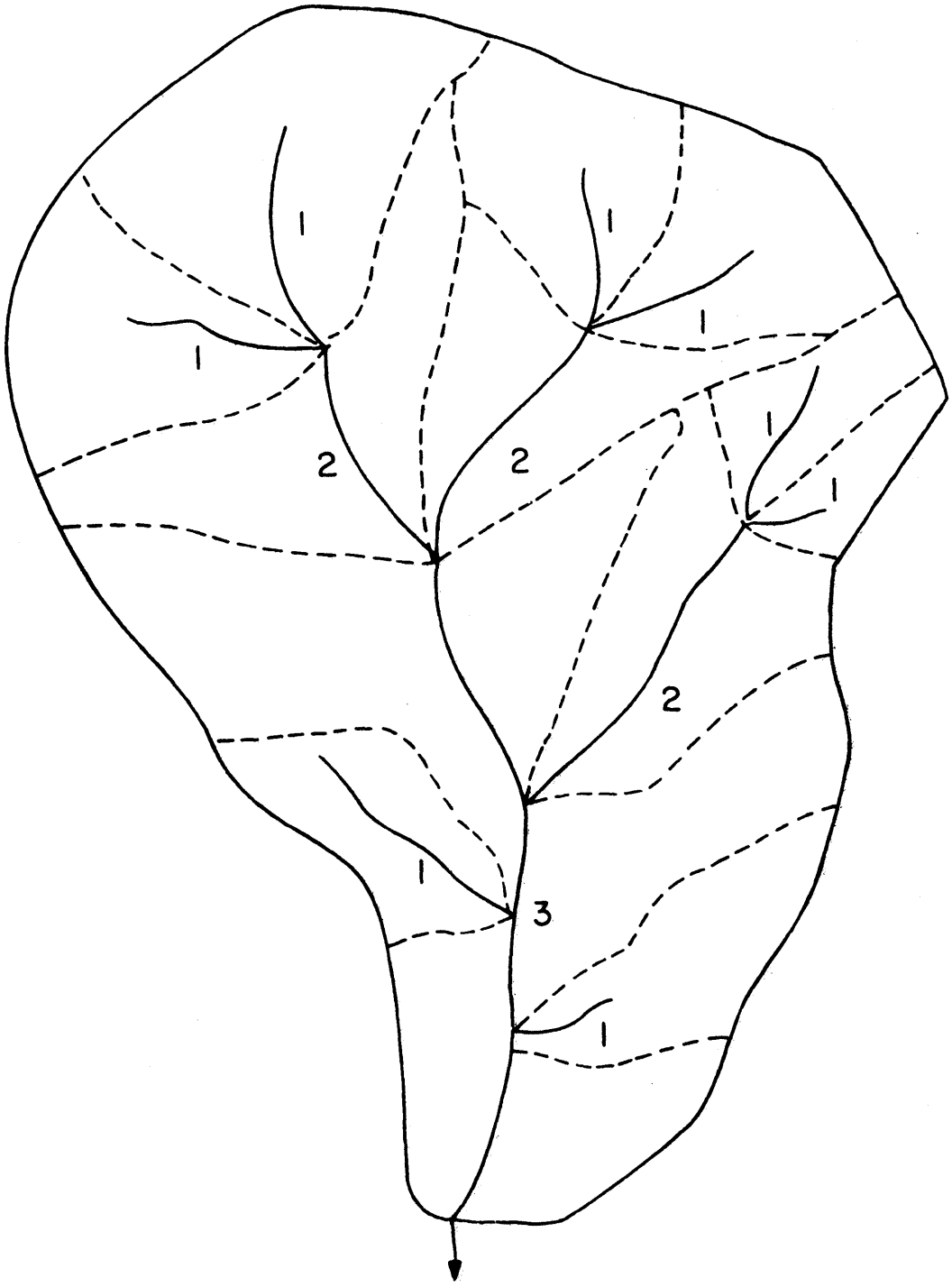

Figure 2.1: Third order basin with Strahler's ordering system (from Rodriguez et al., 1979).

i) channels that originate at a source are defined to be first order streams;

ii) when two streams of order w join, a stream of order w+1 is created;

iii) when two streams of different order join, the channel segment immediately downstream has the higher of the orders of the two continuing streams;

iv) the order of the basin is the highest stream order, W.

The first step in drainage network analysis is the counting of the streams of each order, N_w, w=1,2,...,W. This is followed by the determination of each stream length, L_{w_i}, and stream area, A_{w_i}, i = 1, ... N_w, w=1, ..., W, where A_{w_i} is the area of runoff contributing to the ith stream of order w and its tributaries of lower order. (Note: A_{w_i} is the area that drains directly into the ith stream of order w plus the area contributing from the stream's tributaries). Figures 2.1 and 2.2 present the necessary information for the analysis of a drainage network.

Given the ordering scheme, Horton demonstrated several empirical laws; the law of stream numbers, and the law of stream lengths; Schumm (1956) proposed a Horton-type law for drainage areas, the law of stream areas. The law of stream numbers states that the total number of streams of different orders in a given drainage basin closely approximates an inverse geometric series in which the first term is unity and the ratio of the series is the bifurcation ratio, R_B. The quantitative expression of the law is given by:

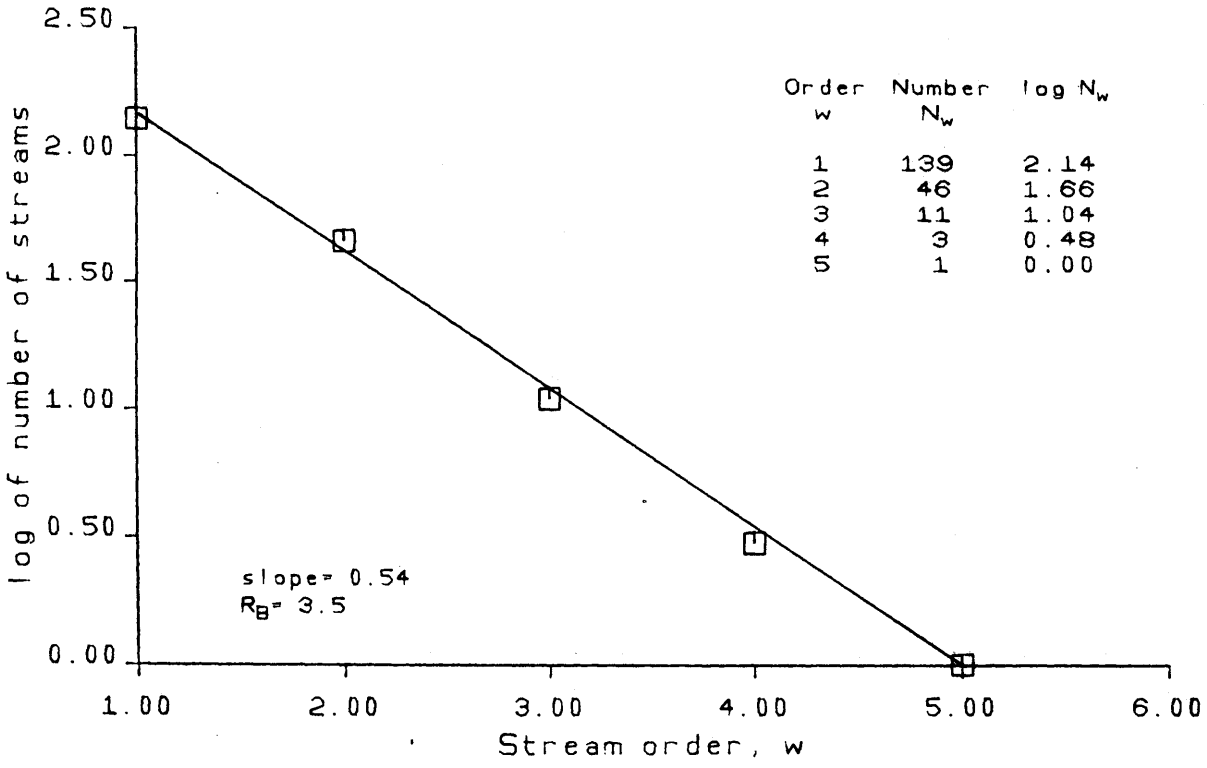

Figure 2.2: Verification of Horton's law of stream numbers.

$$\sum_{W=1}^{W} N_W = R_B^{W-(W)} + R_B^{W-(W-1)} + \ldots R_B^{W-(1)} \qquad (2.1)$$

For a given river basin, the law is easily verified by constructing a plot of the log of number of streams, N_w, versus stream order, w. The plot should be a straight line with very little scatter as shown in Figure 2.2. The anti-logarithm of the slope of the line is R_B. Another interpretation of R_B is obtained from Equation 2.1. From the equation we obtain

$$N_w = R_B^{W-w} \qquad w=1,2,\ldots,W \qquad (2.2)$$

and therefore

$$N_{W-1} = R_B \qquad (2.3)$$

which shows that R_B is the number of streams of order W-1. By substituting the result of Equation 2.3 in Equation 2.2 and rearranging the expression, the following is also obtained:

$$R_B = \frac{N_{w-1}}{N_w}$$

We can therefore interpret Horton's law as ascertaining that the ratio $\frac{N_{w-1}}{N_w}$ for w= 1,...,W approaches a common value given by R_B. The concept

of the laws of stream lengths and stream areas is the same as the law of stream numbers, the ratios of the series being the length ratio, R_L, and the area ratio, R_A, respectively. R_L and R_A are calculated using the following quantities: the average stream length of each order, $\bar{L}_w$, is given by:

$$\bar{L}_w = \frac{1}{N_w} \sum_{i=1}^{N_w} L_{w_i}$$

where L_{w_i} is the length of a stream of order w, and the average stream area of each order, $\bar{A}_w$, is given by

$$\bar{A}_w = \frac{1}{N_w} \sum_{i=1}^{N_w} A_{w_i}$$

where A_{w_i} is the area contributing runoff to a stream of order w and its tributaries. For example, $\bar{A}_W$ is the total area of the basin. The quantitative expressions of Horton's laws are summarized below:

Law of stream numbers: $$\frac{N_{w-1}}{N_w} = R_B$$

Law of stream lengths: $$\frac{\bar{L}_w}{\bar{L}_{w-1}} = R_L$$

Law of stream areas: $$\frac{\bar{A}_w}{\bar{A}_{w-1}} = R_A$$

Empirical results indicate that for natural basins the values for R_B normally range from 3 to 5, for R_L from 1.5 to 3.5, and for R_A from 3 to 6 (Smart 1972). In this study the geomorphologic characteristics, R_B, R_L, and R_A will be the descriptive parameters of the basin on which its response will be based.

2.2 Probabilistic Interpretation of the IUH

By definition the IUH is the response to a unit volume of water instantaneously but uniformly applied to a basin. Its volume (the area under the curve) is equal to 1. The abscissa has units of time and the ordinate units of inverse time. All of the properties are similar to those commonly attributed to a probability density function (pdf). In fact, Gupta and Waymire (1980) clearly prove that the IUH of the basin is the probability density function of the amount of time that an individual drop of water, starting at a random point in the basin, takes to travel to the outlet of the basin. A similar interpretation is valid for the response function of a single channel. The channel IUH gives the probabilistic distribution of the travel time of a drop randomly entering at a point along the channel.

The next section will present how the desired pdf, or basin IUH, can be obtained from the geomorphologic laws of the basin. The development follows Gupta and Waymire's (1980) work as well as Rodriguez et al. (1979). The travel times in a channel are assumed to be exponentially distributed. The subsequent chapter will suggest a different form for the channel IUH.

2.3 Derivation of the Geomorphologic IUH

In order to determine the basin IUH, let's consider the input as a unit volume composed of an infinite number of drops. The following analysis will focus on the travel of one drop, chosen at random, through

the basin. The drop travels throughout the basin making transitions from streams of lower order to those of higher order. A transition can be referred to as a change of state where the state is the order of the channel where the drop is traveling. Rodriguez et al. (1979) agreed that the travel of the drop through the river basin can be modelled as a semi-Markov process. The process is semi-Markov because the time between transitions is dependent on the state presently occupied.

The states of the process are defined to be the overland region or stream of order i where the drop is located at time t. The set of states will be denoted by A = (1,2,...,W+1). The travel of a drop is governed by the following rules.

Rule 1: When the drop is still in the overland phase, the state is the order of the stream to which the land drains directly.

Rule 2: The only possible transitions out of state w are those of the form $w \rightarrow j$ for some $j > w$, $j = w+1, \ldots, W+1$.

Rule 3: Defining the outlet as a trapping state, W+1, the final state of the drop is W+1, from which transitions are impossible.

The above set of rules defines a finite set of possible paths that a drop falling randomly on the basin may follow to reach the outlet. For example, suppose that the basin of interest is of order 3 (see Figure 2.1), then the path space, $S = (s_1, s_2, s_3, s_4)$ is given by

path S_1: $\theta_1 \rightarrow 1 \rightarrow 2 \rightarrow 3 \rightarrow 4$

path S_2: $\theta_1 \rightarrow 1 \rightarrow 3 \rightarrow 4$

path S_3: $\theta_2 \rightarrow 2 \rightarrow 3 \rightarrow 4$

path S_4: $\theta_3 \rightarrow 3 \rightarrow 4$

where i=1,2,3 are as previously defined, 4 represents the basin outlet and θ_i represents the overland phase. Figure 2.3 is a convenient schematic representation of all the alternative paths, the numbered circles representing the elements of a given order.

Following Gupta et al. (1980), the cumulative density function of the time a drop takes to travel to the basin outlet is given by

$$P(T_B \leq t) = \sum_{s \epsilon S} P(T_s \leq t) p(s) \qquad (2.4)$$

where $P(\cdot)$ stands for the probability of the set given in parenthesis; T_B is the time of travel to the basin outlet; T_s is the travel time in a particular path s; p(s) is the probability of a drop taking path s; S is the set of all possible paths that a drop can take upon falling in the basin.

The travel time, T_s, in a particular path, $a_0 \rightarrow a_1 \rightarrow \ldots \rightarrow a_k$, $a_i \epsilon (1,\ldots,W+1)$, must be equal to the sum of travel times in the elements of that path;

$$T_s = T_{a_0} + T_{a_1} + \ldots + T_{a_k} \qquad (2.5)$$

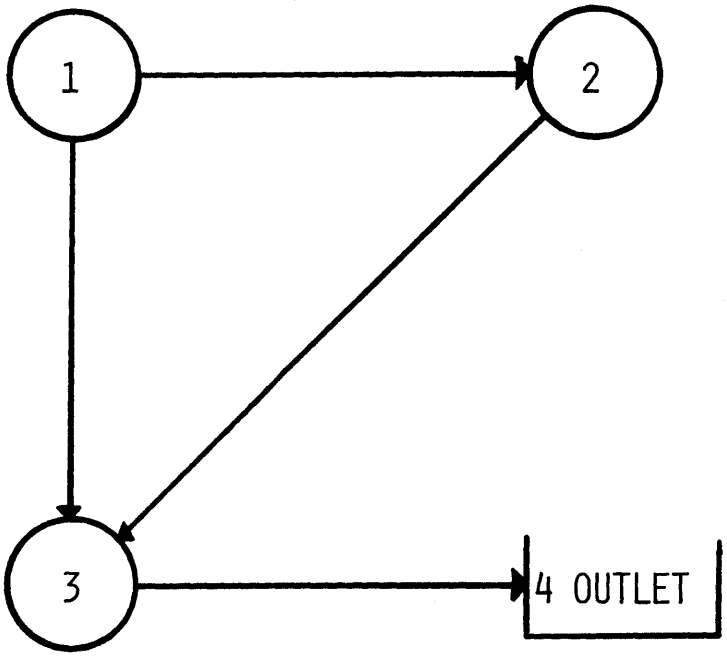

Figure 2.3: Schematic representation of the possible paths for a drop falling in a third order basin.

where T_{a_i} is the travel time in an overland region or stream of order $a_i, a_i \epsilon (1,\ldots,W+1)$ and k is the number of transitions that the drop undergoes. Given the many streams of given orders and their various properties, T_{a_i} must be a random variable with a given probability density function $f_{a_i}(t)$. Furthermore, there is no reason to suspect that the T_{a_i} are anything but independently distributed random variables. The probability density function of T_s must then be the convolution of probability density functions, $f_{a_i}(t)$, corresponding to the elements of path s. The cumulative density of T_s is similarly the convolution of individual cumulative density functions, $F_{a_i}(t)$. Therefore,

$$P(T_s \leq t) = F_{a_0}(t) * F_{a_1}(t) * \ldots * F_{a_k}(t) \tag{2.6}$$

where $a_0 \rightarrow a_1 \rightarrow \ldots \rightarrow a_k$ is path s and * stands for the convolution operation. For example for path s_2, $\theta_1 \rightarrow 1 \rightarrow 3 \rightarrow 4$, $P(T_{s_2} \leq t)$ is given by:

$$P(T_{s_2} \leq t) = \int_0^t \int_0^{t''} F_1'(t') F_1(t''-t') dt' F_3(t-t'') dt''$$

$$= F_1'(t) * F_1(t) * F_3(t) \tag{2.7}$$

where $F_1'(t)$ represents the probability function corresponding to the time the drop spends in the overland region draining into streams of

order 1. Equation 2.7 says that the probability that a drop travels path s_2 in a time less than time t is given by the probability that the drop travels from the overland region to the first order channel in a time less than t'; times the probability that the drop travels through the 1st order streams in time t" - t', where t' can range from 0 to t"; times the probability that the drop travels through the 3rd order stream in the remaining time given by t - t", where t" can range from 0 to t.

The average time that the drop spends as overland waiting time can be inferred from $F_1'(t)$; however, this time will be considered to be negligible when compared to the overall time that the drop spends in the basin. Rodriguez et al. (1979), justify the relative insignifiance of the overland waiting time by the following explanation:

> The importance of the overland waiting time appears to be rather smaller than that of the stream waiting time under the framework of analysis taken in this paper. When one considers drops traveling through a stream of order w, most of them will come from the two streams of order w-1, which make up for the stream in question, or from tributary streams which drain along the route of our stream of order w. The only drops affected by overland waiting time will be those draining directly by overland flow into the stream of order w. These drops are in number considerably fewer, in general, than the above ones, and thus we feel that in average terms the mean waiting time in state w will be the streamflow waiting time. Only for streams of order 1 would one expect that most of the drops, except for channel precipitation, are affected by overland waiting time; because of the smaller size of the order 1 areas, this time is nevertheless considered to be of minor importance in the overall IUH.

The above assumptions simplify equations 2.5 and 2.6 to:

$$T_s = T_{a_1} + \ldots + T_{a_k} \tag{2.8}$$

$$P(T_s \leq t) = F_{a_1}(t) * F_{a_2}(t) * \ldots F_{a_k}(t) \tag{2.9}$$

The probability of following a given path s, p(s), is a direct consequence of the Markovian nature of Strahler's ordering scheme and is given by:

$$p(s) = \theta_{a_0}(0)\, p_{a_0 a_1}\, p_{a_1 a_2} \cdots p_{a_{k-1} a_k} \tag{2.10}$$

where $\theta_{a_0}(0)$ is the probability that the drop starts its travel in an overland segment draining into a stream of order a_0; $p_{a_i a_j}$ is the transition probability from streams of order a_i to streams of order a_j. Remember path s is $a_0 \rightarrow a_1 \rightarrow a_2 \rightarrow \cdots \rightarrow a_k$, where $a_i \varepsilon (1,\ldots,W+1)$ and a_k will be equal to the state which represents the outlet, W+1. The reader should also note that due to rule 1, a drop initially falling in an area which drains to a stream of order i, goes to a stream of order i, thus $a_0 = a_1 = i$ and $p_{a_0 a_1} = 1$. Also the transition probabilities $p_{W-1,W}$ and $p_{W,W+1}$ are equal to 1.

Rodriguez et al. (1979) show that the initial probabilities, $\theta_{a_0}(0)$ and the transition probabilities, $p_{a_i a_j}$ are functions only of the geomorphology and geometry of the river basin. Only general expressions for $\theta_{a_0}(0)$ and $p_{a_i a_j}$ will be presented in this paper, and the reader should refer to Rodriguez et al. (1979) for a more detailed discussion. The physical interpretation of the probabilities is as follows:

$$\theta_w(0) = \frac{\text{total area draining directly into streams of order w}}{\text{total basin area}} \tag{2.11}$$

$$p_{ij} = \frac{\text{number of streams of order i draining into steams of order j}}{\text{total number of streams of order i}} \tag{2.12}$$

The transition probabilities can be derived as a function of R_A and R_B using the following general expression given by Gupta and Waymire (1980):

$$P_{ij} = \frac{(N_i - 2N_{i+1})\ E(j,\ W)}{\sum_{k=j}^{W} E[k,W]\ N_i} + \frac{2N_{i+1}}{N_i}\ \delta_{i+1j} \qquad 1 \leq i < j \leq W \tag{2.13}$$

where $\delta_{i+1j} = 1$ if $j = i+1$ and 0 otherwise. E[i,W] denotes the mean number of interior links of order i in a finite network of order W, an interior link being the segment of the channel network between two successive junctions or between the outlet and the first junction upstream. The expression is given by

$$E[i,W] = N_i \prod_{j=2}^{i} \frac{(N_{j-1} - 1)}{2N_j - 1} \qquad i = 2,\ \ldots,\ W \tag{2.14}$$

Similarly, the probability that a drop falls in an area of order w is derived using the following general expansion

$$\theta_1(0) = \frac{N_1 \bar{A}_1}{\bar{A}_W} \tag{2.15}$$

$$\theta_w(0) = \frac{N_w}{\bar{A}_W}\left[\ \bar{A}_W - \sum_{j=1}^{w-1} \bar{A}_j (N_j\ p_{jw}/N_w)\right] \qquad w = 2,\ \ldots,\ W$$

Table 2.1 presents a complete list of the initial and transition probabilities for a 3rd order basin. As can be observed, all the probabilities are functions of only R_A and R_B. Appendix A presents a summary of the theoretical development of these probabilities.

The probability function for a drop's travel time in a basin, $P(T_B \leq t)$, is now fully defined in terms of the geomorphologic basin properties and the probability functions $F_{a_i}(t)$, corresponding to the travel time of a drop in a given channel, T_{a_i}. As previously stated, the IUH is defined to be the pdf of T_B, and therefore

$$h_B(t) = \frac{dP\ (T_B \leq t)}{dt}$$

$$= \sum_{s\ S} f_{a_1}(t) \ldots {}^{*}f_{a_k}(t)\ p(s) \qquad (2.16)$$

where $f_{a_i}(t)$ is the pdf of the travel time, T_{a_i}.

In summary, the IUH is a function of the probability that a drop initially falls in an area which drains to a channel of order w, the transition probabilities to channels of higher order, w+j (j=1, ..., W-w), and the pdf of the time spent in a channel of a given order. The initial and transition probabilities are functions of the basin's geomorphologic characteristics, R_A and R_B. These transition probabilities provide a probabilistic description of the drainage network and a link between quantitative geomorphology and hydrology.

The next section presents an example of the geomorphologic IUH. The input parameters and mathematical computations will also be presented so that the reader can gain a better understanding of the geomorphologic IUH.

Table 2.1 Initial and transition probabilities for a 3rd order basin.

$$\theta_1(0) = R_B^2 \, R_A^{-2}$$

$$\theta_2(0) = \frac{R_B}{R_A} - \frac{R_B^3 + 2R_B^3 - 2R_B}{R_A^2(2R_B - 1)}$$

$$\theta_3(0) = 1 - \frac{R_B}{R_A} - \frac{R_B(R_B^2 - 3R_B + 2)}{R_A^2(2R_B - 1)}$$

$$P_{12} = \frac{R_B^2 + 2R_B - 2}{2R_B^2 - R_B}$$

$$P_{13} = \frac{R_B^2 - 3R_B + 2}{2R_B^2 - R_B}$$

2.4 Example of the Geomorphologic IUH

As the example, consider a basin of third order, and assume, as is commonly done in hydrology, that each channel responds as a linear reservoir. The response for a stream of order w is therefore given by

$$f_w(t) = y_w e^{-y_w t} \tag{2.17}$$

The parameter y_w is the mean travel time of a drop in a stream of order w, and can be considered to be equal to the mean travel velocity of any drop in the basin, divided by the average stream length. Thus

$$y_w = \frac{V}{\bar{L}_w}$$

where V = average flow velocity

$\bar{L}_w$ = average length of streams of order w.

The response of each stream of order w is now defined. The basin response is determined using Equation 2.16:

$$h_B(t) = \sum_{s \in S} f_{a_1}(t) * f_{a_2}(t) \ \ldots \ f_{a_k}(t) p(s)$$

The derivation of a closed form solution for the basin response is greatly simplified by the use of Laplace transform techniques. The Laplace transform of the convolution operation is the product of the Laplace transform of each function within the integral, so that if the product of the Laplace's can be inverted, a closed-form solution can easily be obtained. For the example, the Laplace of the channel response is given by

$$L[f_w(t)] = \frac{y_w}{s + y_w} \tag{2.18}$$

Recalling that there exists four possible travel paths for a drop falling on a third order basin, the $h_B(t)$ is derived as follows:

$$\begin{aligned} h_B(t) &= p(s_1)f_1(t)*f_2(t)*f_3(t) + p(s_2)f_1(t)*f_3(t) + \\ &\quad p(s_3)f_2(t)*f_3(t) + p(s_4)f_3(t) \\ &= p(s_1)L^{-1}\left[\frac{y_1}{s+y_1}\,\frac{y_2}{s+y_2}\,\frac{y_3}{s+y_3}\right] + p(s_2)L^{-1}\left[\frac{y_1}{s+y_1}\,\frac{y_3}{s+y_3}\right] + \\ &\quad p(s_3)L^{-1}\left[\frac{y_2}{s+y_2}\,\frac{y_3}{s+y_3}\right] + p(s_4)L^{-1}\left[\frac{y_3}{s+y_3}\right] \end{aligned} \tag{2.19}$$

Evaluating the inverses and substituting the probabilities for each path yields:

$$\begin{aligned} h_B(t) &= \\ &\theta_1(0)p_{12}y_1y_2y_3\left[\frac{(y_2-y_3)e^{-y_1t} + (y_3-y_1)e^{-y_2t} + (y_1-y_2)e^{-y_3t}}{(y_2-y_1)(y_2-y_3)(y_3-y_1)}\right] + \\ &\theta_1(0)p_{13}y_1y_3\left[\frac{e^{-y_1t} - e^{-y_3t}}{y_3 - y_1}\right] + \theta_2(0)y_2y_3\left[\frac{e^{-y_2t} - e^{-y_3t}}{y_3 - y_2}\right] + \\ &\theta_3(0)y_3e^{-y_3t} \end{aligned} \tag{2.20}$$

where p_{12}, p_{13}, $\theta_1(0)$, $\theta_2(0)$ and $\theta_3(0)$ are defined in Table 2.1.

For the example assume that the geomorphologic parameters of the basin are as follows:

$$R_B = 4.0,\ R_A = 5.6,\ R_L = 2.8$$
$$\bar{L}_1 = 1.56,\ \bar{L}_2 = 4.38,\ \bar{L}_3 = 12.25 \text{ Km}$$
$$\bar{A}_1 = 3.3,\ \bar{A}_2 = 18.4,\ \bar{A}_3 = 103.0 \text{ Km}^2$$

The mean flow velocity will be assumed to be 2 m/sec which gives the following result for each y_w:

$$y_1 = 4.62/\text{hr} \qquad y_2 = 1.64/\text{hr} \qquad y_3 = 0.59/\text{hr}.$$

A plot of the response of each channel is presented in Figure 2.4. As can be observed, the area under each response is one. Figure 2.5 shows the basin IUH as given by Equation 2.20. Notice that the IUH does not start at zero. A discussion of this will be deferred until later but the reader should note that it differs from the results of Rodriguez et al. (1979) which argued that it should start at zero and devised a scheme to force the result to do so.

The previous results depend on the exponential assumption for the channel IUH and on the "dynamic" parameter which takes the form of a velocity required to compute mean travel time. Notice that following Rodriguez et al. (1979) it was assumed that this velocity is the same for streams of all orders. Next chapter will suggest a different form for the channel IUH and a somewhat different parameterization.

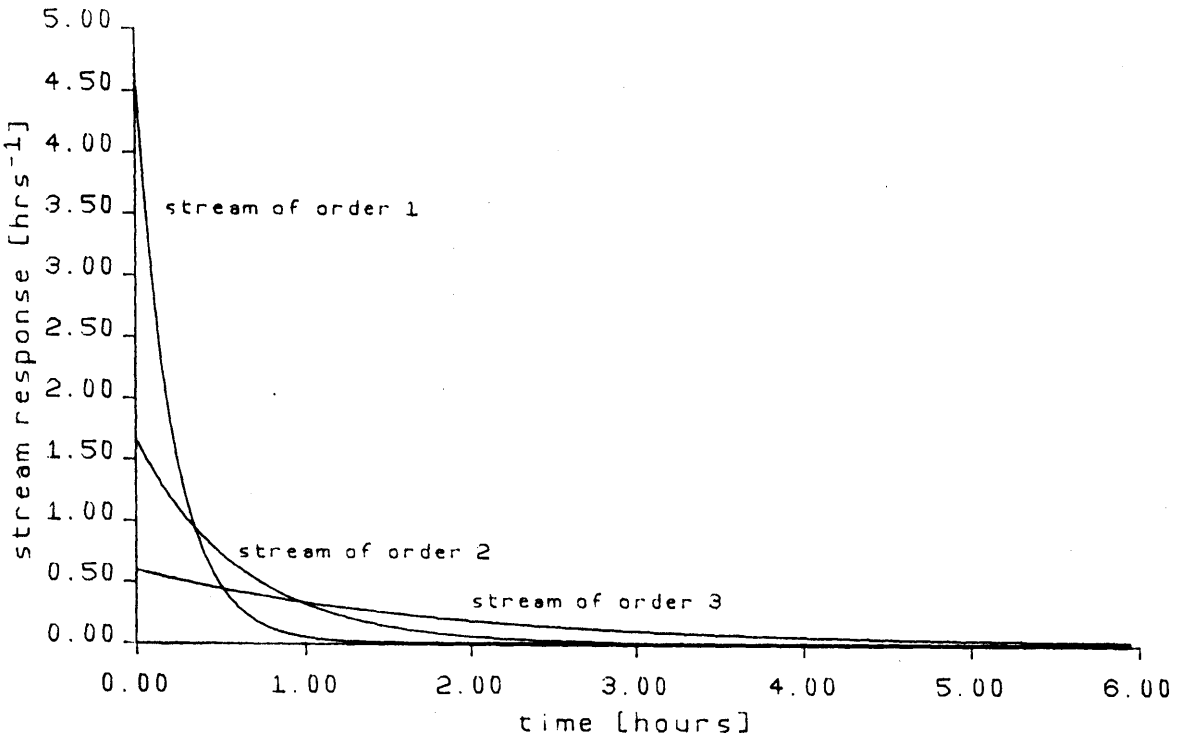

Figure 2.4: Response of each order stream for a third order basin.

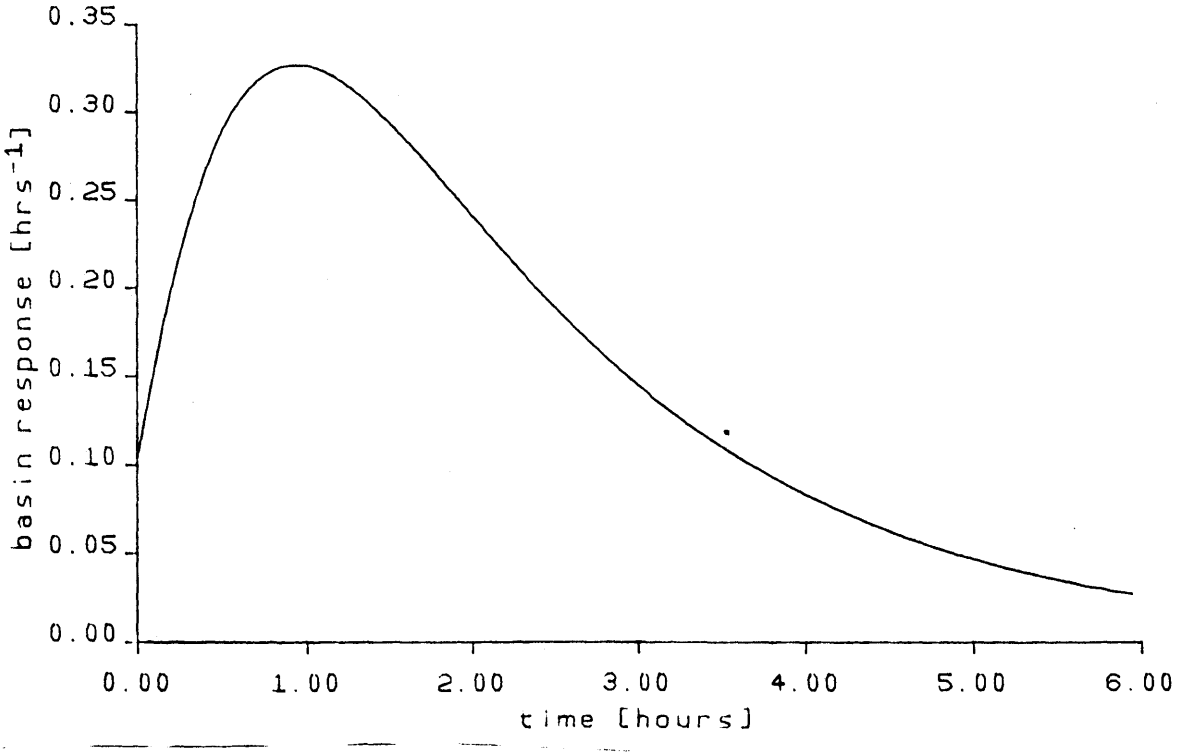

Figure 2.5: Basin IUH for a third order basin.

Chapter 3

THE RESPONSE OF A CHANNEL

3.1 Introduction

Flood routing procedures provide a means of estimating the shape and timing of a flood wave as it progresses along a channel. The procedures are classified according to the following criteria: the physical principles and equations used as the theoretical basis for flood routing, methods used for solving the basic differential equations, specific assumptions and approximations used in treating the flood wave movement, the type of problem to be solved. In this chapter the one-dimensional equations of motion for unsteady flow of an incompressible fluid, in a wide and uniform rectangular channel, will be solved for the conditions imposed by the definition of an IUH. The mathematical treatment of problems concerning unsteady flow is difficult due to the many variables that enter into the functional relationships, and closed form solutions cannot generally be derived for the relevant nonlinear partial differential equations.

We are interested in a flood routing procedure to determine the response of a channel, or equivalently the pdf corresponding to the time of travel of a drop, chosen at random, in a stream of order w. The solution procedure we will use is based on the linearization of the continuity and momentum equations as proposed by Harley (1967). The channel's response to an input at the channel's most upstream point will be derived, and from this closed form solution, the channel's response to a uniform input along the channel's length will be obtained.

3.2 Linear Solution to the Equations of Motion

The one-dimensional equations of motion for unsteady flow in an open channel without lateral inflow are given by:

Continuity:
$$\frac{\partial q}{\partial x} + \frac{\partial y}{\partial t} = 0 \tag{3.1}$$

Momentum:
$$\frac{\partial y}{\partial x} + \frac{v}{g}\frac{\partial v}{\partial x} + \frac{1}{g}\frac{\partial v}{\partial t} = S_o - S_f \tag{3.2}$$

where g = gravitational acceleration

v = mean velocity

y = water depth

$q = vy$ = discharge per unit width

S_o = slope of the channel bottom

S_f = friction slope

x = space coordinate, measured along the channel axis

t = time coordinate

The frictional effects will be described by the Chezy equation, thus:

$$S_f = \frac{v^2}{C^2 R}$$

where R = hydraulic radius

C = Chezy coefficient

which for a wide rectangular channel yields:

$$S_f = \frac{v^2}{C^2 y}$$

The momentum equation can be rearranged to be a function of only two dependent variables, y and q, by substituting the relation for v: $v = q/y$. Substituting the expression for S_f and rearranging yields:

$$(gy^3 - q^2)\frac{\partial y}{\partial x} + 2yq\frac{\partial q}{\partial x} + y^2\frac{\partial q}{\partial t} = gy^3\left(S_o - \frac{q}{C^2 y^3}\right) \qquad (3.3)$$

Combining the continuity and momentum equations, which are two first order partial differential equations in q and y, to give a single second order equation in the same two dependent variables q and y, requires differentiating Equation 3.1 with respect to x, and Equation 3.2 with respect to t. Assuming the Chezy coefficient to be a constant, the result is:

$$(gy^3 - q^2)\frac{\partial^2 q}{\partial x^2} - 2yq\frac{\partial^2 q}{\partial x \partial t} - y^2\frac{\partial^2 q}{\partial t^2} = 3g\left(S_o - \frac{\partial y}{\partial x}\right) y^2\frac{\partial q}{\partial x}$$

$$+ \frac{\partial g}{C^2} q\frac{\partial q}{\partial t} - 2\left(\frac{\partial q}{\partial x}\frac{\partial y}{\partial t} - \frac{\partial q}{\partial t}\frac{\partial y}{\partial x}\right)q \qquad (3.4)$$

The above equation is highly non-linear. In order to linearize Equation 3.4, the following equalities and assumptions are established:

$$q = q_o + \delta q \qquad q_o >> \delta q$$

$$y = y_o + \delta y \qquad y_o >> \delta y \tag{3.5}$$

where q_o and y_o are the steady state reference parameters and δq and δy are perturbations about these values. In other words, the steady state uniform flow is perturbed by an input whose response is given by small deviations or perturbations from the steady state reference values. Substituting Equation 3.5 into 3.4 and elminating less significant terms, yields the following linearized equation in terms of δq:

$$(gy_o^3 - q_o^2)\frac{\partial^2 \delta q}{\partial x^2} - 2q_o y_o \frac{\partial^2 \delta q}{\partial t \partial x} - y_o^2 \frac{\partial^2 \delta q}{\partial t^2} = 3gS_o y_o^2 \frac{\partial \delta q}{\partial x} + \frac{2g}{C^2} q_o \frac{\partial \delta q}{\partial t} \tag{3.6}$$

The value chosen for the Chezy coefficient is that at steady state, thus assuming that $S_f \tilde{} S_o$ at steady state yields:

$$C^2 = \frac{v_o^2}{y_o S_o}$$

Substituting the above expression into Equation 3.6 and expressing the result in terms of y_o and v_o yields:

$$(gy_o - v_o^2)\frac{\partial^2 \delta q}{\partial x^2} - 2v_o \frac{\partial^2 \delta q}{\partial x \partial t} - \frac{\partial^2 \delta q}{\partial t^2} = 3gS_o \frac{\partial \delta q}{\partial x} + \frac{2gS_o}{v_o}\frac{\partial \delta q}{\partial t} \qquad (3.7)$$

The above linear equation can now be solved for various initial and boundary conditions. The analytic solution of Equation 3.7 is the response of the channel to an input causing a small disturbance of the initial and boundary conditions.

In this study we are interested in the response of a channel to a drop landing anywhere along the channel's length. We will first consider the response of a channel to an input at the channel's most upstream point, and then generalize the results such that the point at which the input occurs is random.

3.3 Channel's Response to an Upstream Input

The previous section presented a partial linear differential equation (3.7) dependent on the perturbation δq. This section will use this equation to determine the response of a channel to an input at its most upstream point. The implied upstream boundary condition is

$$\delta q(0,t) = \delta(t)$$

where $\delta(t)$ is the dirac delta function which represents a pulsed upstream inflow.

One initial condition is given by

$$\delta q(x,0) = 0$$

which means that there exists no perturbation about the reference discharge prior to the application of the input. The other initial condition is:

$$\left.\frac{\partial \delta q(x,t)}{\partial t}\right|_{t=0} = 0$$

Harley (1967) solved Equation 3.7 with the above conditions and obtained:

$$\delta q(x,t) = \delta(t - x/c_1)\exp(-px) + \exp(-rt+zx)(x/c_1-x/c_2)h \frac{I_1[2h\sqrt{(t-x/c_1)(t-x/c_2)}]}{\sqrt{(t-x/c_1)(t-x/c_2)}} u(t-x/c_1)dt \tag{3.8}$$

where $\delta q(x,t)$ is the response of a channel to an instantaneous input at the channel's most upstream point, with parameters

$$c_1 = v_o + \sqrt{gy_o}$$

$$c_2 = v_o - \sqrt{gy_o}$$

$$p = \frac{S_o}{2y_o} \frac{2 - F}{F(1+F)}$$

$$r = \frac{S_o v_o}{2y_o} \frac{2 + F^2}{F^2}$$

$$z = \frac{S_o}{2y_o}$$

$$h = \frac{S_o v_o}{2y_o} \frac{\sqrt{(4-F^2)(1-F^2)}}{2F^2}$$

$$F = \frac{v_o}{\sqrt{gy_o}}$$

$I_1[\cdot]$ = modified bessel function of order 1

$u(\cdot)$ is the unit step function

A detailed description of the solution procedure is presented in Appendix B. Also presented is the calculation of the area underneath

the curve, $\delta q(x,t)$. The area is proved to be 1, which is a property of any pdf.

Equation 3.8 is the response of a channel to an instantaneous upstream input and can be interpreted as the pdf corresponding to the travel time of a drop landing at the channel's most upstream point, and travelling a distance downstream given by x. Recalling the derivation of the geomorphologic IUH, the pdf of the travel time of a drop falling anywhere in the channel and travelling to the outlet is required. This pdf will be referred to as $r_{a_i}(t)$, where a_i is the order of the channel where the drop is travelling. The next section presents the derivation of $r_{a_i}(t)$ as a function of the upstream input, $\delta q(x,t)$.

3.4 The Lateral Inflow Case: the pdf of Travel Time of a Drop Entering the Channel Anywhere Along its Length

The definition of the geomorphologic IUH as the pdf of a drop's travel time in a basin or order w requires the pdf of a drop's travel time in each stream of order a_i,($a_i = 1,\ldots,W$). We are interested in the travel time of a drop landing anywhere in the channel and travelling to the channel's most downstream point.

The landing spot, X_{a_i}, of the drop must belong to the interval $Z = (x: \ 0 \leq x \leq \overline{L}_{a_i})$ where $\overline{L}_{a_i}$ is the mean channel length of order a_i; therefore the pdf, $f_{X_{a_i}}(x)$, must be 0 outside of Z. Furthermore since

the drop is equally likely to fall in any equal subinterval in Z, regardless of the location of these subintervals in Z, it follows that $f_{X_{a_i}}(x)$ must be constant throughout Z. Since the pdf, $f_{X_{a_i}}(x)$ must integrate to 1 over the interval Z, $f_{X_{a_i}}(x)$ is given by:

$$f_{X_{a_i}}(x) = \begin{cases} \dfrac{1}{\bar{L}_{a_i}} & 0 \leq x \leq \bar{L}_{a_i} \\ 0 & \text{otherwise} \end{cases} \tag{3.9}$$

The distribution of the random variable X_{a_i} is called the uniform distribution on the interval $(0,\bar{L}_{a_i})$.

The previous section presented the pdf, $\delta q(x,t)$, which corresponds to a drop's travel time over a distance x. Since the drop that we are interested in will fall anywhere on the channel, it will travel a distance anywhere between $\bar{L}_{a_i}$ to 0 to reach the channel's most downstream point. Therefore the determination of the pdf of the drops travel time, $r_{a_i}(t)$, requires that each point of landing be considered. Since there are an infinite number of landing points, in order to obtain the pdf, $r_{a_i}(t)$, of the drops travel time in a channel of order a_i, we must integrate the upstream inflow IUH, $\delta q(x,t)$, over all possible travel distances x. This operation yields:

$$r_{a_i}(t) = \frac{1}{\bar{L}_{a_i}} \int_0^{\bar{L}_{a_i}} \delta q_{a_i}(x,t)\, dx \qquad (3.9)$$

where $\delta q_{a_i}(x,t)$ is the upstream inflow IUH defined by Equation 3.8 with parameters corresponding to those of a stream of order a_i. The pdf, $r_{a_i}(t)$, corresponds to a drop landing anywhere along the channel's length and will be referred to as the lateral input IUH. The response of a drop entering at the channel's most upstream point will be referred to as the upstream input IUH and is defined as:

$$u_{a_i}(t) = \delta q_{a_i}(\bar{L}_{a_i}, t)$$

Substituting in the expression for $\delta q_{a_i}(x,t)$ into Equation 3.9, the following integral is obtained:

$$r_{a_i}(t) = \frac{1}{\bar{L}_{a_i}} \int_0^{\bar{L}_{a_i}} \delta(t-x/c_1)\exp(-px) + \exp(-rt+zx)(x/c_1-x/c_2)h \frac{I_1[2h\sqrt{(t-x/c_1)(t-x/c_2)}]}{\sqrt{(t-x/c_1)(t-x/c_2)}} u(t-x/c_1)\, dx \qquad (3.10)$$

where all the parameters correspond to those of a channel of order a_i.

The integration of the first term in equation 3.10 (see Appendix B, Section B.4) yields,

$$\frac{c_1}{\bar{L}_{a_i}} \exp(-ptc_1)$$

A closed form solution to the second term integral cannot be found. The rearranged expression for $r_{a_i}(t)$, shows that the upper limit of integration for the second term is dependent on the time, t,

$$r_{a_i}(t) = \frac{c_1}{\bar{L}_{a_i}} \exp(-ptc_1) + \int_0^{L'_{a_i}} \exp(-rt+zx)(x/c_1-x/c_2)h \frac{I_1[2h\sqrt{(t-x/c_1)(t-x/c_2)}]}{\sqrt{(t-x/c_1)(t-x/c_2)}} \, dx \tag{3.11}$$

where

$$L'_{a_i} = \begin{cases} c_1 t & \text{for } t \leq \bar{L}_{a_i}/c_1 \\ \bar{L}_{a_i} & t \geq \bar{L}_{a_i}/c_1 \end{cases}$$

Since a closed form solution to the above integral does not exist, the integral must be evaluated numerically.

Up to now, this chapter has presented the derivation of $r_{a_i}(t)$ based on the equations of motion. Inherent in the parameters of $r_{a_i}(t)$ are the physiographic factors relating to the channel's characteristics, which affect the discharge from the channel, and therefore the basin. The next section of this chapter will present a physical interpretation of $r_{a_i}(t)$ and $u_{a_i}(t)$.

3.5 Physical Interpretation of $u_{a_i}(t)$ and $r_{a_i}(t)$

Examination of the parameters of Equations 3.8 and 3.11 indicates that the channel responses will be significantly influenced by the Froude number. Actually the solution is valid only for a Froude number less than 2. In most regions, the Froude number is usually less than 1 which corresponds to subcritical flow. A Froude number greater than 2 indicates that a bore will form and, as indicated by Equation 3.8, the solution breaks down. For Froude numbers between 1 and 2 the first order modified Bessel function of the first kind, $I[\cdot]$, will change to a first order Bessel function of the first kind, $J[\cdot]$. The solution will contain imaginary terms which imply oscillations in the discharge and water surface.

A plot of $u_{a_i}(t)$ for channels with all the same characteristics except for channel length, is presented in Figure 3.1 The spike given by the first term of Equation 3.8 represents the dynamic part of the wave and occurs at time x/c_1. At that time the wavefront, moving at the dynamic propagation speed, $c_1 = v_o + \sqrt{gy_o}$, reaches the outlet. The magnitude of the spike is influenced by the parameter p and provides an indication of the dissipation of the wave along a distance x. The magnitude of the spike can be interpreted as the following ratio:

$$\exp(-px) = \frac{\text{volume under the head of the wave}}{\text{total volume of the complete wave}}$$

where

$$p = \frac{S_o}{2y_o} \frac{2-F}{F(1+F)} \quad , \quad x = \text{channel length}$$

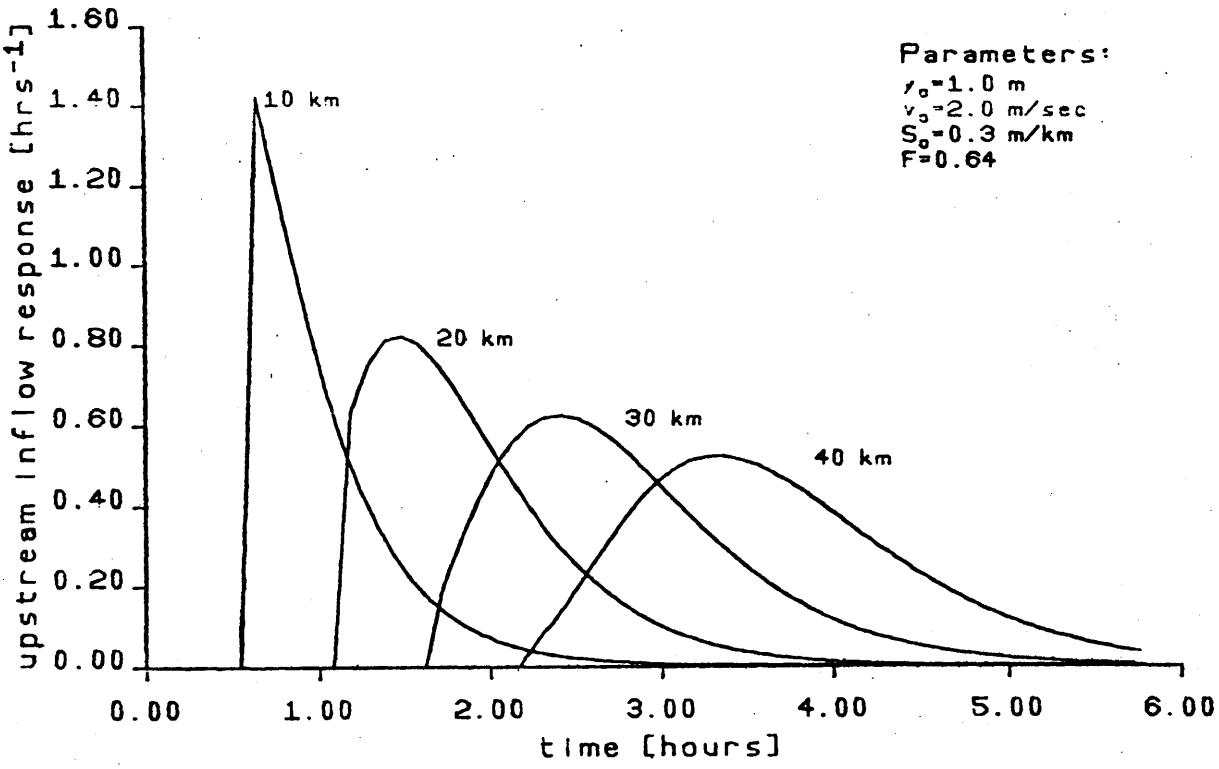

Figure 3.1: Upstream inflow response for different channel lengths.

The term p lumps the flow characteristics into one parameter, as p is a function of S_o, y_o and F which are interdependent parameters in the sense that changing one parameter causes at least one of the other parameters to change. For example increasing S_o, increases v_o, which increases F, and assuming y_o is unchanged, one cannot conclude whether p increases or decreases.

The second term of Equation 3.8 represents the kinematic part of the wave which dissipates more slowly than the dynamic part. The dynamic wave travels at the speed $v_o + \sqrt{gy_o}$, whereas the mean velocity of the center of mass of the kinematic part is 1.5 y_o. This is obtained from the expression of the time lag, t_L, which is the interval between the centroid of effective rainfall and that of direct runoff. In Appendix B t_L is shown to be

$$t_L = \frac{x}{1.5\ v_o} \tag{3.12}$$

The kinematic wave velocity is always smaller than the dynamic since $v_o/\sqrt{gy_o}$ (the Froude number) is always less than 1 for the cases considered in this study.

In contrast to the upstream inflow IUH, $u_{a_i}(t)$, the lateral inflow IUH, $r_{a_i}(t)$, exists for all time. The response at t=0, is given by

$$\frac{c_1}{\overline{L}_{a_i}} = \frac{v_o + \sqrt{gy_o}}{\overline{L}_{a_i}} \tag{3.13}$$

where $c_1 = v_o + \sqrt{gy_o}$ is the dynamic velocity of the wave. The numerator represents the steady state reference condition, and since there is a $1/\bar{L}_{a_i}$ chance that the drop will land at the outlet, the initial response is given by the above expression.

Consider the response $r_{a_i}(t)$ as the summation of two terms,

$$r^1_{a_i}(t) = \begin{cases} c_1/\bar{L}_{a_i} \exp(-pc_1 t) & t \leq \bar{L}_{a_i}/c_1 \\ 0 & t > \bar{L}_{a_i}/c_1 \end{cases} \tag{3.18}$$

$$r^2_{a_i}(t) = \begin{cases} e^{-rt} \int_0^{c_1 t} H(x,t)\,dx & t \leq \bar{L}_{a_i}/c_1 \\ e^{-rt} \int_0^{\bar{L}_{a_i}} H(x,t)\,dx & t > \bar{L}_{a_i}/c_1 \end{cases} \tag{3.19}$$

where

$$H(x,t) = e^{zx}\,(x/c_1 - x/c_2)h\,\frac{I_1[2h\sqrt{(t-x/c_1)(t-x/c_2)}]}{\sqrt{(t-x/c_1)(t-x/c_2)}}$$

$r_{a_i}(t)$ can be interpreted as the channel's response to an input consisting of an infinite number of waves originating at each point along the channel. The response due to the wave fronts and to the bodies of the waves originating along the channel, are given by the Equations 3.18 and 3.19, respectively.

The first term is zero after $\bar{L}_{a_i}/c_1$ as all the wave fronts have responded. Recall that $r_{a_i}(t)$ is the pdf corresponding to the time at

which a drop, falling anywhere in the channel reaches the channel outlet; therefore the possible times at which a wave front could reach the outlet is between times 0 and $\bar{L}_{a_i}/c_1$ where c_1 is the dynamic wave front velocity ($c_1 = v_o + \sqrt{gy_o}$). For example, consider the two extreme cases: case (i): the drop lands at x=0; case (ii): the drop lands at $x = \bar{L}_{a_i}$. In the first case the wave front would reach the channel outlet at $t = \bar{L}_{a_i}/c_1$ and in the second case at time 0. These two cases establish the time interval during which wave fronts reach the outlet. The abrupt change in slope at $t = \bar{L}_{a_i}/c_1$ is due in part to the fact that all wave fronts have responded so that $r^1_{a_i}(t)$ equals zero.

Concerning the second term, the limit of integration changes as the limit cannot exceed the distance travelled by the body of a wave. The first limit, $c_1 t$, for $t \leq \bar{L}_{a_i}/c_1$, represents the distance from the most downstream channel point, to the point where a wave can originate and contribute to the response at time t. Those waves originating beyond distance $c_1 t$ have not yet contributed to the response at the end of the channel. For $t > \bar{L}_{a_i}/c_1$ all waves originating along the channel are contributing to the response, and the limit changes to $\bar{L}_{a_i}$, which is the greatest distance a wave will travel to reach the most downstream point.

Plots of $r_{a_i}(t)$ for channels of different lengths, are presented in Figure 3.2. As can be observed, the ordinate of each curve starts at $c_1/\bar{L}_{a_i}$, remains relatively constant and then rapidly decreases at time $\bar{L}_{a_i}/c_1$. The abrupt change in slope the time $t = \bar{L}_{a_i}/c_1$ is due to the previously mentioned facts concerning the response of the wave fronts and wave bodies. The response due to wave fronts and wave bodies are

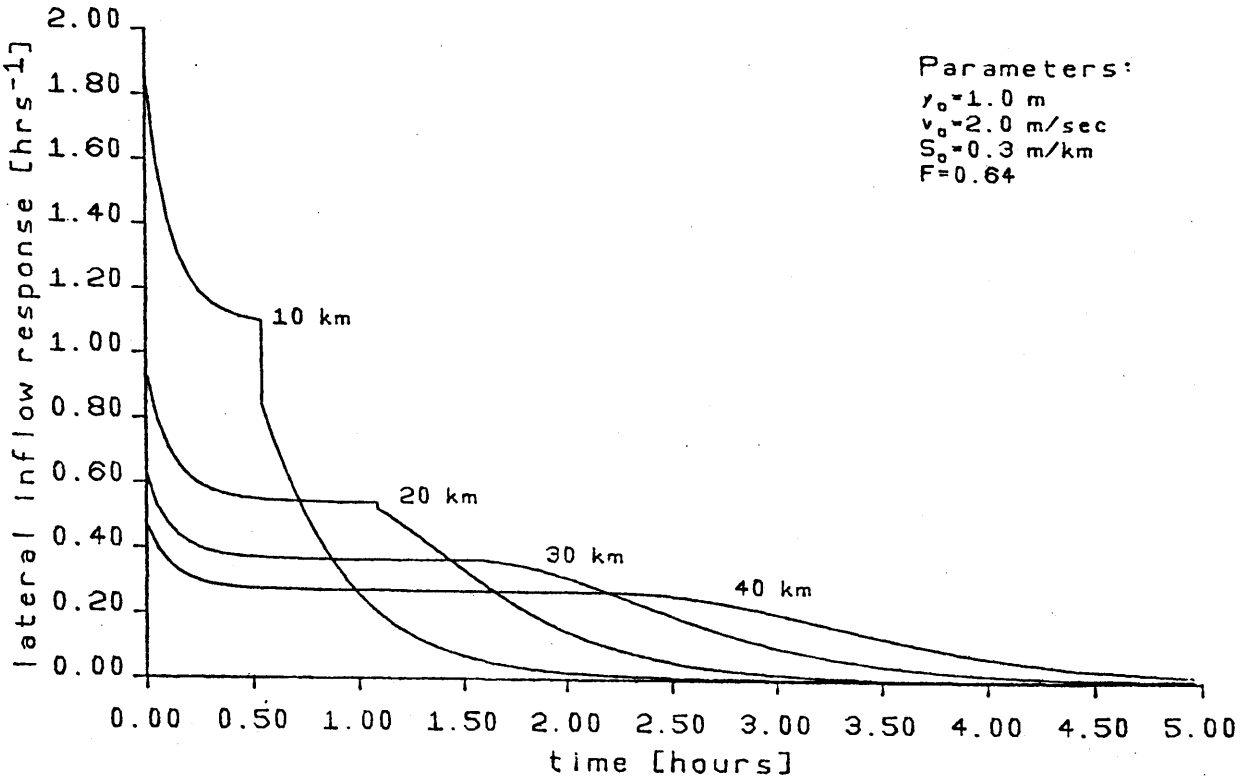

Figure 3.2: Lateral inflow response for different channel lengths.

plotted separately in Figures 3.3 and 3.4 for channels of length 10 and 20 km. As can be observed, the longer the channel, the less significant are the effects of the wave fronts, vice versa for shorter channels.

3.6 The Effect of the Input Parameters on the Channels' Response

As previously presented, both the upstream and lateral input channel IUHs are expressed as functions of the channels' physiographic characteristics, and the reference parameters, v_o and y_o. This section will present a sensitivity analysis in order to determine the effects of the input parameters on the shape of the upstream and lateral input IUHs.

3.6.1 The Upstream Input Channel IUH

The upstream input IUHs for different parameter sets are presented in Figures 3.5 to 3.6. Figures 3.5 and 3.6 have channel lengths of 10 to 20 km, respectively. The channel IUH in Figures 3.5.1 and 3.6.1 have the same velocity (v_o), and Figures 3.5.2 and 3.6.2 have the same Froude number (F). As can be observed the translation of the IUH is affected by both a change in velocity and Froude number. A more interesting observation is that the attenuation is relatively independent of the velocity for a given F. For in Figures 3.5.2 and 3.6.2, the IUHs have the same F and different velocities, yet the attenuation of the wave is approximately the same in each case.

For a constant velocity, the reference parameter, y_o, determines the Froude number, and for these cases of constant velocity, the time to

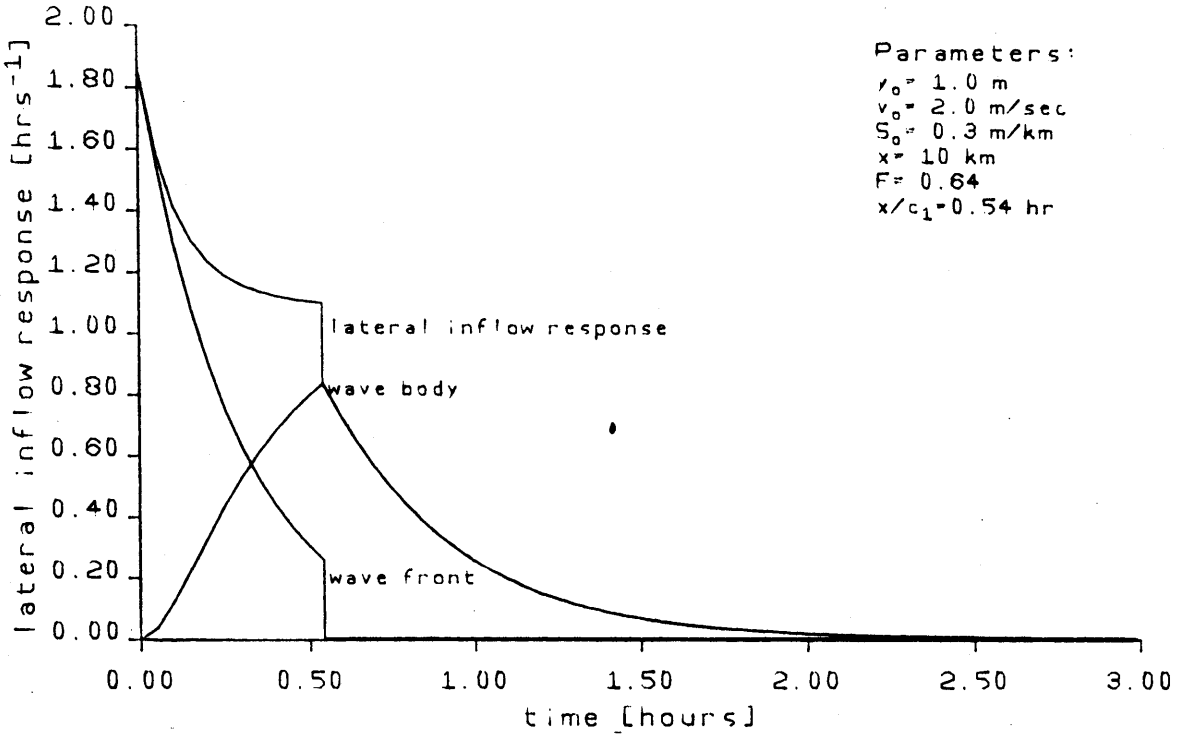

Figure 3.3: Contribution of the wave front and wave body to the lateral inflow response.

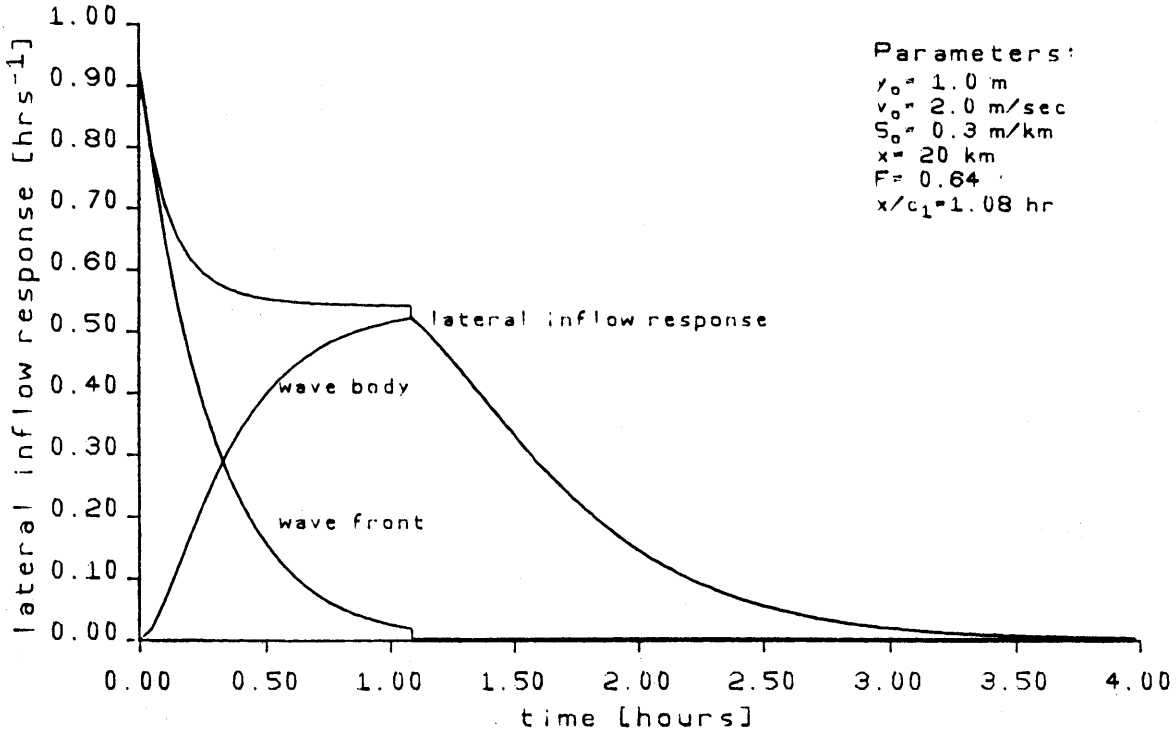

Figure 3.4: Contribution of the wave front and wave body to the lateral inflow response.

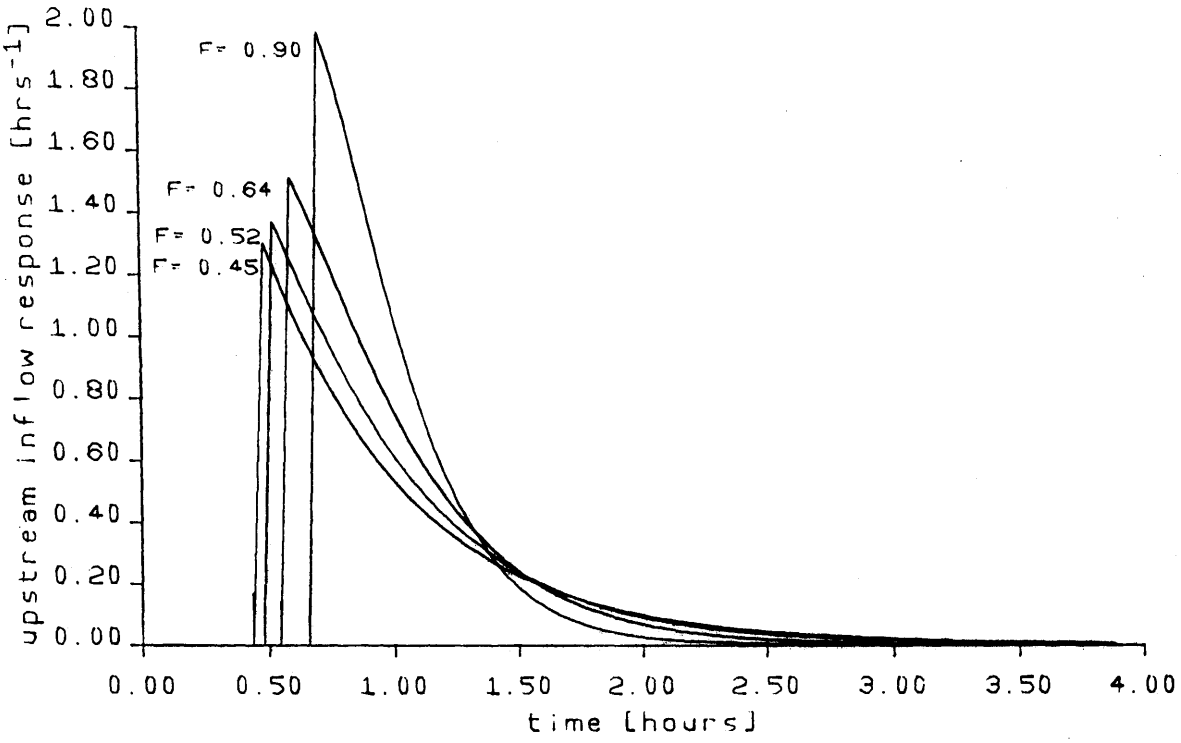

Figure 3.5.1: Upstream inflow response for different Froude numbers.

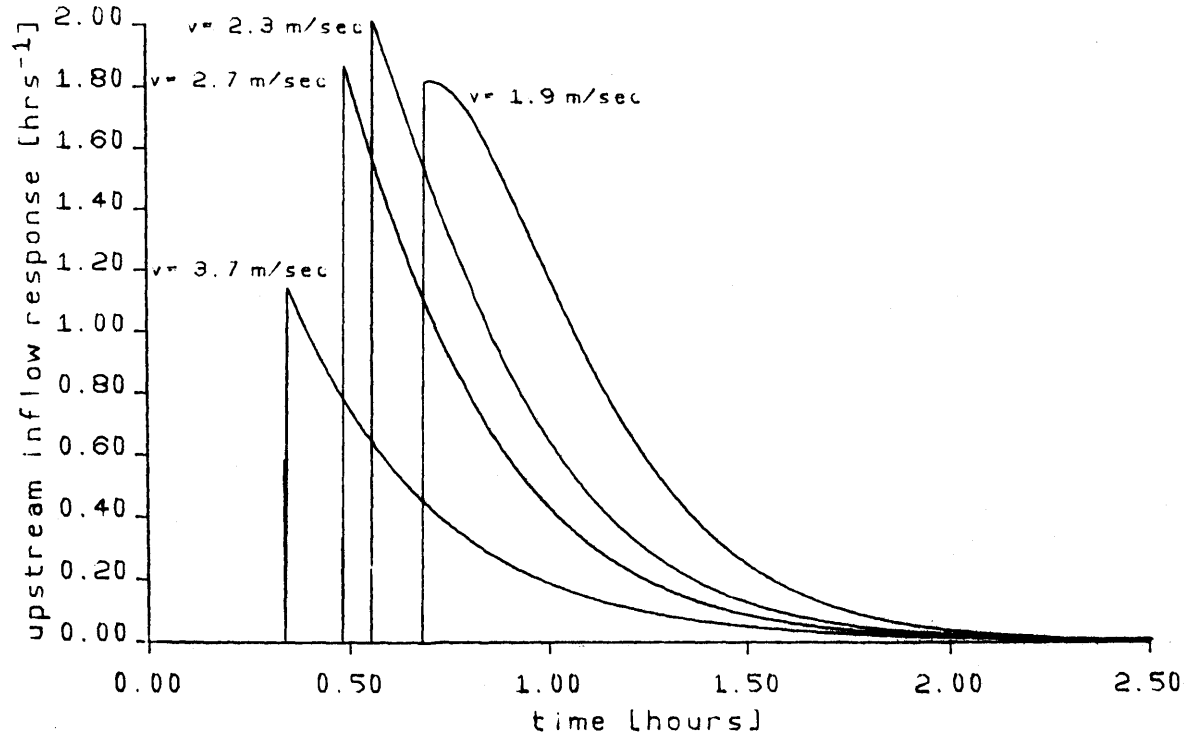

Figure 3.5.2: Upstream inflow response for different reference velocities.

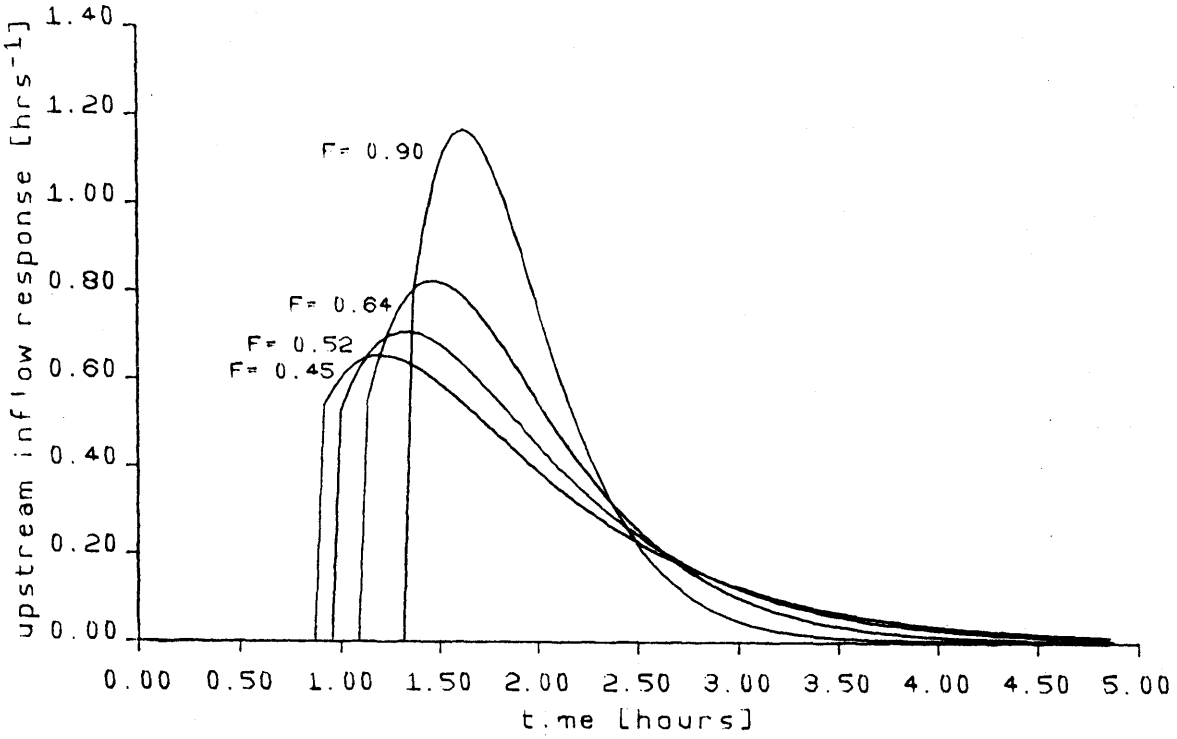

Figure 3.6.1: Upstream inflow response for different Froude numbers.

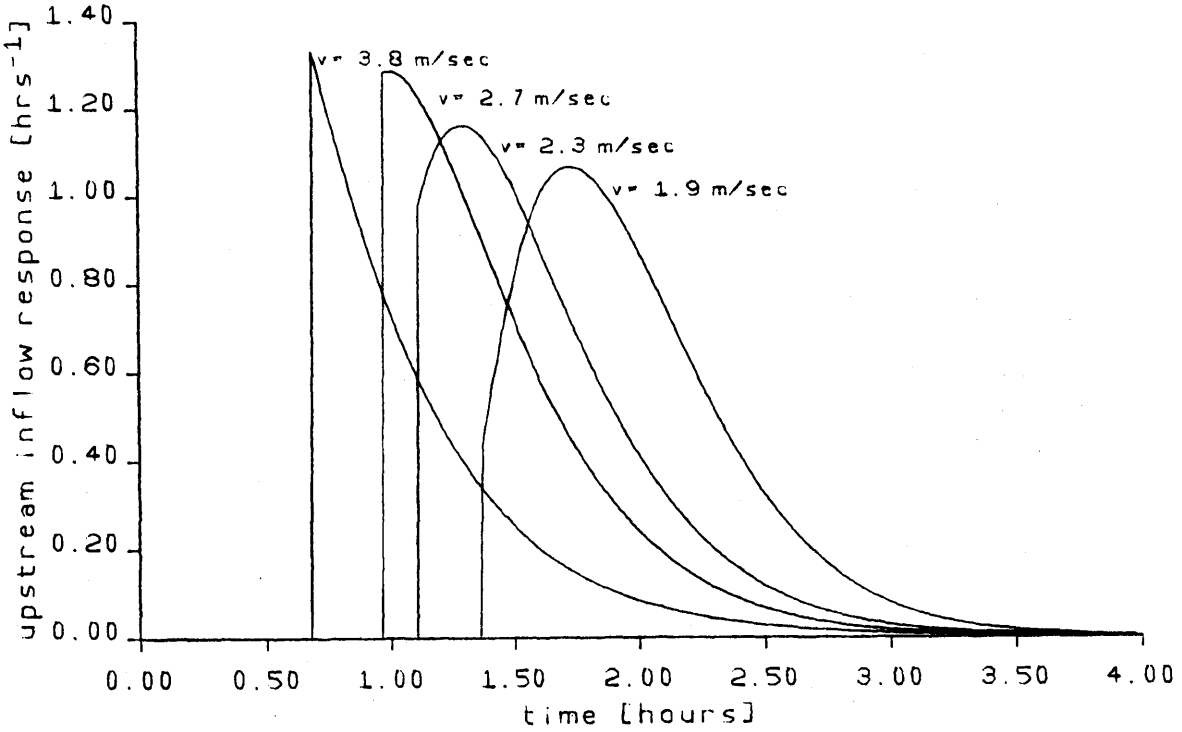

Figure 3.6.2: Upstream inflow response for different reference velocities.

peak and peak response both increase with decreasing y_o and increasing F. The time to peak is influenced by the dynamic wave speed, c_1; c_1 decreases with y_o and thus the time to the initial response, x/c_1, increases, and the time to peak occurs later for cases where y_o is smaller. The peak response also increases. Even though the time to the initial response is delayed, the greater F implies a faster response once the channel begins to respond.

The effect of the channel's slope on the upstream input channel response is exhibited in Figures 3.7.1 and 3.7.2. For each case the velocity and Froude number are equivalent. In Figure 3.7.1 the slope ranges from 0.15 to 0.35 m/km, but the overall change in the IUH is negligible. However, in Figure 3.7.2 the slopes vary by factors of 10, and the variation in the IUHs is signficant between the different cases. Thus the slope must be within a reasonable range of the actual slope.

3.6.2 The Lateral Input IUH

In contrast to the upstream input IUH, the lateral input IUH is only significantly dependent on the reference velocity, v_o. The lateral input IUH is presented in Figures 3.8 and 3.9, where 3.8 and 3.9 have channel lengths of 10 and 20 km respectively. Figures 3.8.1 and 3.9.1 have the same velocity, and Figures 3.8.2 and 3.9.2 have the same Froude number. The insignificance of F can be observed in Figures 3.8.1 and 3.9.1. In these Figures the Froude number ranges from .45 to .90, yet the responses are similar. The significance of v_o can be concluded by observing the difference between the responses presented in Figures 3.8.2 and 3.9.2.

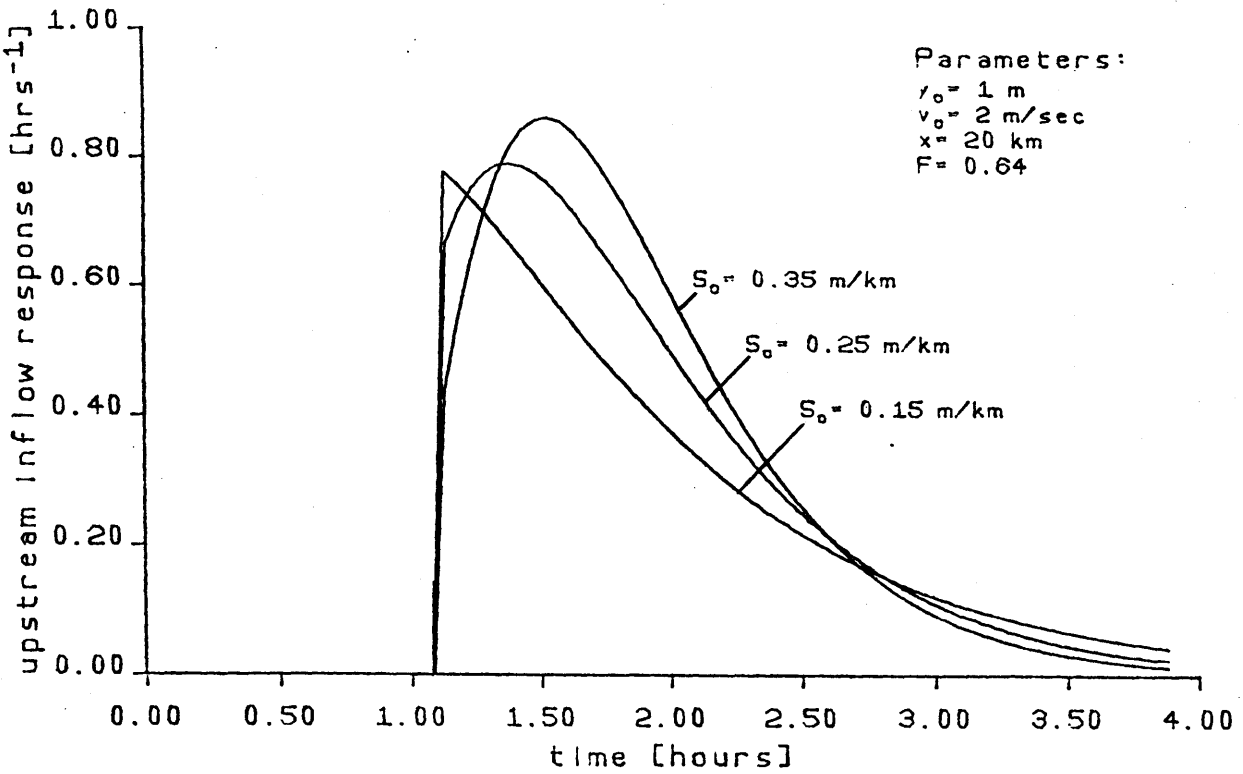

Figure 3.7.1: Upstream inflow response for different channel slopes.

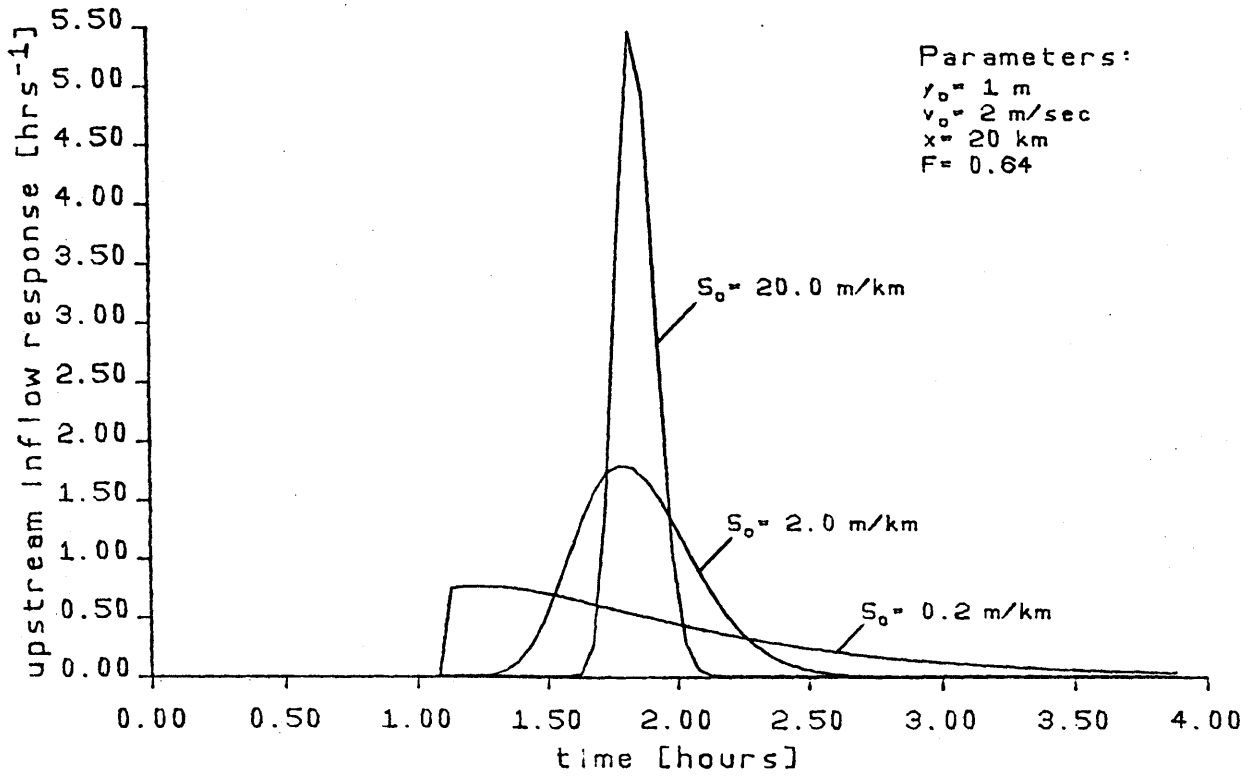

Figure 3.7.2: Upstream inflow response for different channel slopes.

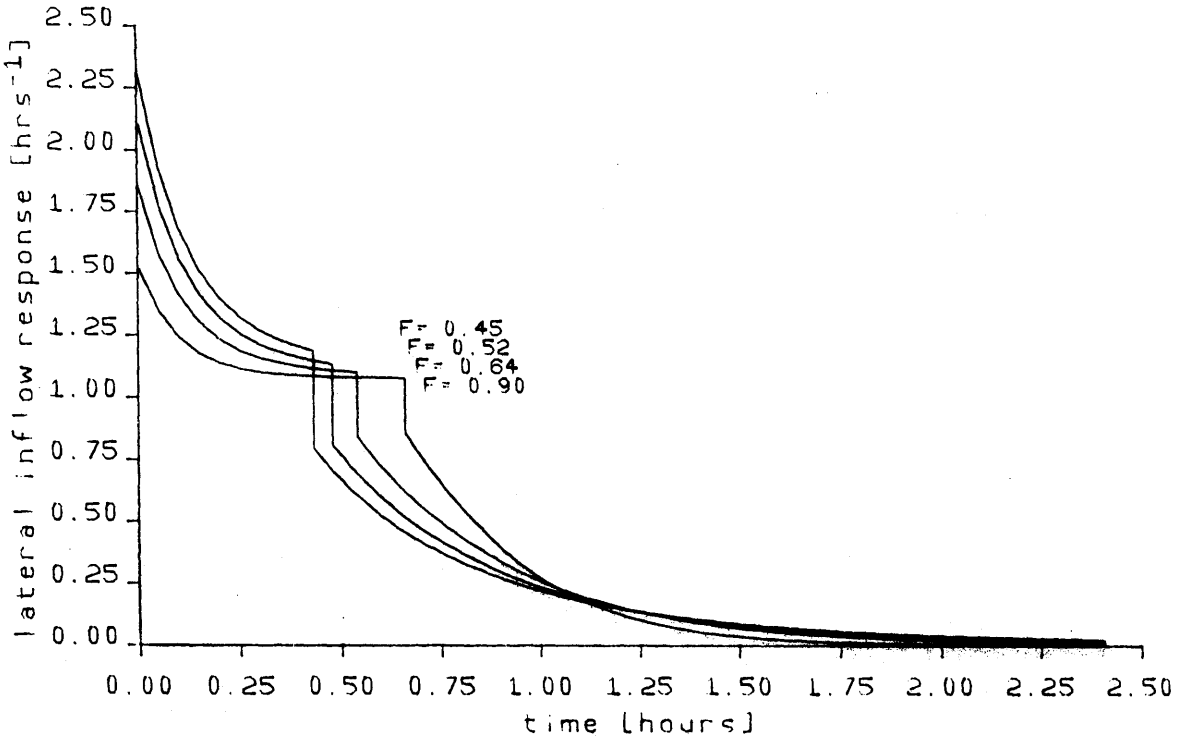

Figure 3.8.1: Lateral inflow response for different Froude numbers.

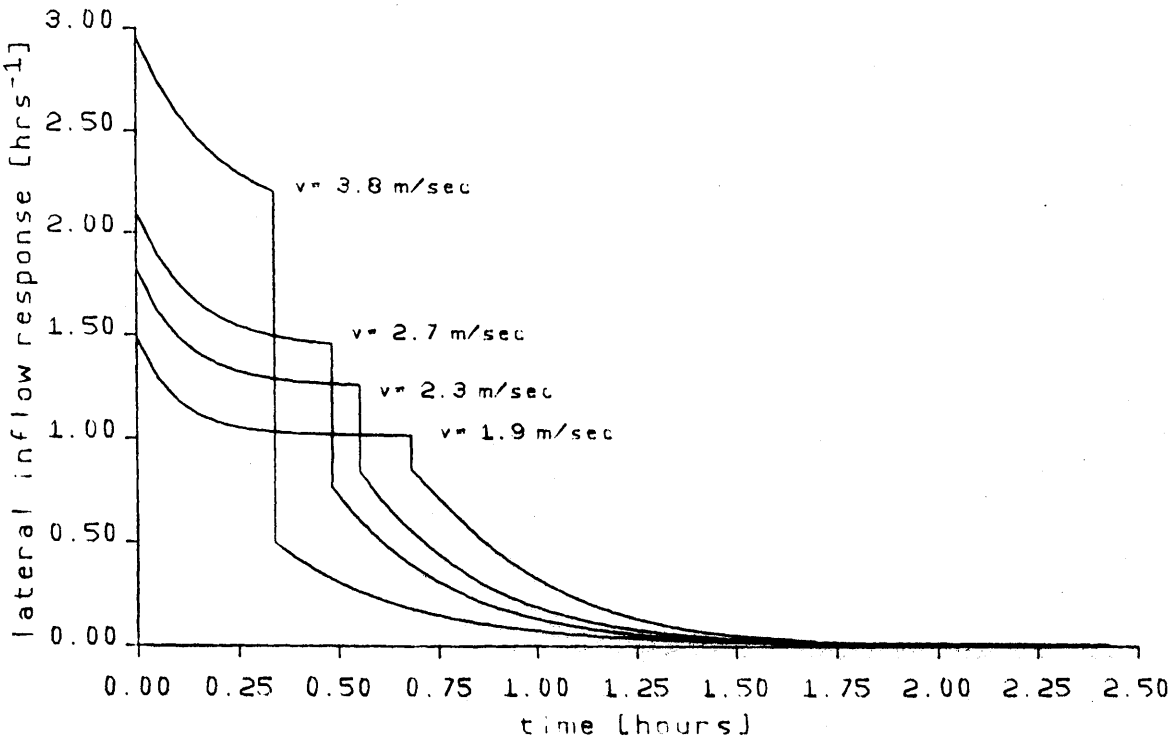

Figure 3.8.2: Lateral inflow response for different reference velocities.

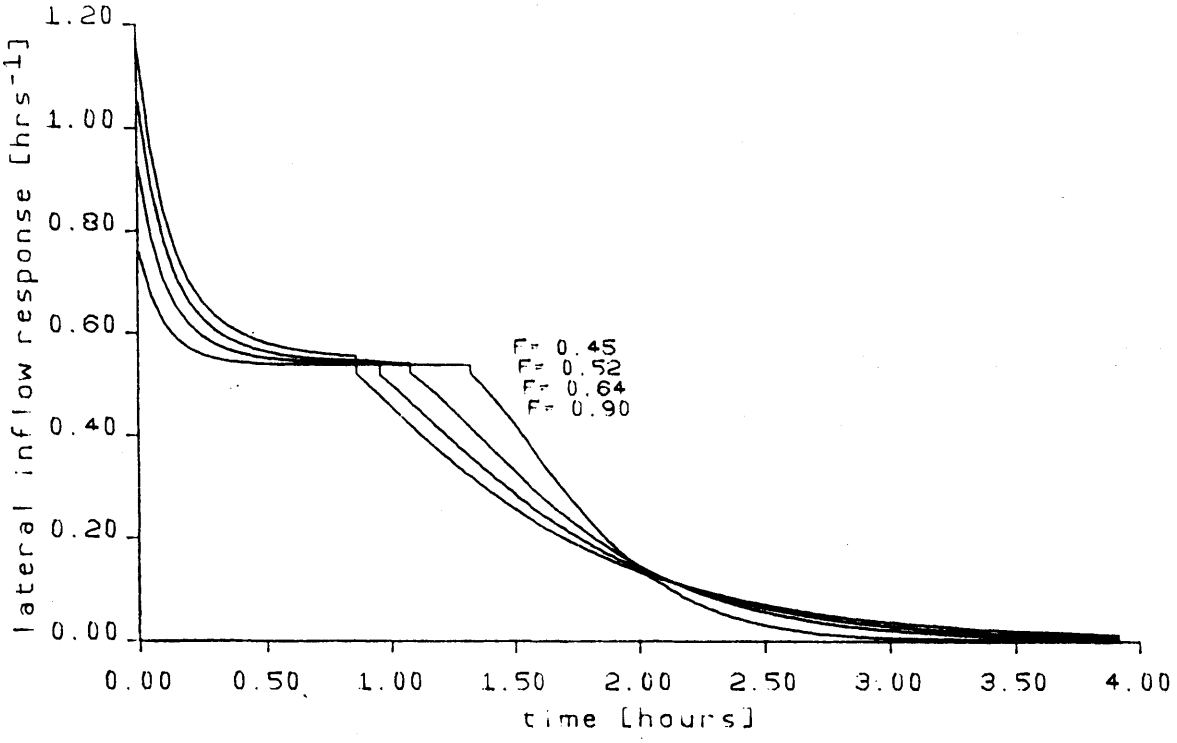

Figure 3.9.1: Lateral inflow response for different Froude numbers.

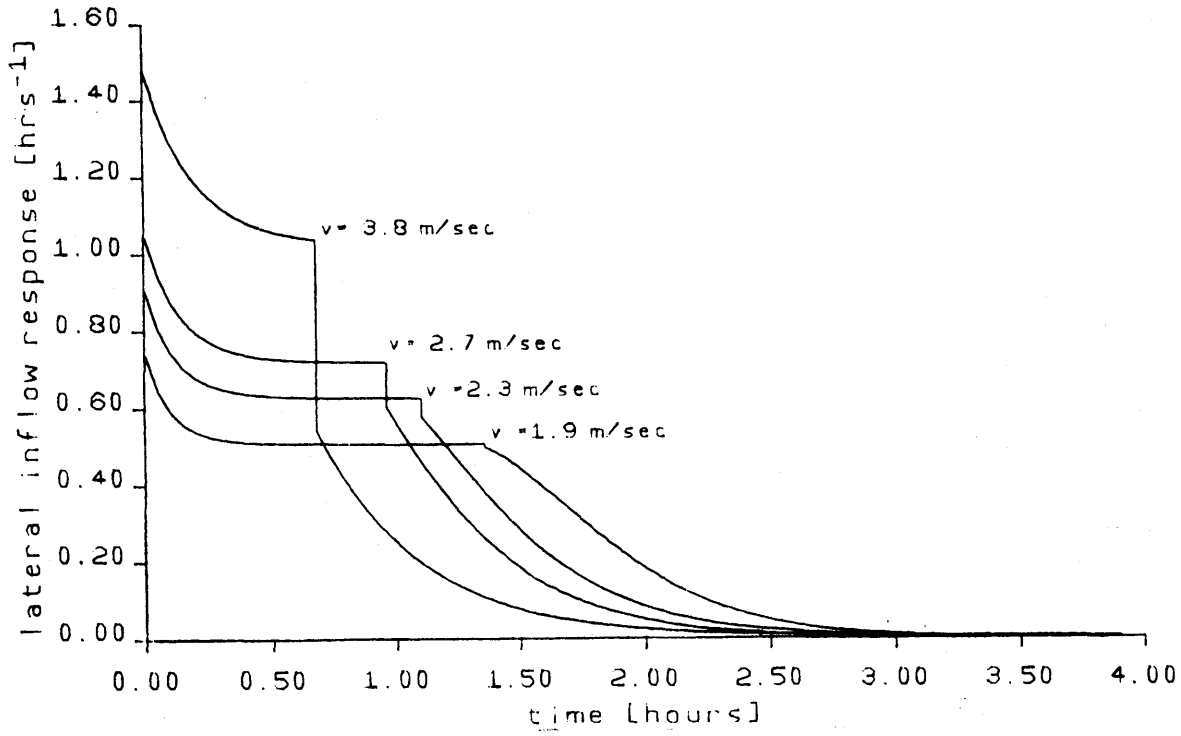

Figure 3.9.2: Lateral inflow response for different reference velocities.

Figures 3.10.1 and 3.10.2 present the difference in the lateral inflow IUH due to changes in the channel slope. In Figure 3.10.1 the slope ranges from 0.15 to 0.35 m/km, with the steepest channel responding the fastest. In Figure 3.10.2, the slopes vary by factors of 10, yet the responses are quite similar. Compared with the other parameters, the channel IUH is the least sensitive to the slope parameter.

3.7 Summary

This chapter presented the derivation of analytical expressions for the response of a channel. The channel responds according to where the input originates along the channel. The response to an input at the channel's most upstream point is denoted by $u_{a_i}(t)$, and that to an input originating anywhere along the channel by $r_{a_i}(t)$. The responses describe the flood wave's movement along the channel as the pdfs corresponding to the time a drop, whose travel begins in the channel of order a_i, takes to reach the channel's most downstream point. Inherent in the pdf is the physics of the flood wave movement as functions of channel slope, acceleration due to gravity and the reference parameters, v_o and y_o. The expressions for $u_{a_i}(t)$ and $r_{a_i}(t)$ and their corresponding Laplaces are summarized below.

$$u_{a_i}(t) = \delta(t-x/c_1)\exp(-px) +$$

$$\exp(-rt+zx)(x/c_1-x/c_2)h\,\frac{I_1[2h\sqrt{(t-x/c_1)(t-x/c_2)}\,]}{\sqrt{(t-x/c_1)(t-x/c_2)}}\;u(t-x/c_1) \qquad (3.20)$$

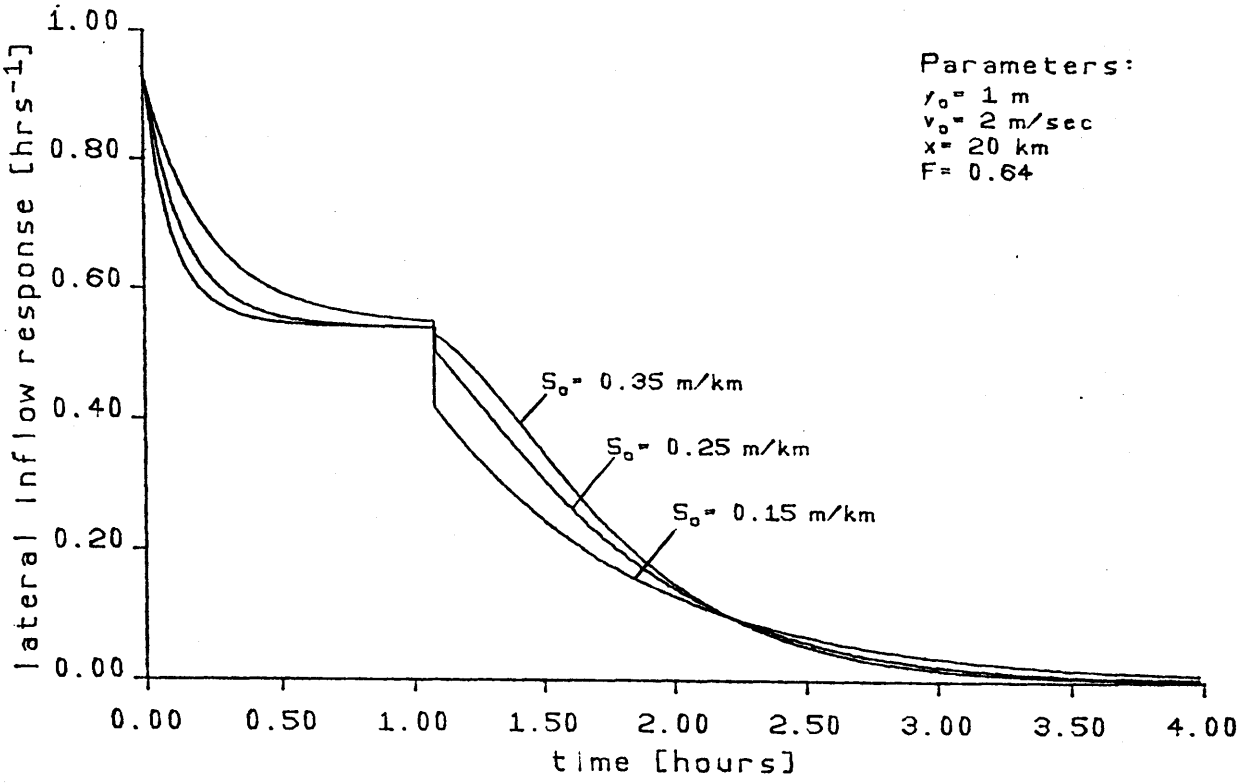

Figure 3.10.1: Lateral inflow response for different channel slopes.

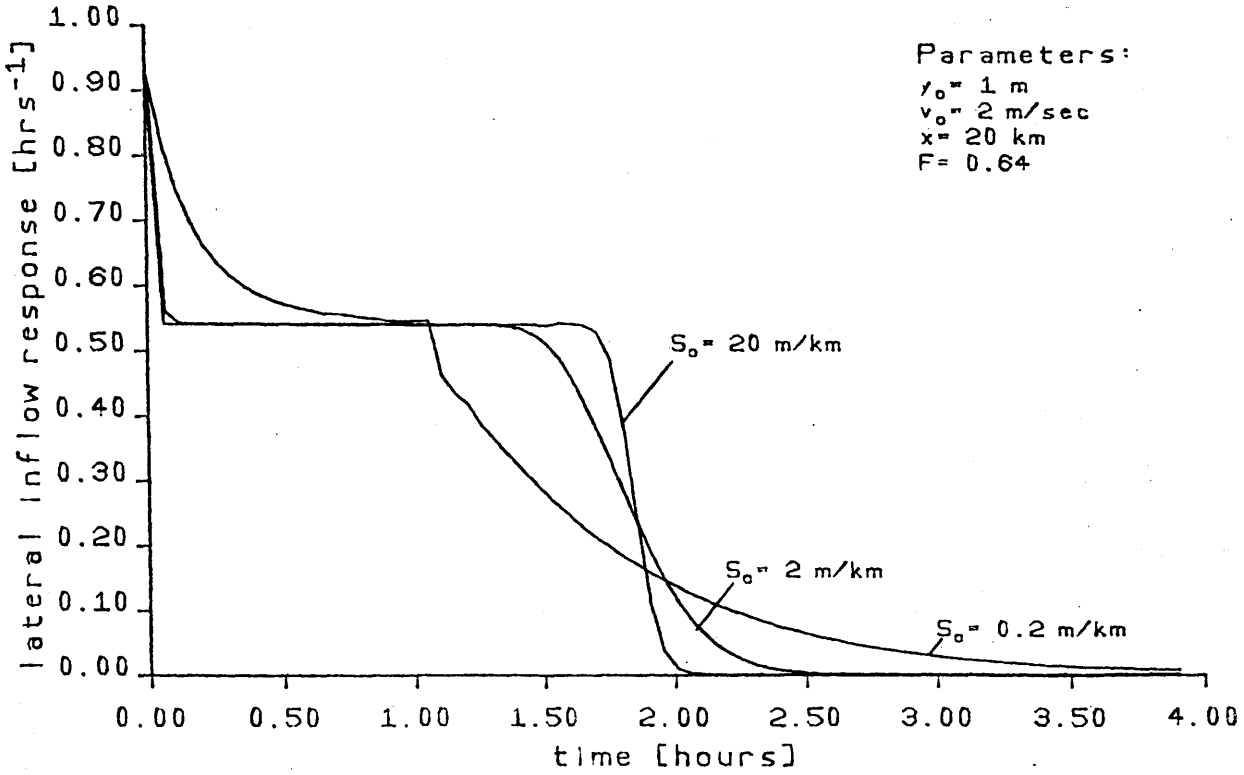

Figure 3.10.2: Lateral inflow response for different channel slopes.

$$L[u_{a_i}(t)] = \exp[(-\sqrt{as^2+bs+c}+es+f)\bar{L}_{a_i}] \tag{3.21}$$

$$r_{a_i}(t) = \begin{cases} \dfrac{c_1}{\bar{L}_{a_i}} \exp(-pc_1 t) + e^{-rt}\displaystyle\int_0^{c_1 t} H(x,t)dx & t \leq \bar{L}_{a_i}/c_1 \\ e^{-rt}\displaystyle\int_0^{\bar{L}_{a_i}} H(x,t)\,dx & t > \bar{L}_{a_i}/c_1 \end{cases} \tag{3.22}$$

where

$$H(x,t) = e^{zx}(x/c_1 - x/c_2)h\ \frac{I_1[2h\sqrt{(t-x/c_1)(t-x/c_2)}\ ]}{\sqrt{(t-x/c_1)(t-x/c_2)}}$$

$$L[r_{a_i}(t)] = \frac{1}{\bar{L}_{a_i}(-\sqrt{as^2+bs+c}+es+f)}\ [\exp(L_{a_i}(-\sqrt{as^2+bs+c}+es+f))-1] \tag{3.23}$$

where

$$c_1 = v_o + \sqrt{gy_o}$$

$$c_2 = v_o - \sqrt{gy_o}$$

$$p = \frac{S_o}{2y_o} \frac{(2-F)}{F(1+F^2)}$$

$$r = \frac{S_o v_o}{2y_o} \frac{2 + F^2}{F^2}$$

$$z = \frac{S_o}{2y_o}$$

$$h = \frac{S_o v_o}{2y_o} \frac{\sqrt{(4-F^2)(1-F^2)}}{2F^2}$$

$$F = \frac{v_o}{\sqrt{gy_o}}$$

$$a = \frac{1}{gy} \frac{1}{(1-F^2)^2}$$

$$b = \frac{S_o}{q_o} \frac{2+F^2}{(1-F^2)^2}$$

$$c = \frac{9}{4} \left(\frac{S_o}{y_o}\right)^2 \frac{1}{(1-F^2)^2}$$

$$e = \frac{v_o}{gy_o(1-F^2)}$$

$$f = \frac{3}{2} \frac{S_o}{y_o} \frac{1}{1-F^2}$$

The following chapter will present several geomorphologic IUH's, and a sensitivity analysis will be conducted to decipher the significant parameters which influence the shape of the IUH. The results will be summarized in terms of the time to the peak response and the peak response of the basin IUH.

Chapter 4

THE RESPONSE OF A RIVER BASIN

4.1 Introduction

The ultimate aim of this study is to determine the runoff from ungaged river basins. Estimation of runoff is based on a wide variety of approaches, both empirical and theoretical. This study specifically investigates a theoretical approach which focuses on the relationship between runoff and the physiographic and geomorphologic characteristics of the river basin.

The response of a channel has been derived as a function of its physiographic characteristics and the origin of the input. This chapter presents how both the upstream input response, $u_{a_i}(t)$, and the lateral input response, $r_{a_i}(t)$, are used to determine the basin IUH. A sensitivity analysis will illustrate how the channels' physiographic and the basin's geomorphologic characteristics affect the shape of the basin IUH.

4.2 The Basin Instantaneous Unit Hydrograph

The upstream input and channel responses discussed in the previous chapter can be used to enhance the hydrogeomorphologic theory. Referring to the hypothetical basin presented in Figure 2.1, the flow contributing to some higher order streams is mainly due to flow from the intersection of the lower order tributaries which form these higher order streams. Streams of this type respond according to the upstream inflow channel response. River basins with bifurcation ratios approximately equal to 2 would have streams where most of the contributing flow is from the

upstream lower order channels and where there are few tributaries contributing along the stream.

Basins with bifurcation ratios much larger than 2 will have high order streams heavily dependent on lateral tributaries inflows. The lateral inflow stream IUH would then be important in these cases. Differentiating between the possible configurations of the streams (e.g., whether the lower order streams flow into the higher order streams' most upstream point or along the streams' length) requires reevaluating the possible paths a drop can take.

According to Strahler's ordering procedure, two streams of lower order combine to form a stream of higher order, thus the paths containing a transition of the form, ... $i \rightarrow i+1$ ..., can be further divided into two paths. One path represents those drops that enter along the channel laterally, and the other path represents those drops that enter at the channel's most upstream point. For a third order basin, the possible paths are:

$$
\begin{aligned}
s_1&: \ \theta_1 \rightarrow r_1 \rightarrow r_2 \rightarrow r_3 \rightarrow r_4 \\
s_2&: \ \theta_1 \rightarrow r_1 \rightarrow u_2 \rightarrow r_3 \rightarrow r_4 \\
s_3&: \ \theta_1 \rightarrow r_1 \rightarrow r_2 \rightarrow u_3 \rightarrow r_4 \\
s_4&: \ \theta_1 \rightarrow r_1 \rightarrow r_3 \rightarrow r_4 \\
s_5&: \ \theta_2 \rightarrow r_2 \rightarrow r_3 \rightarrow r_4 \\
s_6&: \ \theta_2 \rightarrow r_2 \rightarrow u_3 \rightarrow r_4 \\
s_7&: \ \theta_3 \rightarrow r_3 \rightarrow r_4 \\
s_8&: \ \theta_1 \rightarrow r_1 \rightarrow u_2 \rightarrow u_3 \rightarrow r_4
\end{aligned}
\qquad (4.1)
$$

where θ_i (i=1, ..., W) refers to the overland phase, r_i refers to the drop entering anywhere along the channel's length, u_i refers to the drop entering at the channel's most upstream point, and r_{W+1} refers to the basin outlet. In order to account for the additional paths, the transition probabilities previously presented need to be modified and the transition probabilities of the form $r_i \rightarrow u_{i+1}$ and $u_i \rightarrow r_{i+1}$ need to be determined.

Two streams of order i are required to form a stream of order i+1, thus the probability of a transition from a stream of order i to the upstream point of a stream of order i+1, is the fraction $\frac{2N_{i+1}}{N_i}$. Using Equation 2.13, the transition probabilities are given by:

$$P_{r_i r_j} = \frac{(N_i - 2N_{i+1})\, E[j,W]}{\sum_{k=j}^{w} E[k,W] N_i} \qquad 1 \leq i < j \leq W \qquad (4.2)$$

$$P_{r_i u_{i+1}} = \frac{2N_{i+1}}{N_i} \qquad 1 \leq i \leq W \qquad (4.3)$$

$$P_{u_i r_{i+1}} = P_{r_i r_{i+1}} \qquad 1 \leq i \leq W \qquad (4.4)$$

$$P_{u_i u_{i+1}} = P_{r_i u_{i+1}} \qquad 1 \leq i \leq W \qquad (4.5)$$

where $p_{r_i r_j}$ is the transition probability for a drop going from a stream of order i to a point along a stream of order j, $p_{r_i u_{i+1}}$ is the probability that a drop from a stream of order i goes to the upstream point of a stream of order i+1, and E[k,W] is given by Equation 2.14. A drop following this path travels along the stream that forms the stream of higher order. Transition probabilities of the form $p_{u_i r_{i+1}}$ and $p_{u_i u_{i+1}}$ are equivalent to $p_{r_i r_{i+1}}$ and $p_{r_i u_{i+1}}$, respectively, as the drop's transition from a stream of order i is independent of where it originally entered the stream of order i.

Taking into account the 8 paths, the initial and transition probabilities for a 3rd order basin are presented in Table 4.1 as functions of R_A and R_B. The result that the transition probabilities of the form, $p_{r_i u_{i+1}}$, are always equal to $2/R_B$ is a consequence of Horton's law of stream numbers. The transition probabilities account for the fact that the lower the bifurcation ratio, the greater the number of streams which respond according to the upstream input channel response. For as R_B decreases, $p_{r_i u_{i+1}}$ and $p_{u_i u_{i+1}}$ increase, and the other transition probabilities of the form, $p_{r_i r_j}$ and $p_{u_i r_j}$ (j>i), decrease; thus paths defined by one or more upstream inflow channel responses will have more influence on the overall basin IUH, in accordance with the basin's configuration.

The more detailed classification of the paths requires two types of pdfs for a drop's travel time in a stream of order a_i. Recall that the expression of the basin response function is given by:

Table 4.1: Initial and transition probabilities for a 3rd order basin.

$$\theta_1(0) = R_B^2 \, R_A^{-2}$$

$$\theta_2(0) = \frac{R_B}{R_A} - \frac{R_B + 2R_B - 2R_B}{R_A^2 \, (2R_B - 1)}$$

$$\theta_3(0) = 1 - \frac{R_B}{R_A} - \frac{R_B + 2R_B - 2R_B}{R_A^2(2R_B - 1)}$$

$$p_{r_1 r_2} = \frac{(R_B - 2R_B)}{R_B(2R_B - 1)}$$

$$p_{r_1 u_2} = \frac{2}{R_B}$$

$$p_{r_1 r_3} = \frac{R_B^2 - 3R_B + 2}{R_B(2R_B - 1)}$$

$$p_{r_2 r_3} = \frac{R_B - 2}{R_B}$$

$$p_{r_2 u_3} = \frac{2}{R_B}$$

$$p_{u_2 r_3} = p_{r_2 r_3}$$

$$p_{u_2 u_3} = p_{r_2 u_3}$$

$$h_B(t) = \sum_{s \in S} f_{a_1}(t) * \ldots * f_{a_k}(t)\, p(s) \qquad (4.6)$$

where $f_{a_i}(t)$ represents the pdf of travel time for a drop travelling a a stream of order a_i. Depending on the particular path, $f_{a_i}(t)$ will be defined as $r_{a_i}(t)$, if the drop enters laterally along the stream, or $u_{a_i}(t)$, if the drop enters at the most upstream point of the stream.

The expressions for $u_{a_i}(t)$ and $r_{a_i}(t)$ are given by Equations 3.20 and 3.22, respectively. Substitution of the expressions into Equation 4.6 for each path given in Equation 4.6 leads to an extremely complicated expression for which no closed form numerical solution exists. Noting that the Laplace of a convolution operation is the product of the Laplaces of each term, Equation 4.6 can be more readily solved using Laplace transform techniques. The Laplace of the expression representing a path in Equation 4.6 is given by the product of the Laplaces of $f_{a_i}(t)$, $a_i = a_1 \ldots a_k$, and is inverted numerically using a mathematical routine available on the Honeywell 6180, Multics operating system. (See Crump, 1976, for details concerning the mathematics.)

The next section will present examples of the geomorphologic basin IUH and will discuss the effect of the geomorphologic parameters and the reference parameters, y_o, v_o, and S_o, on the shape of the IUH.

4.3 The Effect of the Input Parameters on the Basin IUH

The basin response is expressed in terms of the channel responses and the geopmorphological parameters, R_A, R_B, and R_L. This section will demonstrate how the initial response, $h_B(0)$, time to peak, t_p, and the peak response, q_p, vary due to both changes in the geomorphologic parameters and in the reference parameters v_o, y_o, and S_o. The analysis will use a third order basin for the case study.

4.3.1 Geomorphologic Parameters

Examples of the geomorphologic basin IUH are presented in Figures 4.1 to 4.3. In all cases the linearizing velocity is 2.5 m/sec for all streams, and the linearizing depths are 0.80, 0.85 and 0.95 meters for streams of order 1 through 3, respectively. First order streams are 2.78 km in length, implying a small basin. Average channel slope is 0.3 m/km. The figures differ only in the geomorphological parameters. The time to peak, t_p, peak discharge, q_p, and initial response, $h_B(0)$, are summarized in Table 4.2.

The significant difference in all three basin IUHs presented in Figure 4.1 is due to the shorter distance a drop must travel to reach the basin outlet as R_L decreases. The cases with the shorter higher order streams have greater peaks and the time to peak occurs earlier. Obviously the shorter distance a drop has to travel to reach the outlet the faster the response, and thus this change in the IUH as R_L decreases.

As can be observed in Figures 4.2 and 4.3, the time to peak, t_p, is insensitive to changes in R_A and R_B for a given R_L, and only the initial response $h_B(0)$, and the peak, q_p, vary. Recall that for a

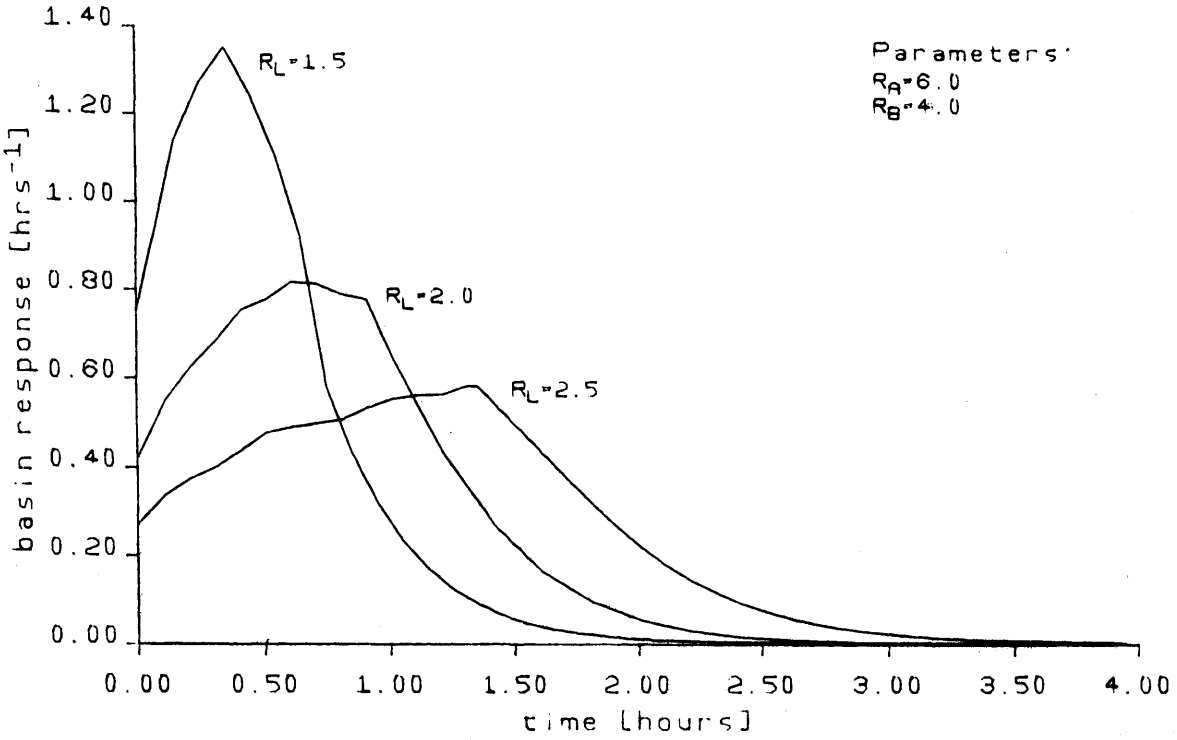

Figure 4.1: Basin IUHs for different length ratios, R_L.

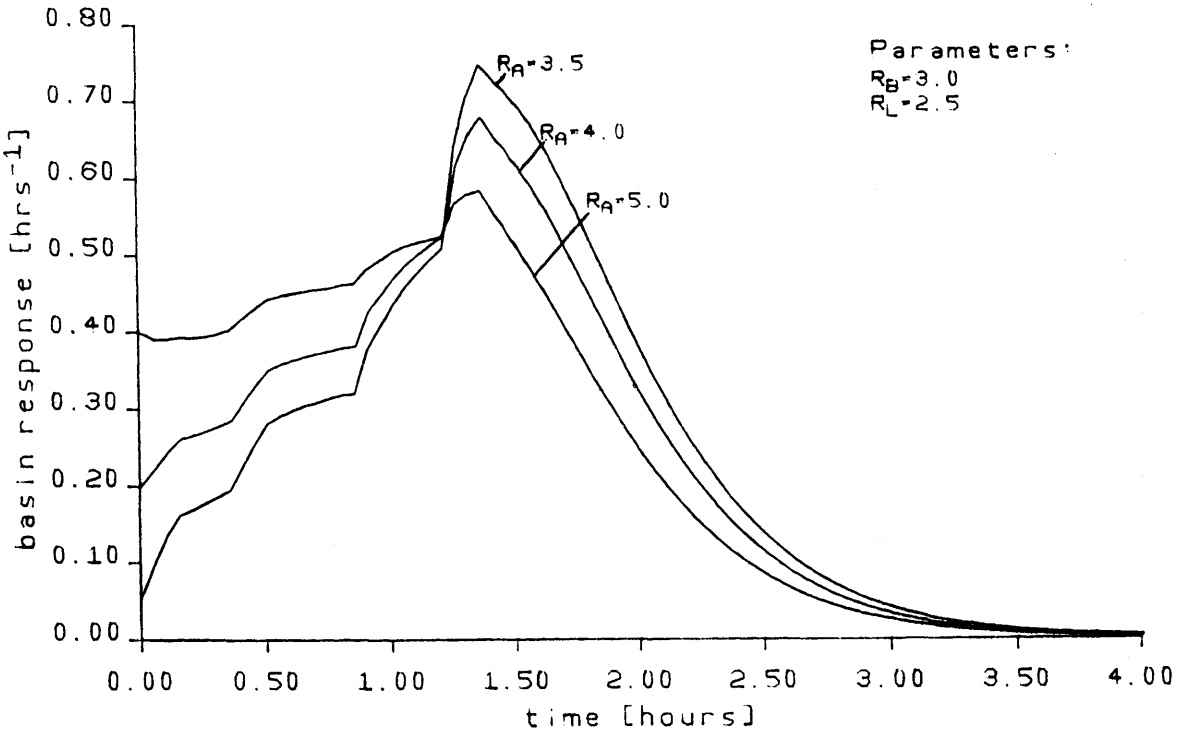

Figure 4.2: Basin IUHs for different area ratios, R_A.

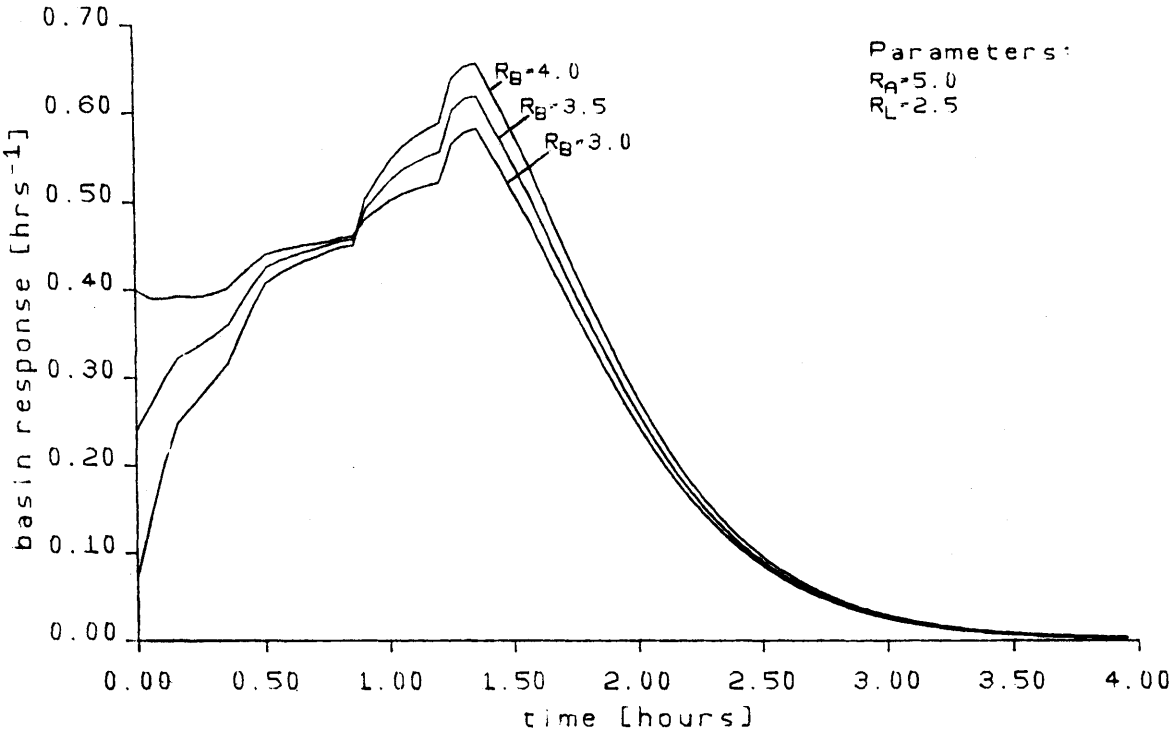

Figure 4.3: Basin IUHs for different bifurcation ratios, R_B.

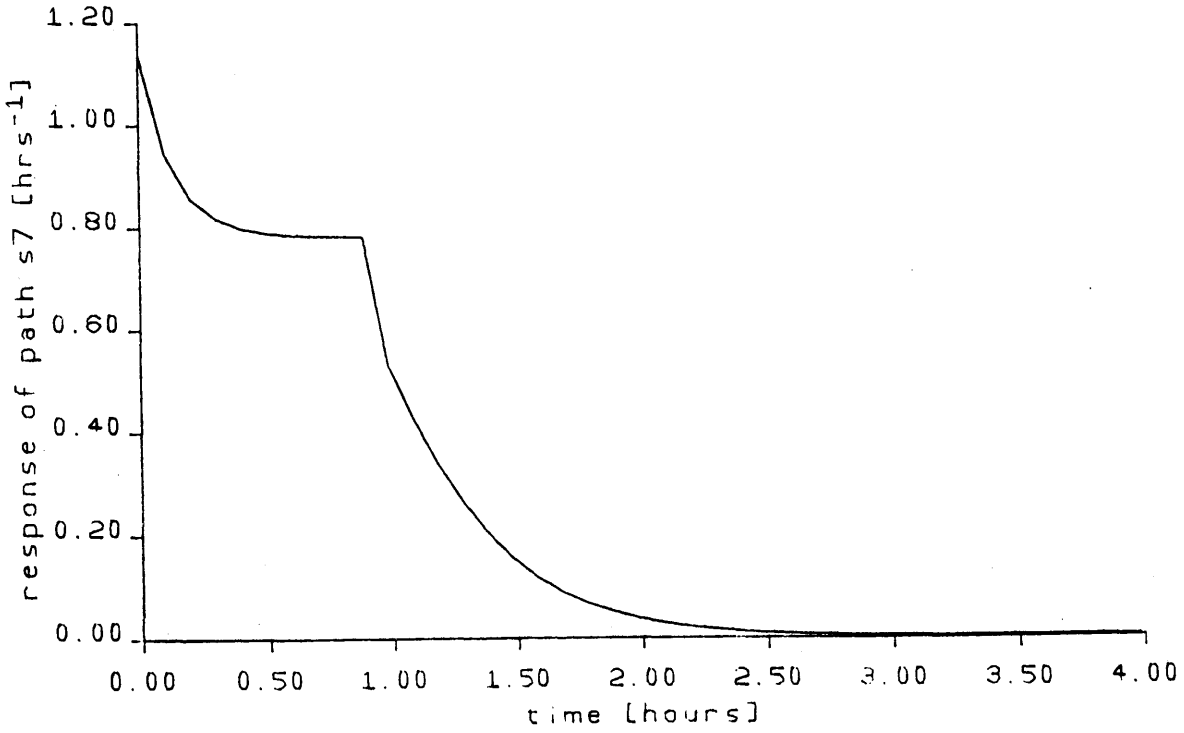

Figure 4.4: Response of path s_7.

Table 4.2: Characterisitics of the basin IUH for different geomorphological parameters.

Figure	R_A	R_B	R_L	$h_B(0)$ hr^{-1}	t_p hr	q_p hr^{-1}
	6.0	4.0	1.5	0.75	0.35	1.35
4.1	6.0	4.0	2.0	0.42	0.61	0.82
	6.0	4.0	2.5	0.27	1.31	0.58
	3.5	3.0	2.5	0.05	1.36	0.75
4.2	4.0	3.0	2.5	0.20	1.36	0.68
	5.0	3.0	2.5	0.40	1.36	0.58
	5.0	4.0	2.5	0.07	1.36	0.66
4.3	5.0	3.5	2.5	0.24	1.36	0.62
	5.0	3.0	2.5	0.40	1.36	0.58

3rd order basin there exists 8 possible paths that a drop can take. Each path response is a function of the individual channel responses, both upstream and lateral input responses, which compose the path. (See equations 4.1 and 4.6 for the list of possible paths and the general expression for the basin response.) The relative contribution of each path response is given by the probability of each particular path which change only with R_A and R_B; thus the change in the basin IUH's shape.

Figure 4.2 presents the basin IUH for different values of R_A. As R_A decreases the peak increases and the initial response decreases. A decrease in R_A implies that the area draining into lower order streams increases, thus there is less probability for a drop to drain directly to the highest order stream, which is the only stream contributing to the initial response, and so the initial response decreases. Physically, the increase in the peak can be attributed to the fact that more drops are entering the mainstream from the lower order streams, and thus the peak is greater as more drops coincidentally reach the outlet. The increase in peak can also be understood exploiting the property that all IUHs must have a volume of 1. If the initial response decreases, then one way of preserving an area of 1 is to increase the peak.

The basin's response to decreasing bifurcation ratios, R_B, is opposite to that for decreasing area ratios, R_A. The smaller R_B implies that the basin has few lower order steams in comparison to the higher order streams. Thus the initial response is greater for smaller R_B as

most drops drain directly to the highest order stream. The peak increases with R_B as there exists a greater number of contributing streams to the mainstream.

The behavior of the initial response due to different values of R_A and R_B is also depicted in the initial probabilities given in Table 4.1. As can be determined, the greater R_A or the smaller R_B, the greater $\theta_3(0)$ and correspondingly a greater initial response will result. The initial response is due to path s_7, which is plotted in Figure 4.4.

In some cases, path s_7 has a significant effect on the overall shape of the basin IUH. As can be observed in Figure 4.4, there is a higher initial response, and then the response rapidly decreases, remains relatively constant and then gradually decreases. The dominance of path s_7 is reflected in the less well defined peak for higher R_A or lower R_B. In some cases the probability of path s_7 is so high that the basin IUH decreases immediately after the initial response, as does path s_7. Several cases where this occurred are shown in Figures 4.5, 4.6 and 4.7. The corresponding parameters and path probabilities are presented in Table 4.3. This type of behavior would occur for basins which have most of the tributaries to the main channel in the upper regions of the basin. Thus initially the basin responds according to the highest order stream's response, leading to a sharp rise and fall. As the upper tributaries response reach the outlet, this basin IUH again increases.

The extent of the initial decrease is dependent on the length of the first order streams and R_L. Figure 4.5 corresponds to a case

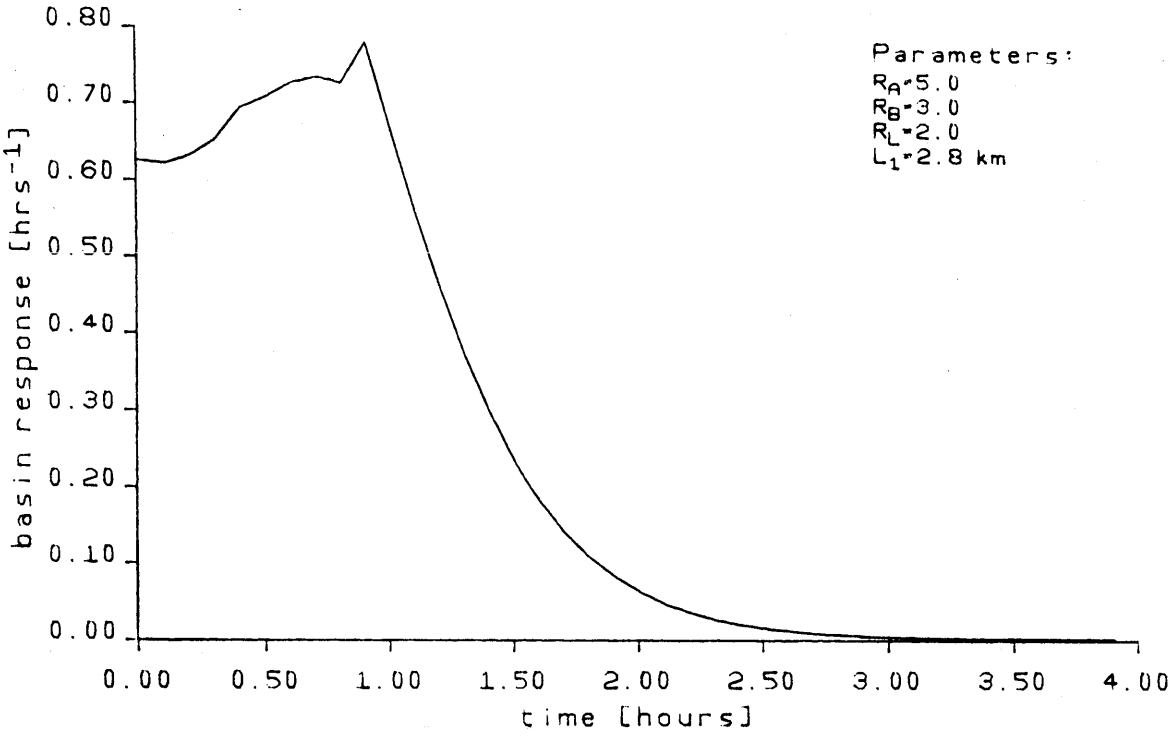

Figure 4.5: Case where the basin IUH initially decreases.

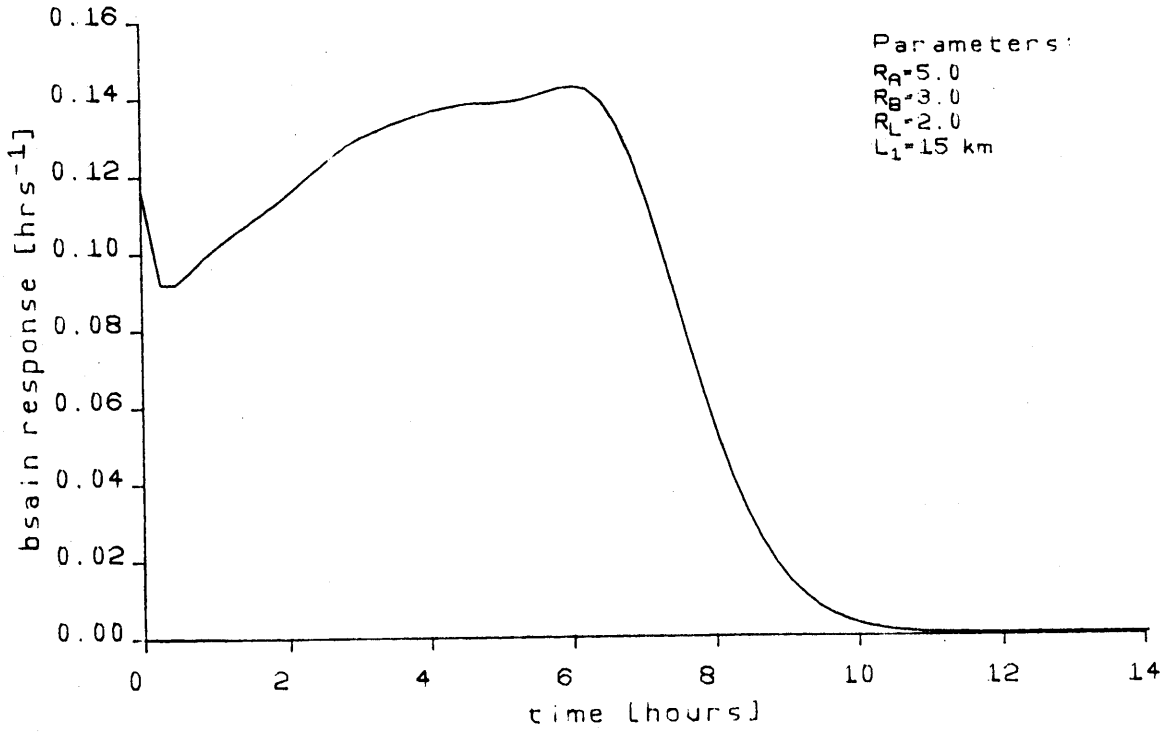

Figure 4.6: Case where the basin IUH initially decreases.

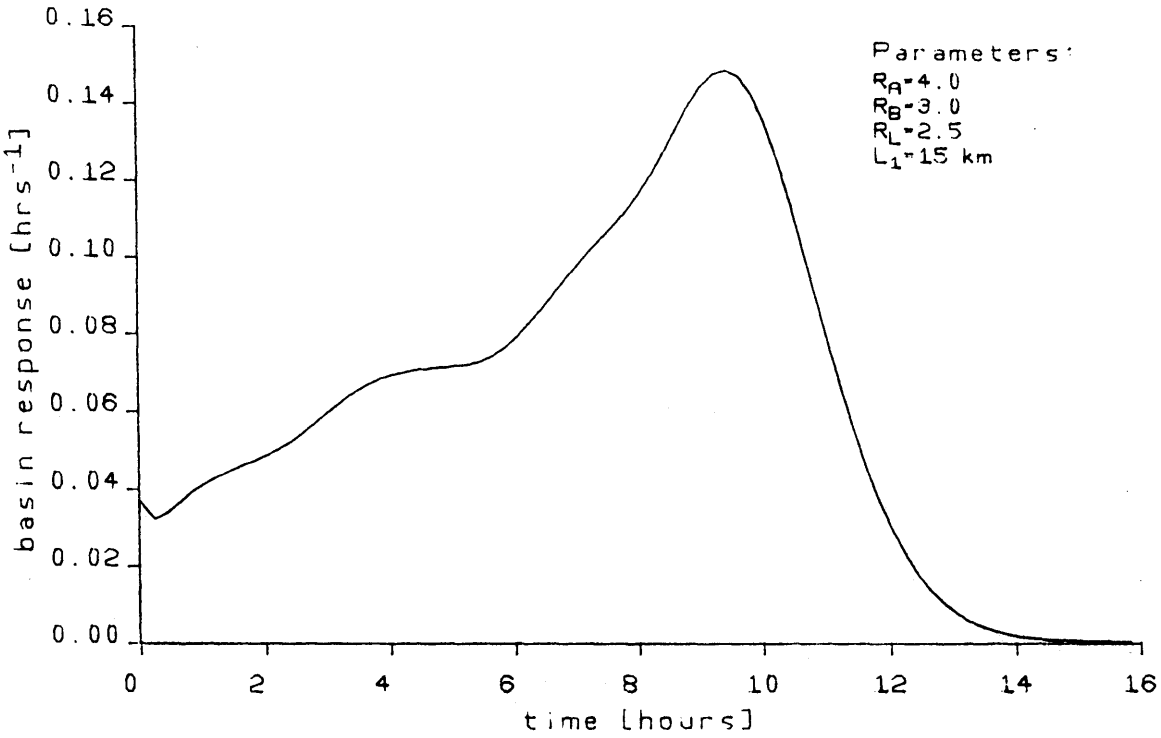

Figure 4.7: Case where the basin IUH initially decreases.

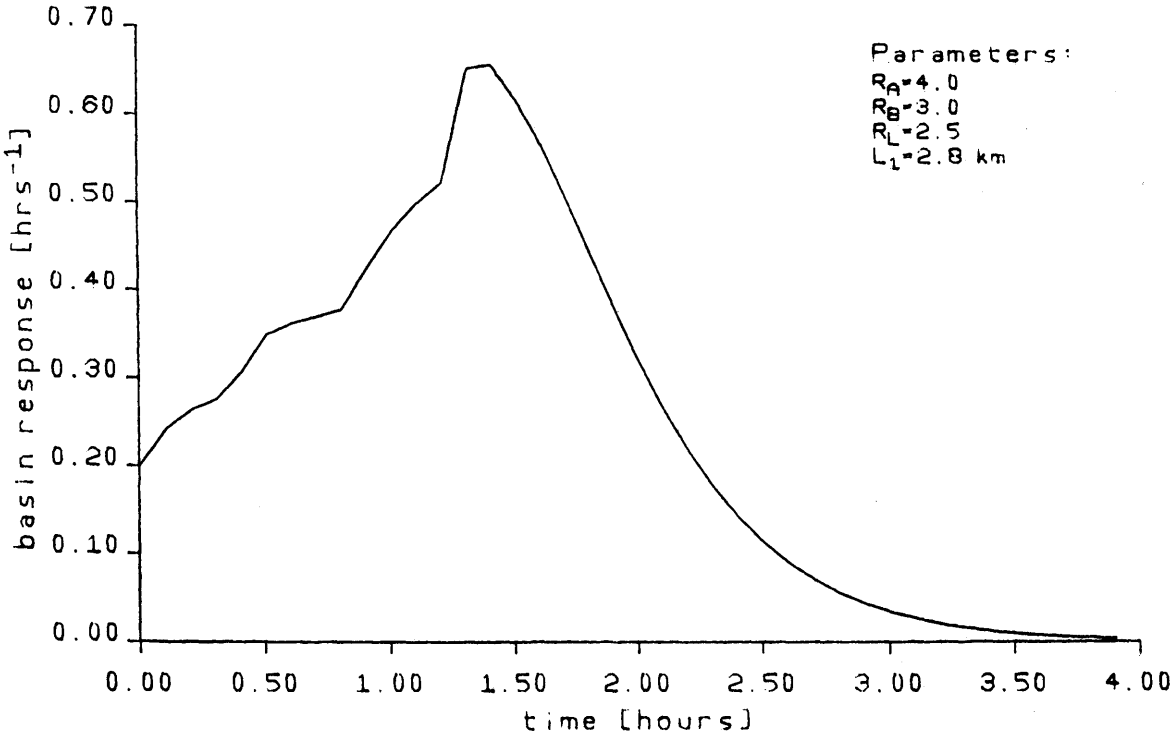

Figure 4.8: Basin IUH with no initial decrease in the response.

Table 4.3 Parameters Corresponding to Figures 4.5, 4.6, and 4.7:

Stream Characteristics:

	y_o	v_o	S_o	F	c_1	C
	m	m/sec	m/km		m/sec	$m^{1/2}$/sec
1st order streams	0.80	2.5	0.3	0.89	5.30	161
2nd order streams	0.85	2.5	0.3	0.87	5.39	156
3rd order streams	0.90	2.5	0.3	0.84	5.47	152

Difference between figures:

	Figure 4.5	Figure 4.6	Figure 4.7
$\bar{L}_1$(km)	2.8	15	15
Geomorphological Parameters R_A; R_B; R_L	5.0; 3.0; 2.0	5.0; 3.0; 2.0	4.0; 3.0; 2.5
Initial Probabilities: $\theta_1(0)$; $\theta_2(0)$; $\theta_3(0)$	0.36;0.29;0.35	Same as Figure 4.5	0.56;0.26;0.18
Transition Probabilities: $Pr_{1\,2}$ r ; $Pr_{1\,2}$ u	0.20; 0.67	Same as Figure 4.5	0.20; 0.67
$Pr_{1\,3}$ u ; $Pr_{2\,3}$ r	0.13; 0.33		0.13; 0.33
$Pr_{2\,3}$ u ; $Pu_{2\,3}$ r	0.67; 0.33		0.67; 0.33
$Pu_{2\,3}$ u	0.67		0.67
Path Probabilities: $p(s_1)$; $p(s_2)$	0.02; 0.08	Same as Figure 4.5	0.04; 0.12
$p(s_3)$; $p(s_4)$	0.05; 0.05		0.07; 0.07
$p(s_5)$; $p(s_6)$	0.10; 0.19		0.09; 0.18
$p(s_7)$; $p(s_8)$	0.35; 0.16		0.18; 0.25

where $\overline{L}_1$ = 2.8 km, and Figures 4.6 and 4.7 correspond to cases where $\overline{L}_1$ = 15 km. In each of these cases the IUH initially decreased. Figure 4.8 presents a case where $\overline{L}_1$ = 2.8 km, and the geomorphological and reference parameters are the same as those in Figure 4.7, yet there is no initial decrease in the response.

4.3.2 The Reference Velocity, v_o, Reference Depth, y_o, and Slope, S_o

For the following examples, the reference velocities and slopes for each order stream are assumed equal. These assumptions are obviously not true for all basins, especially in mountaineous regions, but they are used to reduce the number of parameters.

Figure 4.9 shows three possible responses of a basin with R_A = 4.0, R_B = 3.0, R_L = 3.5, and $\overline{L}_1$ = 2.78 km. Linearizing velocities are 3.0, 2.5, and 2.0 m/sec with Froude numbers being kept relatively constant (i.e., linearizing depths increase with velocity). As the reference velocity increases, the initial response and peak response increase. Table 4.4 presents the parameter used to calculate each response.

Figures 4.10 and 4.11 present several basin IUHs for different reference depths and slopes, respectively. The difference between the parameters is quite substantial, 1 meter for the reference depths, and a factor of 10 for the slopes. Comparing Figures 4.9, 4.10, and 4.11 and recognizing that representative slopes can be obtained from

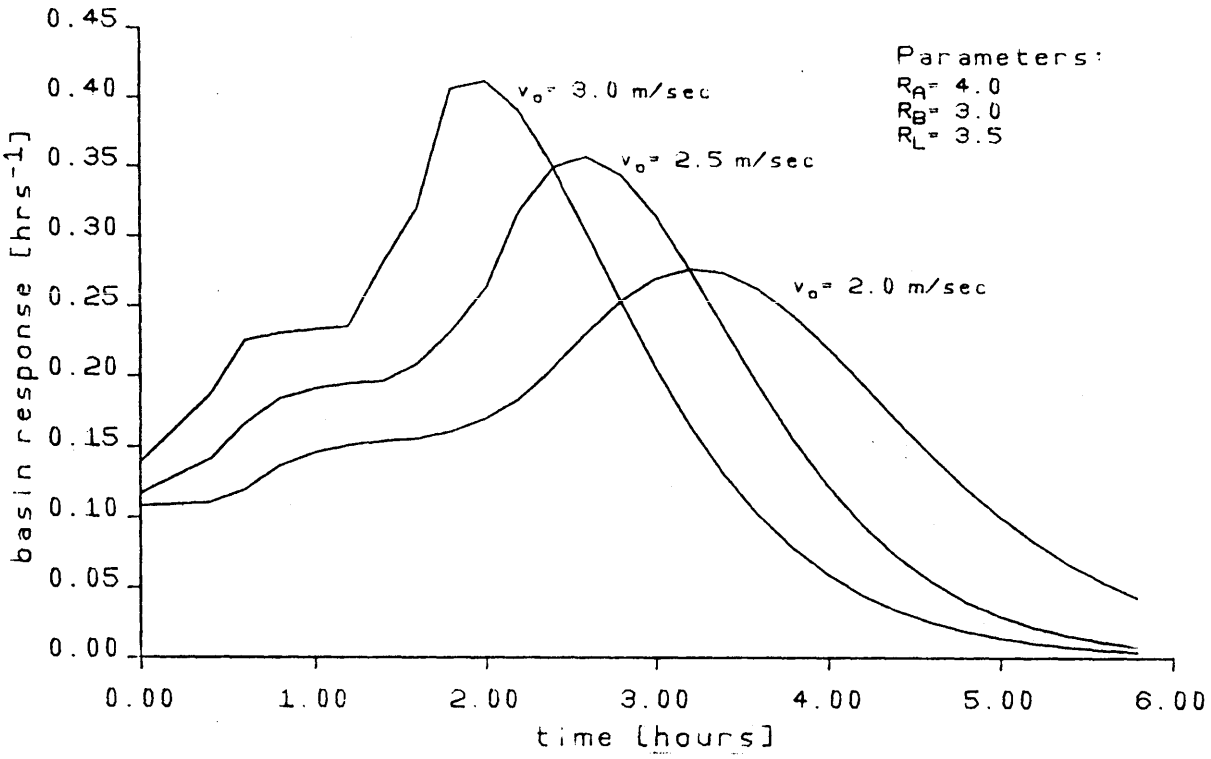

Figure 4.9: Basin IUHs for different reference velocities, v_o.

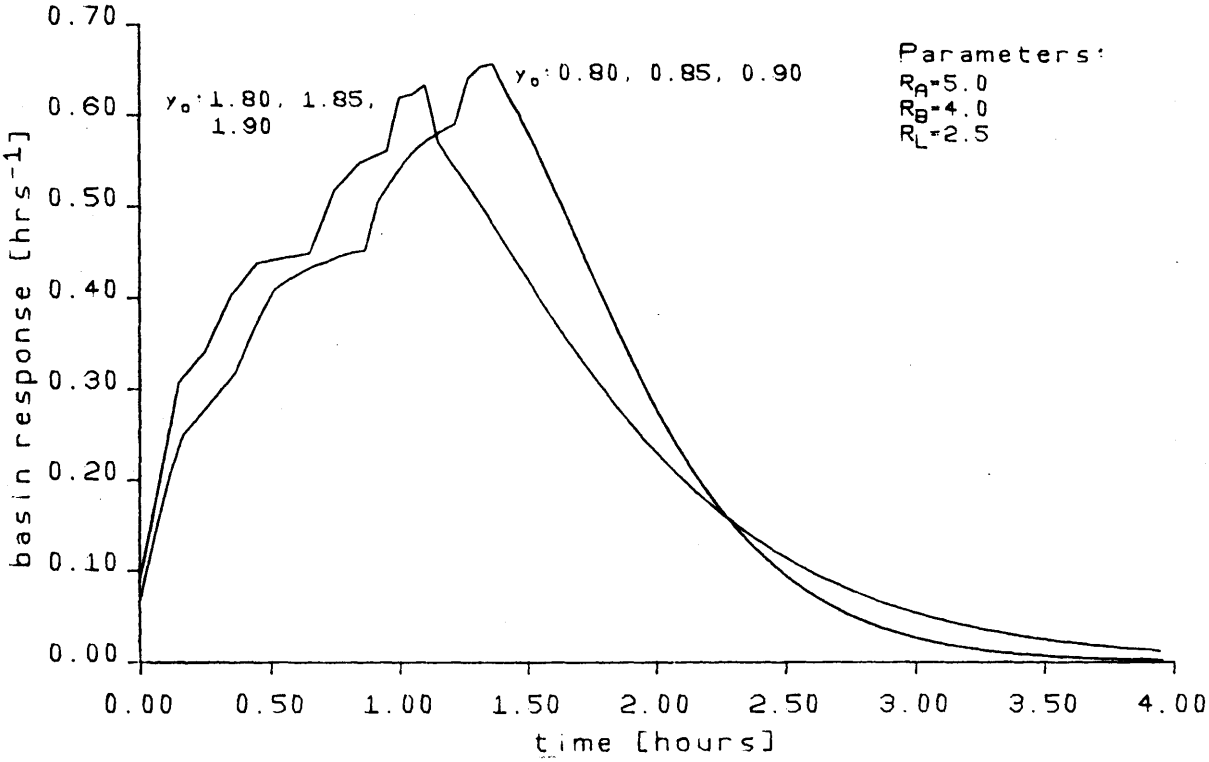

Figure 4.10: Basin IUHs for different reference depths.

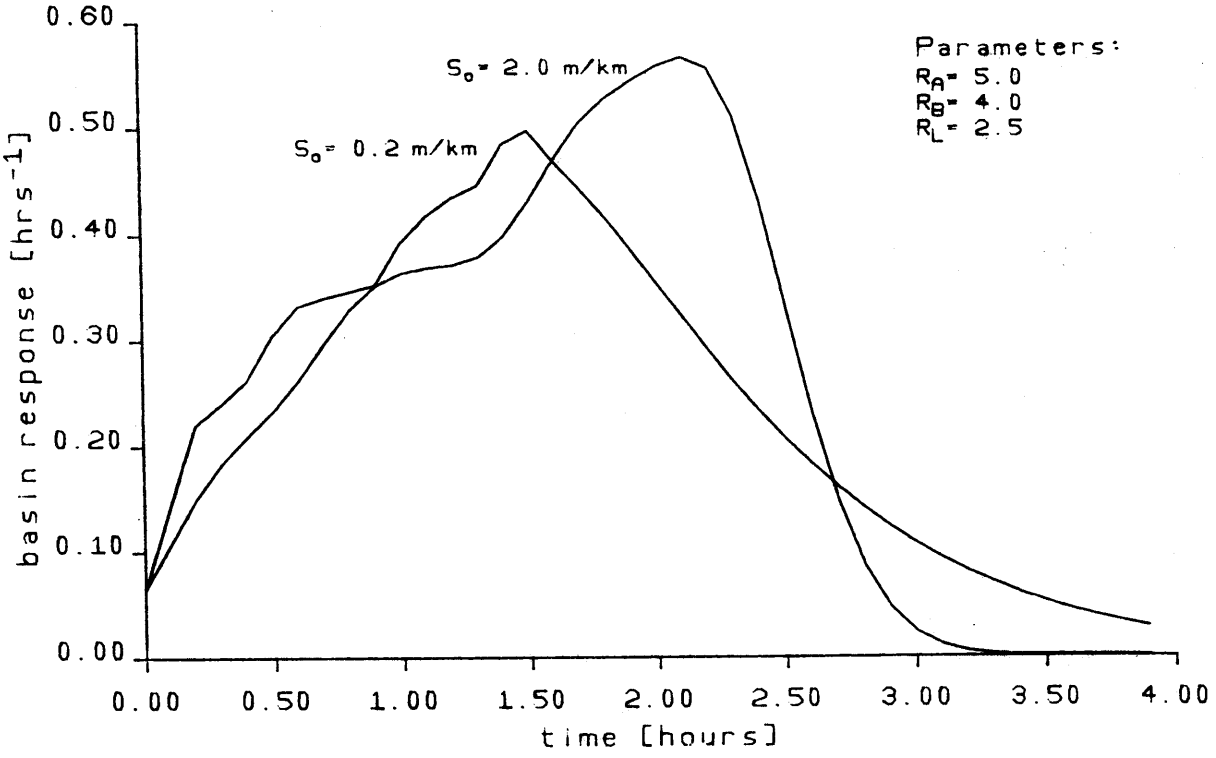

Figure 4.11: Basin IUHs for different channel slopes.

Table 4.4: Parameters for Figure 4.9

Case	y_o	v_o	S_o	$\bar{L}$	c_1	F	C
	m	m/sec	m/km	km	m/sec		$m^{1/2}/sec$
1st order streams	1.1	3.0	0.3	2.8	6.3	0.91	165
2nd order streams	1.6	3.0	0.3	9.7	7.0	0.76	136
3rd order streams	2.1	3.0	0.3	34.0	7.5	0.66	119
1st order streams	0.7	2.5	0.3	2.8	5.1	0.95	172
2nd order streams	1.0	2.5	0.3	9.7	5.6	0.80	144
3rd order streams	1.5	2.5	0.3	34.0	6.3	0.65	117
1st order streams	0.5	2.0	0.3	2.8	4.2	0.90	163
2nd order streams	1.0	2.0	0.3	9.7	5.1	0.90	115
3rd order streams	1.5	2.0	0.3	34.0	5.8	0.52	94

Geomorphlogical Parameters: $R_A=4.0$ $R_B=3.0$ $R_L=3.5$

Initial Probabilities: $\theta_1(0)=0.56$ $\theta_2(0)=0.26$ $\theta_3(0)=0.18$

Transition Probabilities:

$p_{r_1 r_2}=0.20$ $p_{r_1 u_2}=0.67$ $p_{r_1 r_3}=0.13$ $p_{r_2 r_3}=0.33$

$p_{r_2 u_3}=0.67$ $p_{u_2 r_3}=0.33$ $p_{u_2 u_3}=0.67$

Path Probabilities:

$p(s_1)=0.04$ $p(s_2)=0.12$ $p(s_3)=0.07$ $p(s_4)=0.08$

$p(s_5)=0.09$ $p(s_6)=0.17$ $p(s_7)=0.18$ $p(s_8)=0.25$

topographic maps, one can conclude that the basin IUH is most sensitive to the reference velocity. Thus the reference depths and slope can be approximated, but a procedure must be developed to determine the reference velocity.

4.4 Summary

The basin IUH is now fully defined in terms of the basin's geomorphological and channel's physiographic characteristics. The actual configuration of the streams which compose the basin is accounted for by the initial and transition probabilities which are dependent on the geomorphological parameters. The probabilities determine the relative contribution of each path, where the paths are indicative of tributaries joining a stream at its most upstream point or along the streams' length.

The input parameters required to determine the basin include R_A, R_B, R_L, and for each order stream, the average length, slope, reference velocity and depth. A sensitivity analysis showed that the basin IUH is most sensitive to the velocity.

The next chapter will present a means to estimate the velocity given the previously mentioned parameters and the properties of the storm.

Chapter 5

THE DISCHARGE HYDROGRAPH

5.1 Introduction

For a given drainage basin the discharge hydrograph due to a given period of rainfall reflects all the combined physical characteristics of the basin plus the surrounding hydrometerological effects. For the model presented in this work, the basin IUH reflects the effects of the basin's physiographic and geomorphologic characteristics on the runoff, and the the time distribution of the effective rainfall reflects the hydrometerological effects. These effects are combined through the convolution equation which determines the discharge.

As an example, consider a storm of constant intensity, i, for a duration, t_d, with a uniform spatial pattern over the catchment. Thus the time distribution of effective rainfall is given by:

$$I(t) = i\{u(t) - u(t-t_d)\} \tag{5.1}$$

where u(t) = 1 if $t \geq 0$ and 0 otherwise.

The discharge hydrograph is given by:

$$Q(t) = \int_0^t i(t-\tau)h_B(t)d\tau \tag{5.2}$$

which for the I(t) given in Equation 5.1, can be divided into two components:

$$O(t) = \int_0^t i h_B(\tau) d\tau \qquad t \leq t_d \qquad (5.3)$$

$$O(t) = \int_{t-t_d}^t i h_B(\tau) d\tau \qquad t > t_d \qquad (5.4)$$

In this work the effective rainfall will be assumed to be uniform in space and in time as implied by Equation 5.1.

This chapter presents the discharge hydrographs for several different basins. Prior to presenting the hydrographs, a way to calibrate the model and estimate the input parameters is suggested. The peak discharge, Q_p, and time to peak, T_p, are used to compare the discharge hydrograph with the results of a rainfall-runoff model. The hydrograph is also compared to the hydrograph determined using the assumption that the channels respond as linear reservoirs.

Based on the suggested method to estimate the input parameters, an analysis of a basin in Egypt is presented. The basin consists of wadis which are valleys that remain dry except during the rainy season. A description of the rainfall and basin characteristics will be presented.

5.2 Model Calibration

The parameters required to determine the hydrologic response or runoff from a basin can be divided into three classes: the parameters representing the physiographic characteristics of the basin and individual channels, the dynamic component of the response, and those representing the input characteristics. This section will discuss the issues relating to the estimation of these parameter sets.

The physiographic characteristics of the basin are expressed in terms of the geomorphological parameters, R_A, R_B, and R_L, defined by Horton's laws. The characteristics of the individual channels are lumped according to the order of the channel. The average channel length and slope for each stream order are used to represent the channel's physiographic characteristics. Note that when calculating the average channel slope, the geometric mean rather than the arithmetic mean, should be used. All these parameters are easily accessible from a topographic map, aerial photograph or satellite imagery.

The most difficult parameters to estimate are the reference depth and reference velocity used to linearize the continuity and momentum equations. Recalling the derivation of the upstream inflow IUH (see Chapter 3), the IUH represents the perturbation about these reference parameters ($q = vy$, thus $\delta q = \delta v \cdot \delta y$), which in an ideal situation are the steady state conditions. In fact, due to the nonlinearities in the rainfall-runoff process, there does not exist an individual, characteristic basin IUH which when convolved with any given input will produce a representative discharge hydrograph. The IUH is actually a function of <u>both</u> the input and geomorphology (see Rodriguez et al., 1981), and thus there exists no one set of steady state parameters, y_o and v_o, which can be used to represent a unique basin's IUH. Incorporation of the storm effects into the IUH is beyond the scope of this work and the procedure taken to estimate y_o and v_o is similar to the one used by Rodriguez et al., 1979.

In Rodriguez's et al., 1979, work they used the peak velocity of flow during an event to determine the parameter for the exponential distribution, which was assumed to be the channels' IUH. In this work there are two possible velocities which could be calibrated to the peak velocity, the reference velocity, v_o, or the dynamic velocity, c_1, where $c_1 = v_o + \sqrt{gy_o}$. As will be shown in the following section, equating the dynamic velocity for each order stream to be approximately equal to the peak velocity, produces a representative hydrograph for several different storms.

The following section presents the discharge hydrographs for several basins and various storms. The hydrographs are calibrated as described in this section where the peak stream velocity is that determined by a rainfall-runoff model for each particular storm.

5.3 Discharge Hydrographs for Several Subbasins

In this section several discharge hydrographs are presented, and the peak and time to peak are compared to that determined by a rainfall-runoff model. The results indicate that equating the dynamic wave speed to the peak velocity determined by the rainfall-runoff model produces peaks and times to peak similar to those determined by the rainfall-runoff model.

In their paper, "Discharge Response Analysis and Hydrologic Similarity: The Interrelation Between the Geomorphologic IUH and the Storm Characteristics," Rodriguez et al., 1979, present the peak discharge, Q_p^*, time to peak, T_p^*, and peak velocity, v_p^*, determined by a

rainfall-runoff model of basins in Puerto Rico for several storms. They used a rainfall-runoff model originally developed by Schaake (1971), where every stream segment is modeled as an individual segment. The model is based on the continuity equation and the kinematic wave approximation to the equations of motion. Throughout this section the results obtained from Rodriguez's et al. paper will be denoted by Q_p^*, T_p^*, and v_p^*, and are used to compare to the peak discharge, Q_p, and time to peak, T_p, determined by the discharge hydrograph where the dynamic wave speed, c_1, is set equal to v_p^*.

The basins to be investigated are subbasins of the Indio River basin located in Puerto Rico. Each subbasin is of order three, as presented in Figure 5.1. The Unibon and Morovis basins are characterized by the following parameter sets, respectively: $R_A = 5.6$, $R_B = 4.0$, $R_L = 2.8$, $\bar{L}_W = 8.6$ km, $\bar{A}_W = 23$ km^2, and $R_A = 5.0$, $R_B = 3.2$, $R_L = 2.7$, $\bar{L}_W = 8$ km, $\bar{A}_W = 13$ km^2. The slope of each channel segment was obtained from topographic maps, and the geometric mean slope for each stream order was determined and is presented in Tables 5.1 and 5.2, along with the other input parameters and corresponding Q_p^*, T_p^* and v_p^*.

The discharge hydrographs corresponding to storms of 3 and 2 hours durations with an intensity of 3 cm/hr are presented in Figures 5.2.1 through 5.5.1. The corresponding geomorphologic IUH used to determine each hydrograph are presented in Figures 5.2.2 through 5.5.2. As can be observed, the results are excellent and thus equating the dynamic wave speed c_1 to the peak velocity provides a hydrograph whose T_p and Q_p are representative for these particular storms. However, there does exist

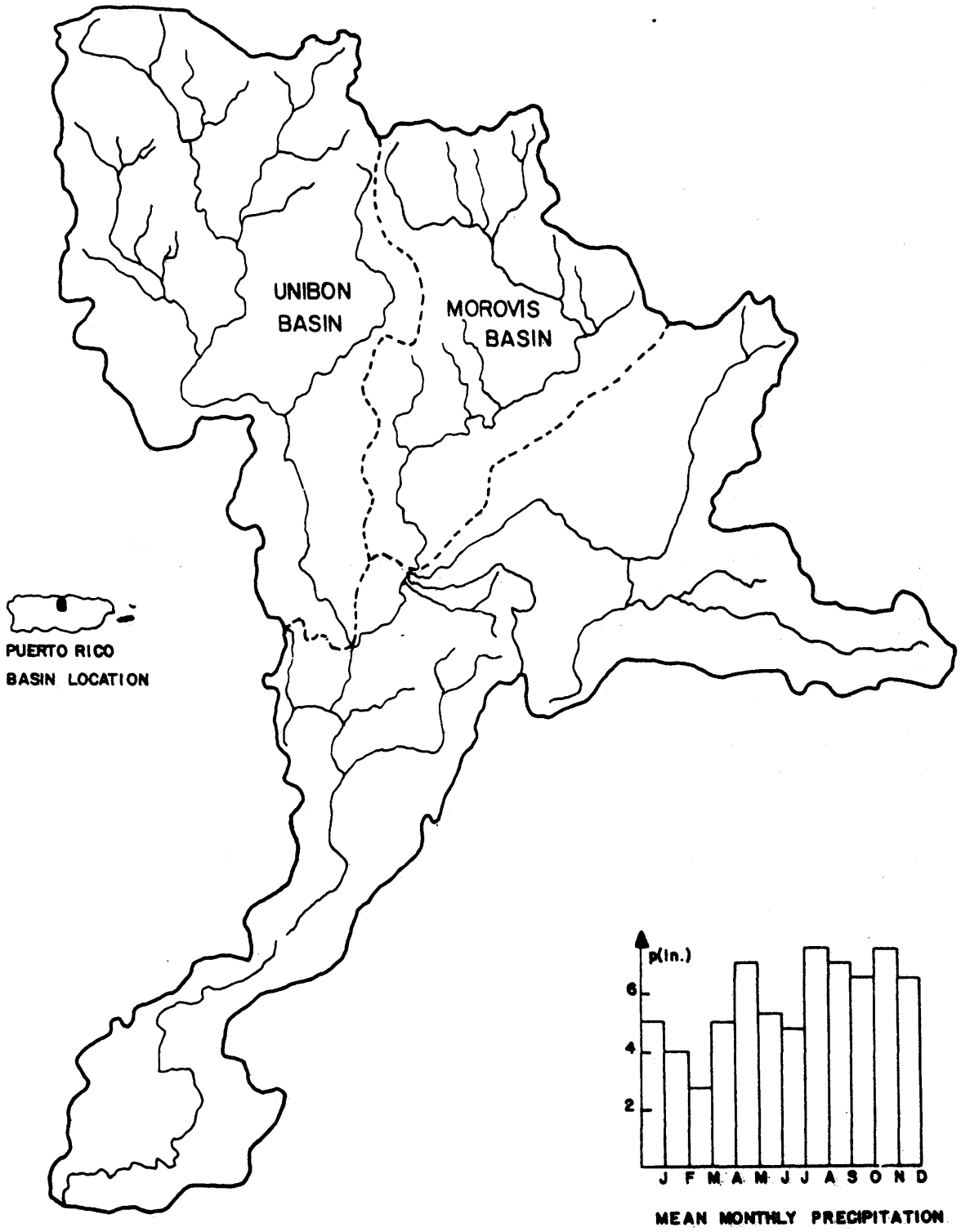

Figure 5.1: Indio basin (Puerto Rico) with the Morovis and the Unibon subbasins (from Valdes et al., 1979).

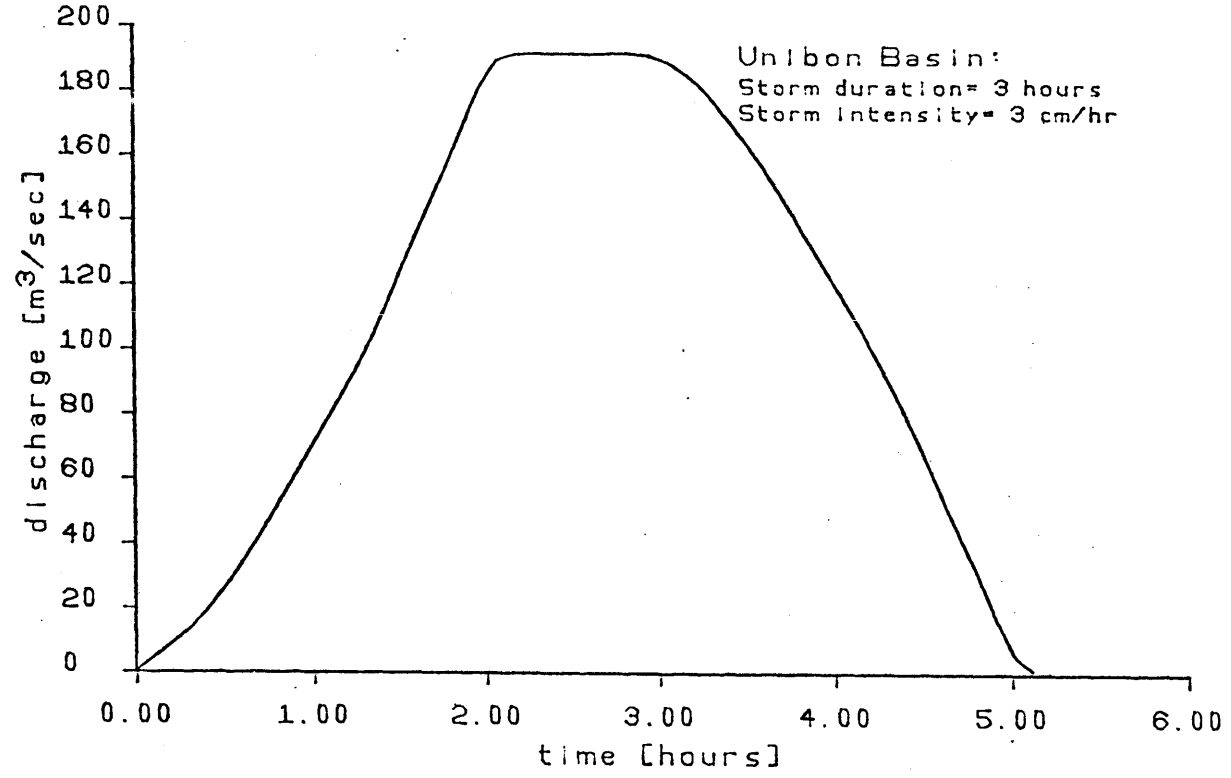

Figure 5.2.1: Discharge hydrograph for Unibon basin.

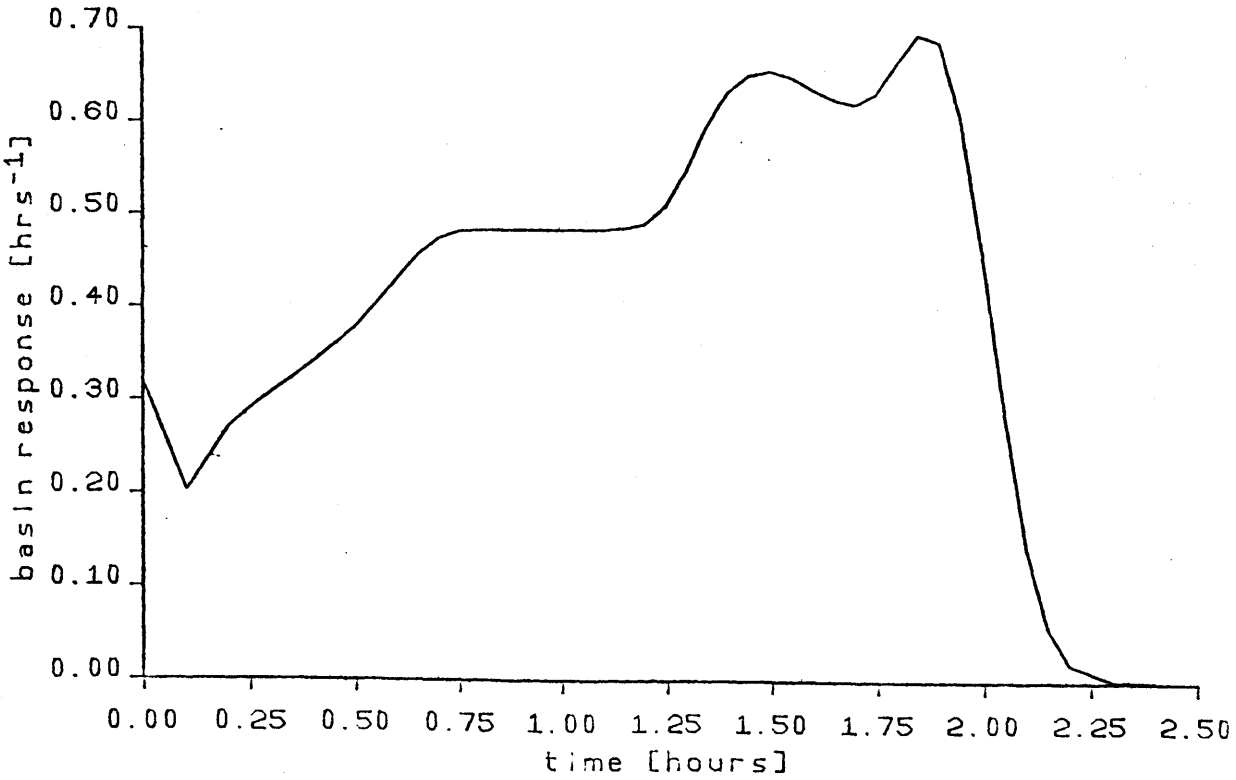

Figure 5.2.2: Geomorphologic IUH used to determine hydrograph in Figure 5.2.1.

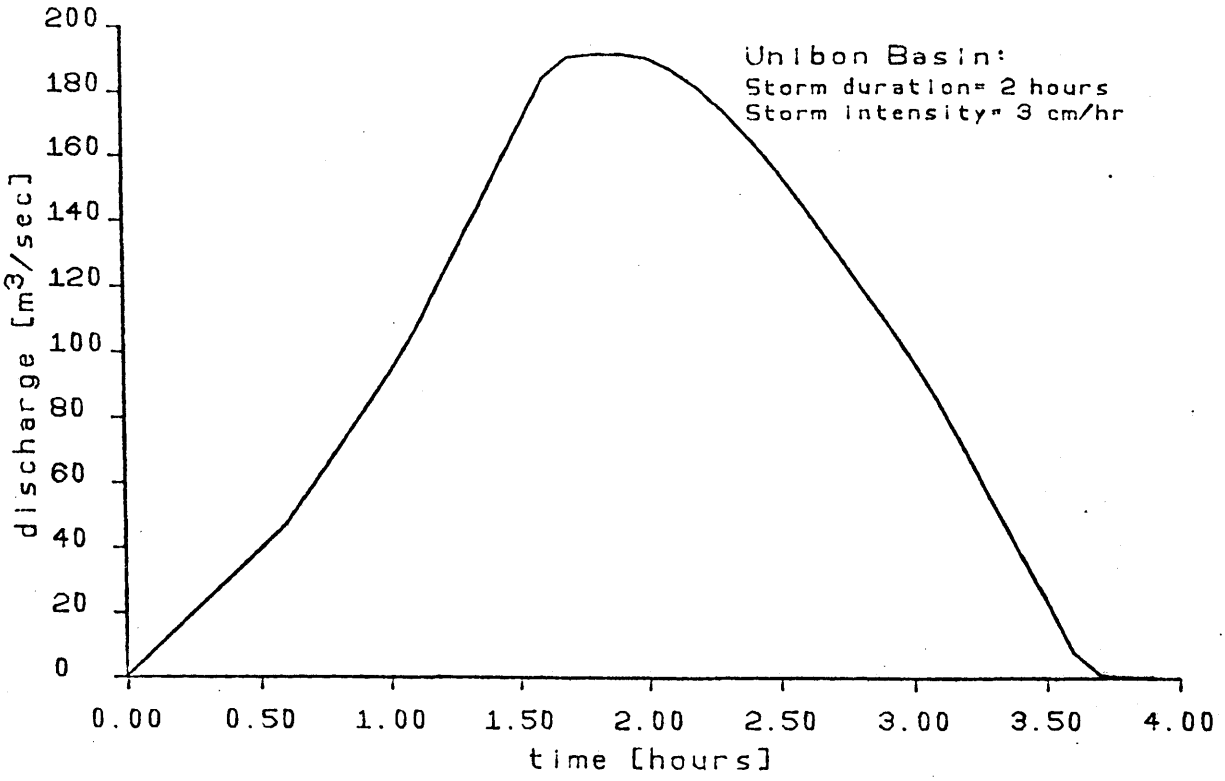

Figure 5.3.1: Discharge hydrograph for Unibon basin.

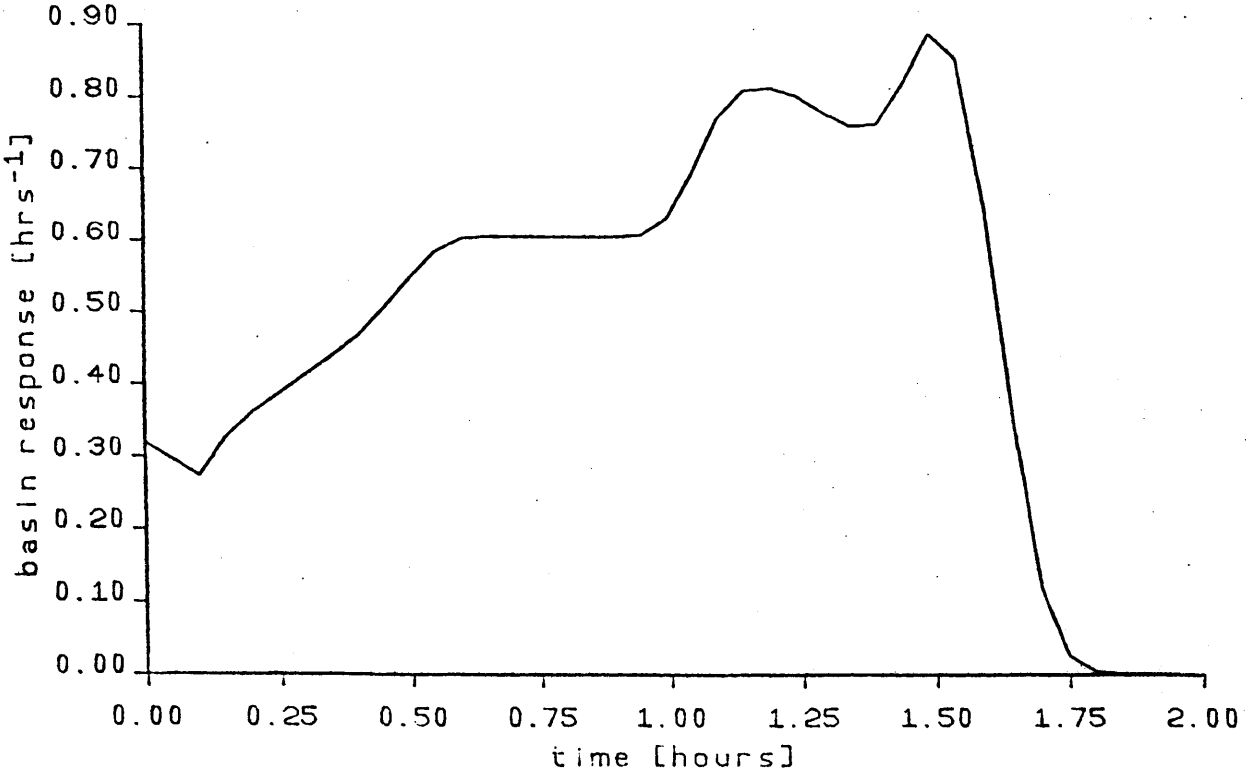

Figure 5.3.2: Geomorphologic IUH used to determine hydrograph in Figure 5.3.1.

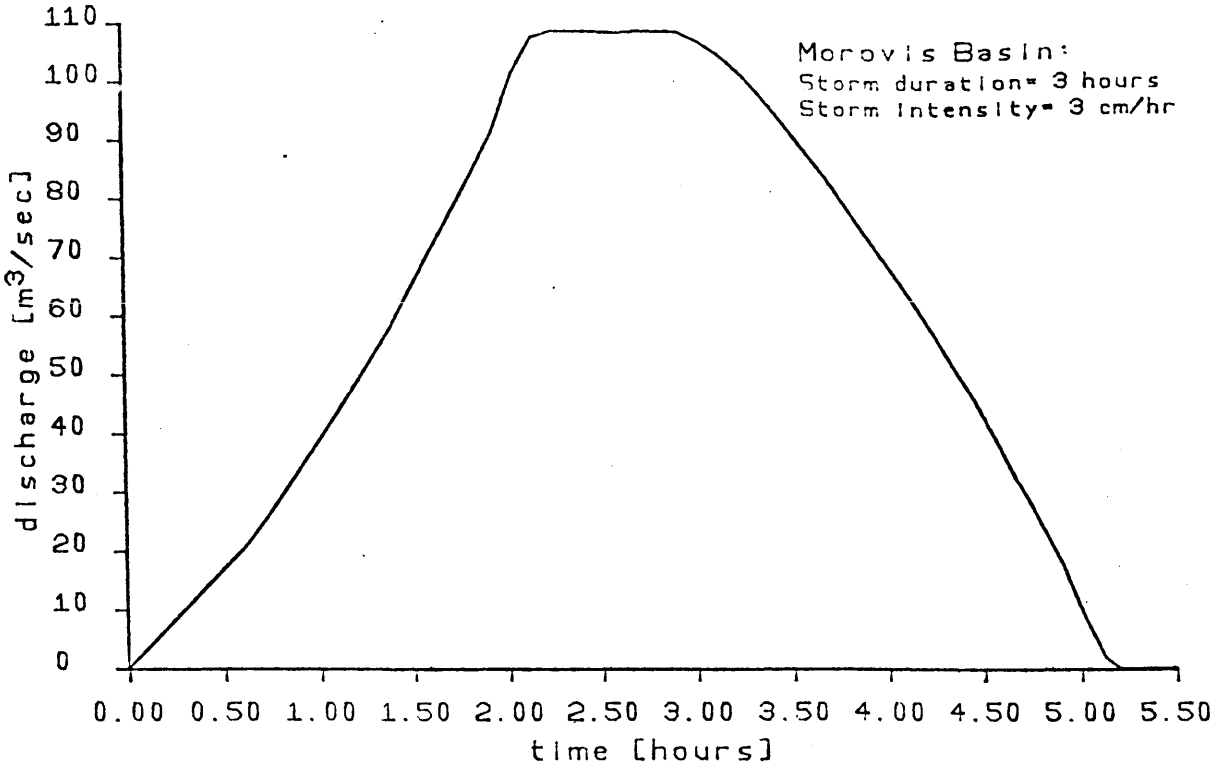

Figure 5.4.1: Discharge hydrograph for Morovis basin.

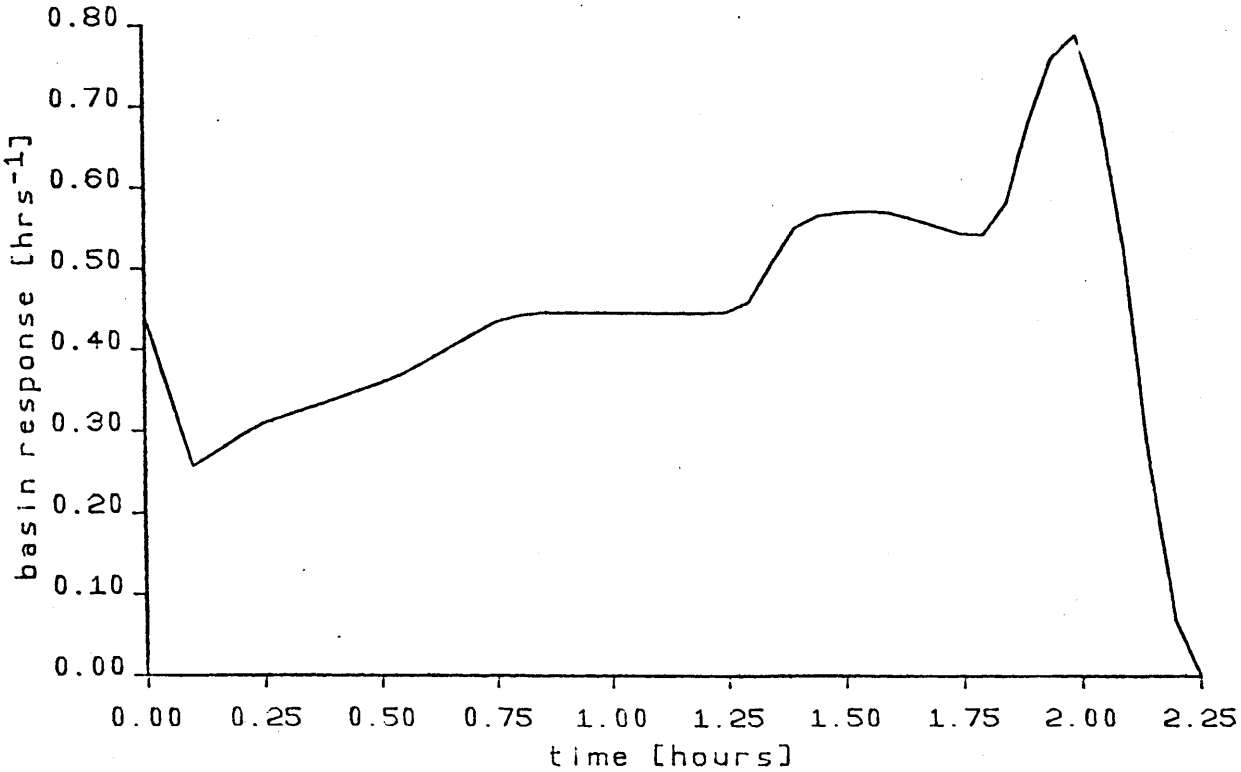

Figure 5.4.2: Geomorphologic IUH used to determine hydrograph in Figure 5.4.1.

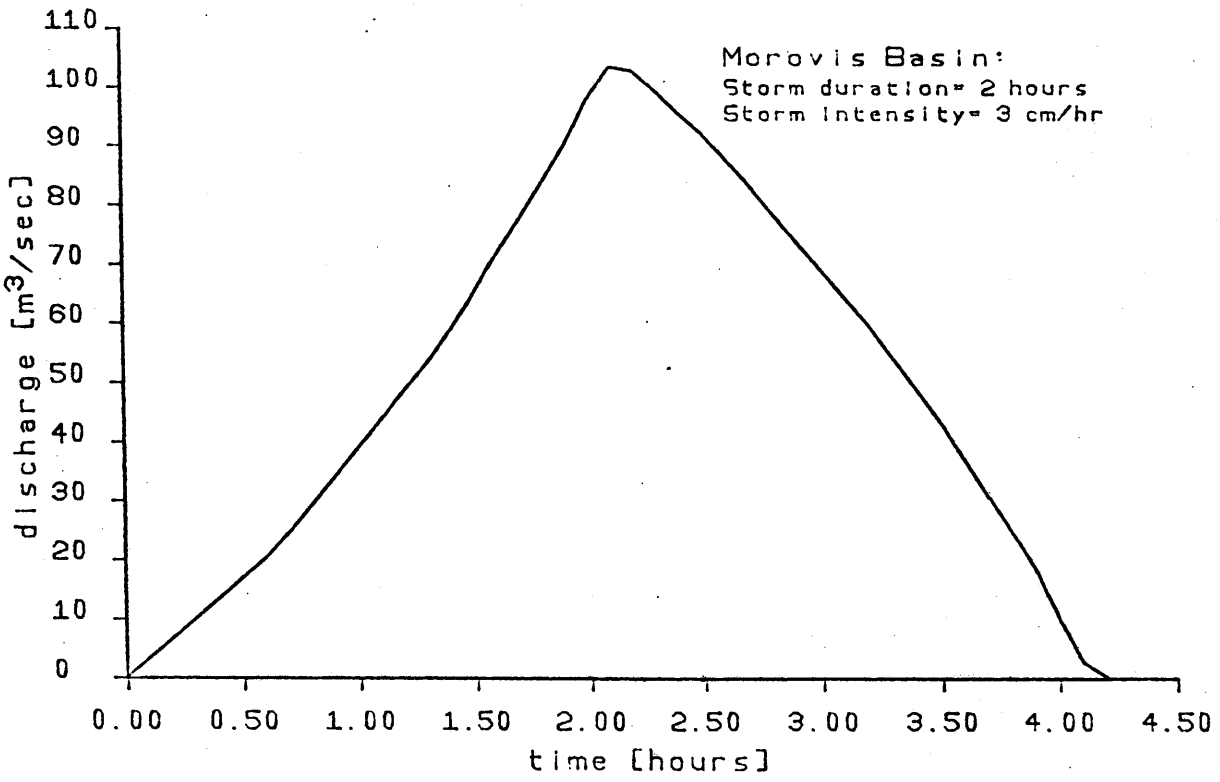

Figure 5.5.1: Discharge hydrograph for Morovis basin.

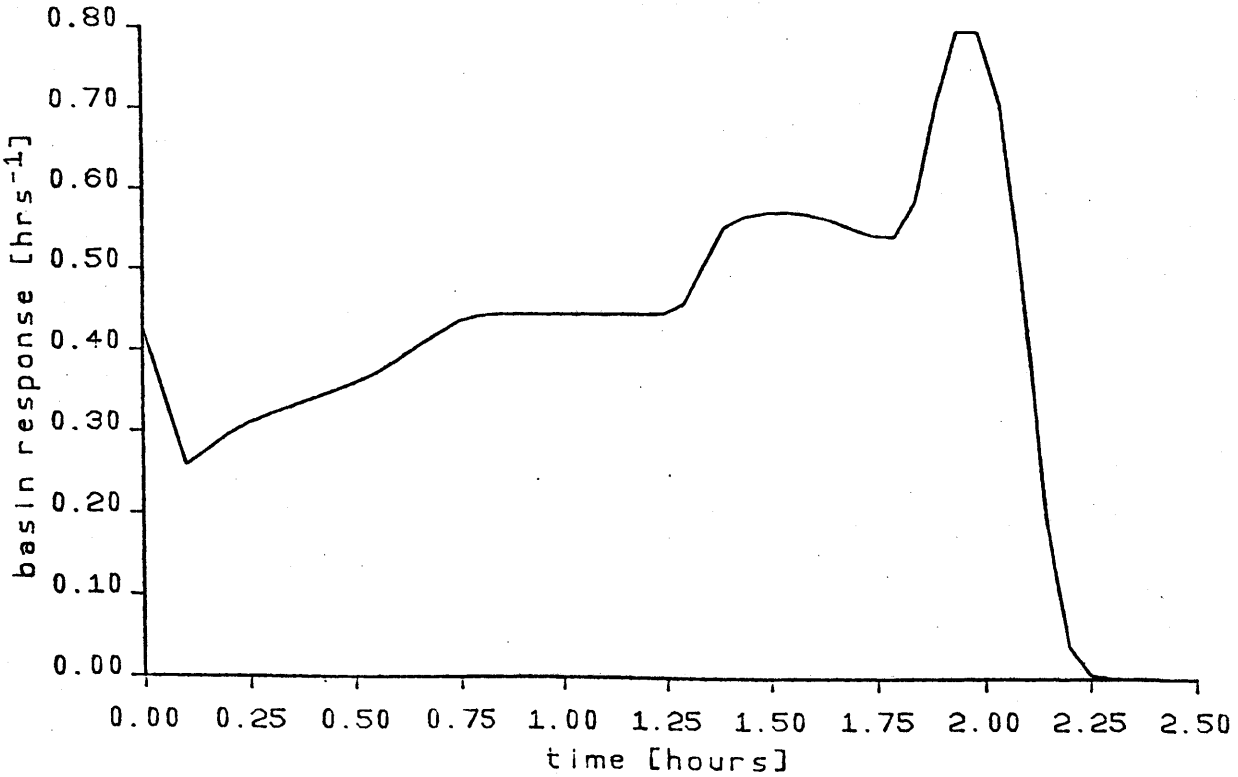

Figure 5.5.2: Geomorphologic IUH used to determine hydrograph in Figure 5.5.1.

Table 5.1: Parameters used to determine the discharge hydrographs for Unibon basin.

Storm Properties: duration = 3 hours; intensity = 3 cm/hr

Rainfall-runoff Results: $v_p^* = 4.1$ m/sec; $Q_p^* = 194$ m^3/sec; $T_p^* = 3$ hours.

Stream Characteristics:

	v_o (m/sec)	y_o (m)	S_o (m/km)	L (km)	c_1 (m/sec)	F
1st order stream:	0.80	1.00	82.7	1.1	3.8	0.36
2nd order stream:	0.90	1.13	46.6	3.1	4.1	0.38
3rd order stream:	1.00	1.20	23.3	8.6	4.3	0.38

Storm Properties: duration = 2 hours; intensity = 3 cm/hr

Rainfall-runoff results: $v_p^* = 4.0$ m/sec; $Q_p^* = 188$ m^3/sec; $T_p^* = 2$ hours

Stream Characteristics:

	y_o (m)	v_o (m/sec)	S_o (m/km)	L (km)	c_1 (m/sec)	F
1st order stream:	0.50	1.25	82.7	1.1	3.5	0.56
2nd order stream:	0.70	1.38	46.6	3.1	4.0	0.53
3rd order stream:	0.80	1.50	23.3	8.6	4.3	0.54

Geomorphologic Characteristics: $R_A = 5.6$; $R_B = 4.0$; $R_L = 2.8$

Initial Probabilities: $\theta_1(0) = 0.51$; $\theta_2(0) = 0.31$; $\theta_3(0) = 0.18$

Transition Probabilities:

$p_{r_1 r_2} = 0.286$ $p_{r_1 u_2} = 0.500$ $p_{r_1 r_3} = 0.214$ $p_{r_2 r_3} = 0.500$

$p_{r_2 u_3} = 0.500$ $p_{u_2 r_3} = 0.500$ $p_{u_2 u_3} = 0.500$

Path Probabilities:

$p(s_1) = 0.073$ $p(s_2) = 0.128$ $p(s_3) = 0.073$ $p(s_4) = 0.109$

$p(s_5) = 0.157$ $p(s_6) = 0.157$ $p(s_7) = 0.176$ $p(s_8) = 0.128$

Table 5.2: Parameters used to determine the discharge hydrographs for Morovis basin

Storm Properties: duration = 3 hours; intensity = 3 cm/hr

Rainfall-runoff Results: $v_p^* = 3.0$ m/sec; $Q_p^* = 112$ m^3/sec; $T_p^* = 3$ hours

Stream Characteristics:

	y_o (m)	v_o (m/sec)	S_o (m/km)	L (km)	c_1 (m/sec)	F
1st order stream:	0.34	0.85	71.9	1.1	2.7	0.47
2nd order stream:	0.41	1.00	32.1	3.0	3.0	0.50
3rd order stream:	0.48	1.10	39.2	8.0	3.3	0.51

Storm Properties: duration = 2 hours; intensity = 3 cm/hr

Rainfall-runoff Results: $v_p^* = 2.9$ m/sec; $Q_p^* = 103$ m^3/sec; $T_p^* = 2.2$ hours

Stream Characteristics:

	y_o (m)	v_o (m/sec)	S_o (m/km)	L (km)	c_1 (m/sec)	F
1st order stream:	0.34	0.90	71.9	1.1	2.7	0.49
2nd order stream:	0.37	1.00	32.1	3.0	2.9	0.52
3rd order stream:	0.44	1.10	39.2	8.0	3.2	0.53

Geomorphologic Characteristics: $R_A = 5.0$; $R_B = 3.2$; $R_L = 2.7$

Initial Probabilities: $\theta_1(0) = 0.41$; $\theta_2(0) = 0.29$; $\theta_3(0) = 0.30$

Transition Probabilities:

$p_{r_1 r_2} = 0.222$ $p_{r_1 u_2} = 0.625$ $p_{r_1 r_3} = 0.153$ $p_{r_2 r_3} = 0.375$

$p_{r_2 u_3} = 0.625$ $p_{u_2 r_3} = 0.375$ $p_{u_2 u_3} = 0.625$

Path Probabilities:

$p(s_1) = 0.034$ $p(s_2) = 0.096$ $p(s_3) = 0.057$ $p(s_4) = 0.063$

$p(s_5) = 0.110$ $p(s_6) = 0.183$ $p(s_7) = 0.297$ $p(s_8) = 0.160$

many combinations of y_o and v_o such that c_1 is equivalent to v_p^*, and for all the hydrographs, both v_o and y_o were varied until the peak and time to peak given by the rainfall-runoff model were obtained. Obviously, another parameter is needed to define the shape of the hydrograph and corresponding IUH.

The Froude number is an indicator of the type of flow in free-surface flow, and if used properly within this model could provide additional information concerning the flow situation for different storms. A detailed study of the incorporation of the Froude number into the model calibration is beyond the scope of this work; but given a Froude number, F, and dynamic wave speed, c_1, there would exist only one combination of y_o and v_o satisfying F and c_1 and the IUH would be completely defined in terms of three parameters. For the cases investigated in this work, the Froude number was restricted to be less than 1.

Although the results of this section are encouraging, the mathematics involved in the solution procedure are rather complex and may limit the use of the model in practice. A common assumption by many hydrologists is that the response of each channel is given by the exponential distribution. Mathematically the exponential distribution is easier to work with than the channel IUHs derived in this study, and the following section compares the discharge hydrographs determined by the two different types of channel IUHs.

5.4 Comparison of the Discharge Hydrographs Determined Using Different Channel IUHs

A common practice in hydrology is to assume that the channel's response is given by the exponential distribution, and in this section the discharge hydrographs determined using the response functions derived in this work, namely $u_{a_i}(t)$ and $r_{a_i}(t)$, given by Equations 3.20 and 3.22, and that determined using the exponential response function, Equation 2.17, will be compared.

The assumption that the channels' IUH is given by the exponential response functions limits the number of paths that a drop can take to reach the basin outlet as this type of channel IUH does not differentiate between the response for a drop entering at the stream's most upstream point and for a drop entering anywhere along the channel. The possible paths for a drop whose response is assumed to be an exponential distribution are given below as presented in Chapter 2:

path s_1: $\theta_1 \rightarrow 1 \rightarrow 2 \rightarrow 3 \rightarrow 4$

path s_2: $\theta_2 \rightarrow 1 \rightarrow 3 \rightarrow 4$

path s_3: $\theta_3 \rightarrow 2 \rightarrow 3 \rightarrow 4$

path s_4: $\theta_4 \rightarrow 3 \rightarrow 4$

where $i \rightarrow j$ represents a transition from a stream of order i to a stream of order j. Initial and transition probabilities are as given in Table 2.1.

Both the basin IUHs used in this section to determine the discharge hydrograph are based on the theory of the geomorphologic IUH as presented in Chapter 2. The difference between the IUHs is in number of possible paths that a drop can take to reach the channel outlet and in the response

of the individual channels which are indicative of the drop's travel time in a particular stream.

The basins to be used for the comparison are the ones presented in the previous section, and thus only the discharge hydrographs using the exponential assumption will be presented in this section. The dynamic component, i.e., the velocity parameter, required for the exponential distribution is determined as suggested by Rodriguez et al., where the velocity is equated to the peak stream velocity associated with a particular storm.

The discharge hydrographs for different storms and corresponding basin IUHs for Unibon and Morovis basins are presented in Figures 5.6.1 to 5.7.2 and 5.8.1 to 5.9.2, respectively. The peaks and times to peak approximate those determined by the rainfall-runoff model, Q_p^* and T_p^*, presented in Tables 5.1 and 5.2. Comparing these discharge hydrographs with those presented in the previous section, the peaks and times to peak are approximately equal, but the majority of the hydrograph volume is positioned differently. As can be concluded by comparing the two different types of basin IUHs, the assumption of the exponential channel response implies a much faster response than that determined by solving the momentum and continuity equations. Thus although the peaks are almost equal for each basin and for each storm, in the case where the exponential asusmption is used, more of the total volume is discharged prior to the peak, whereas for the cases where the response is that derived in this work, more volume is discharged after the peak.

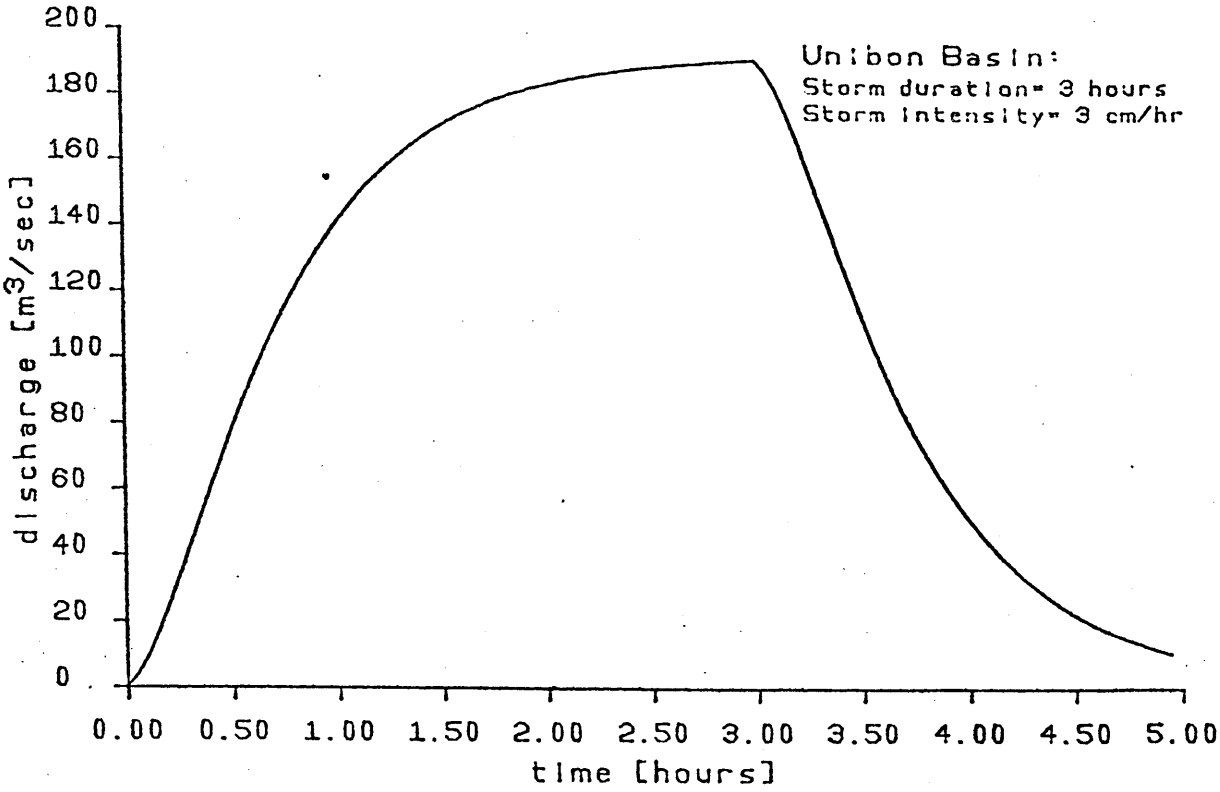

Figure 5.6.1: Discharge hydrograph for Unibon basin using exponential assumption.

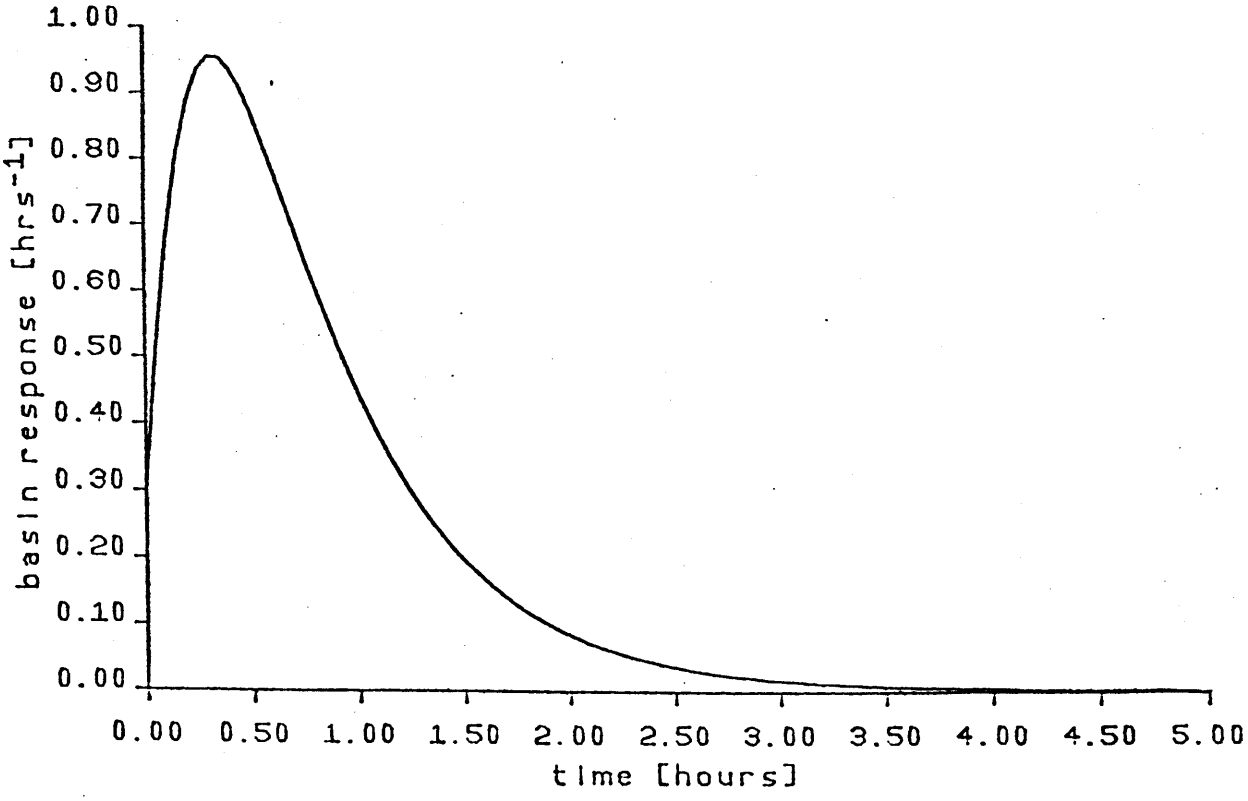

Figure 5.6.2: Geomorphologic IUH used to determine hydrograph in Figure 5.6.1.

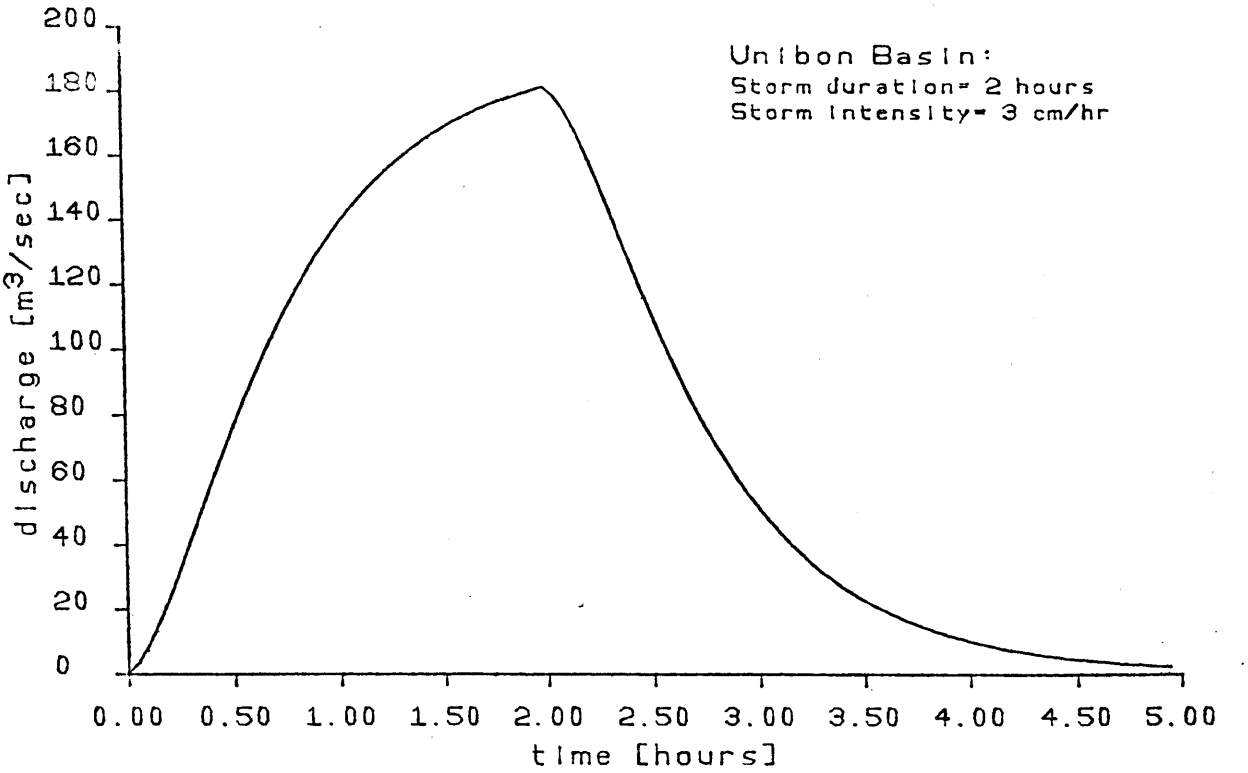

Figure 5.7.1: Discharge hydrograph for Unibon basin using exponential assumption.

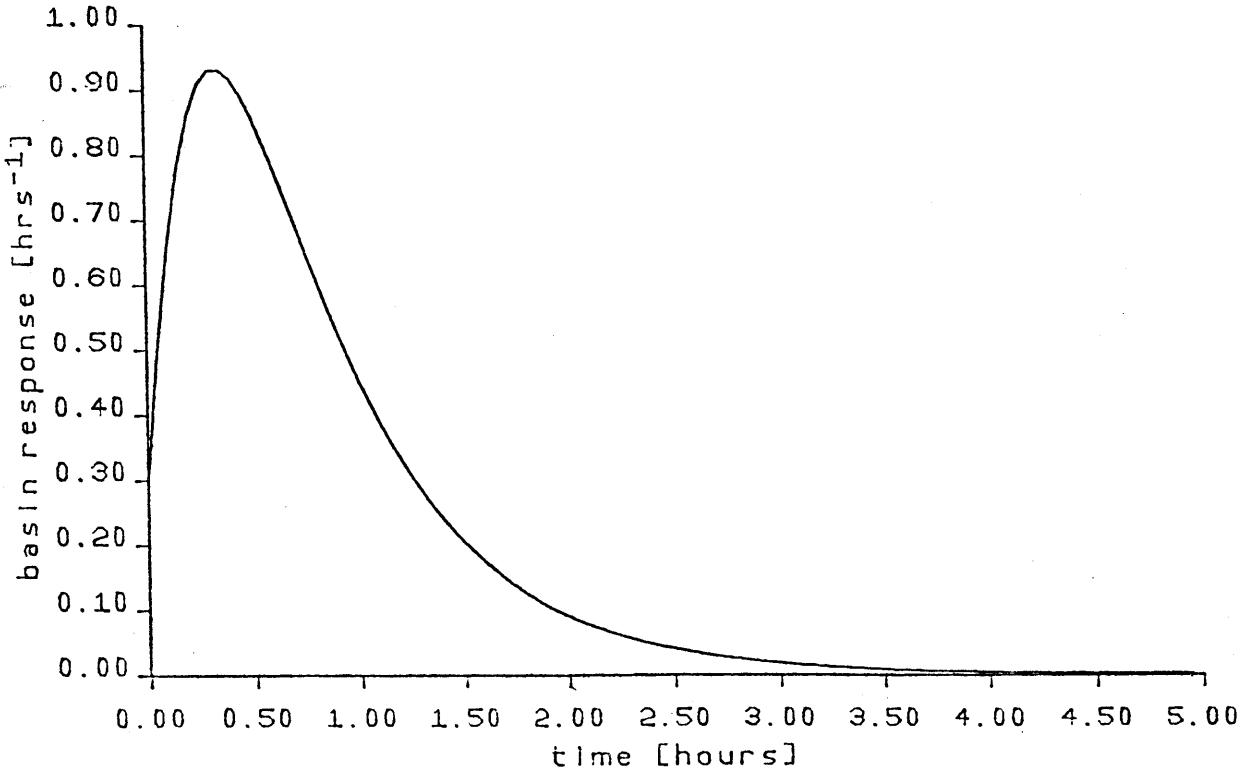

Figure 5.7.2: Geomorphologic IUH used to determine hydrograph in Figure 5.7.1.

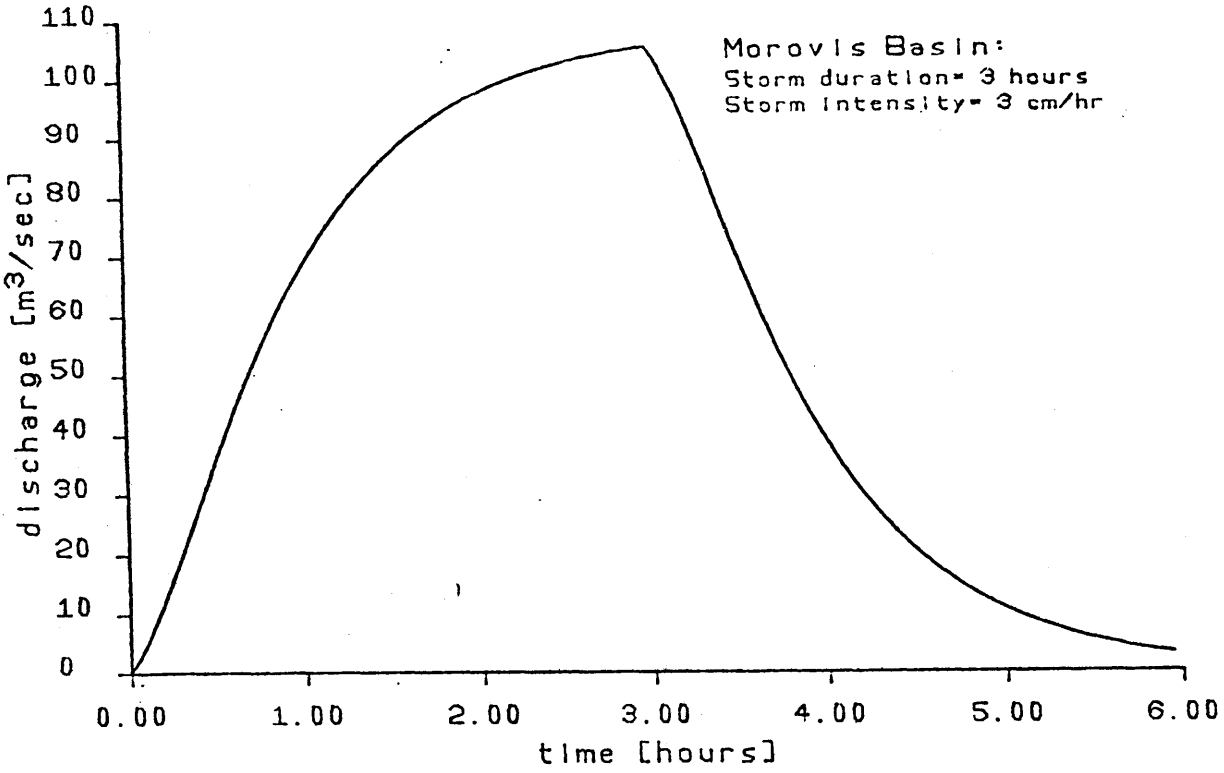

Figure 5.8.1: Discharge hydrograph in Morovis basin using exponential assumption.

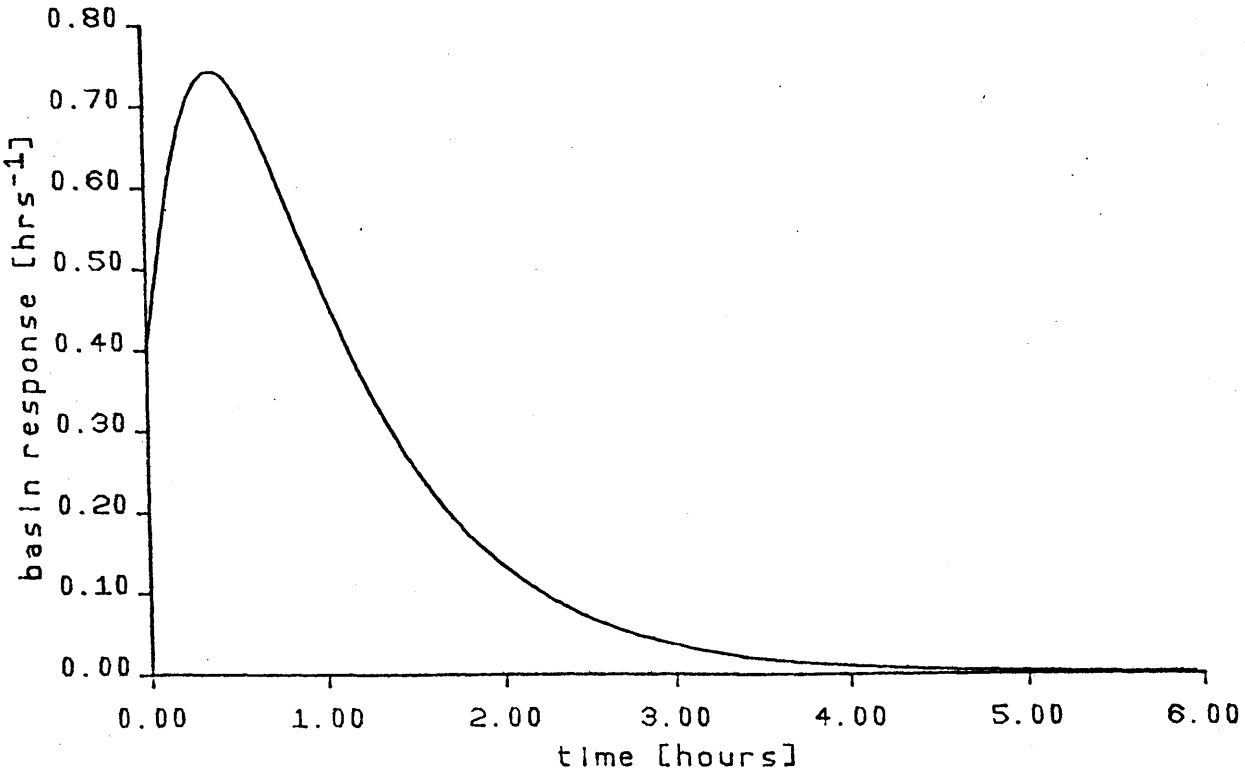

Figure 5.8.2: Geomorphologic IUH used to determine hydrograph in Figure 5.8.1.

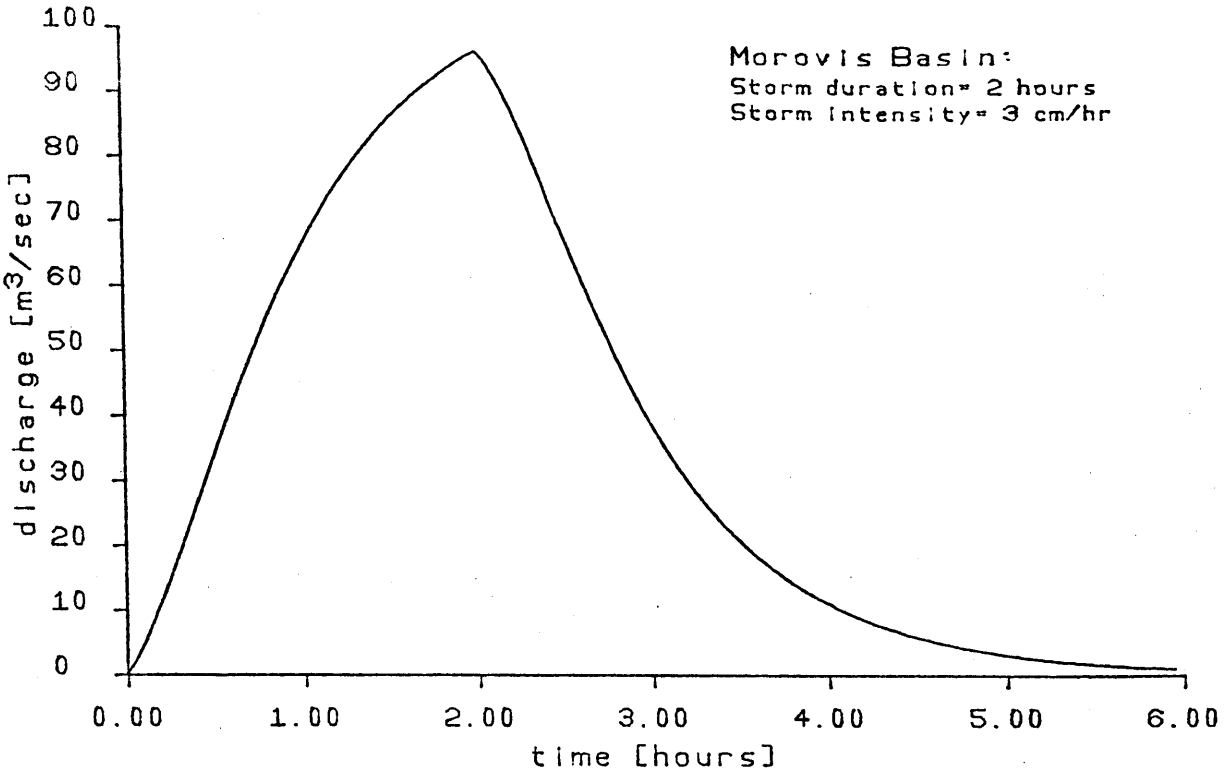

Figure 5.9.1: Discharge hydrograph for Morovis basin using exponential assumption.

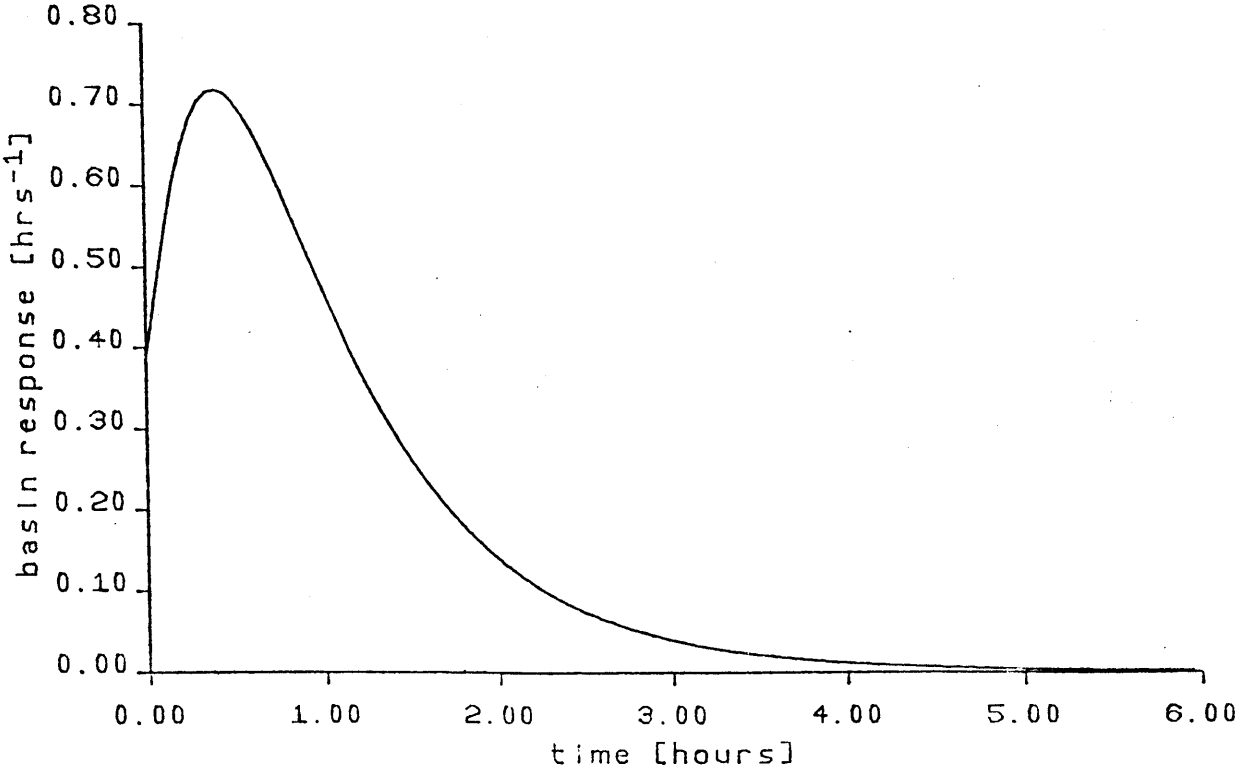

Figure 5.9.2: Geomorphologic IUH used to determine hydrograph in Figure 5.9.1.

This discrepancy between the hydrographs' shape could be significant. For example, in designing protective measures against floods, the hydrograph shape provides useful information to the planner. The hydrograph shape is a function of both the individual basin and the climate, and thus no generalized conclusion can be made concerning the shape of all the hydrographs for a particular basin. Nor can a conclusive statement be made concerning the shape of all the hydrographs determined using a particular channel IUH, as too many factors, such as channel configuration, channel slope and length, influence the shape of the hydrograph. This work has focused on obtaining a basin IUH which is indicative of both the basin's geomorphologic characteristics and the channels' physiographic characteristics, and thus one would expect that the IUH derived in this work provides more of a representative IUH for the particular basin than that obtained using the exponential assumption. However a more detailed investigation is needed before such a conclusion can be made.

The next section presents a case study where the choice of the basin IUH makes a significant difference in the discharge hydrograph.

5.5 Discharge Hydrographs for Wadi Umm Salam

In the last few years, some areas close to the Nile Valley in Upper Egypt have been subjected to occasional flash floods which cause considerable damage to the villages downstream. At the the outlet of these wadis are vast plain areas where villages have developed and people have cultivated the lands from which they obtain their major source of income. The severe

losses over the past few years has prompted the government of Egypt to develop a master plan to provide protection to the surrounding villages. The wadis are quite large in size and extend to the mountainous regions alongside the Nile. Discharge estimates are obtained from the people in the village or are estimated from the flood level water marks. The rainfall for a year is obtained from stations located along the Nile. Thus no rainfall measurements are available for locations within the wadis, nor are direct measurements of the discharges. The model presented in this work provides a feasible way to estimate the discharge due to a given storm. With just a topographic map or aerial photograph and an estimation of the storm properties, the discharge can be estimated.

As an example of the use of the model, Wadi Umm Salam has been selected for study. Wadi Umm Salam is a subbasin of Wadi Abbad which is one of the largest wadis in Upper Egypt. Wadi Abbad has an area of 5700 km^2. Its mouth is located to the east of the city of Idfu (see Figure 5.10). The basin extends up to the Red Sea mountains. Wadi Umm Salam is located in the northern part of Wadi Abbad and has an area of 39 km^2, see Figure 5.11.

The geomorphologic parameters corresponding to Wadi Umm Salam were obtained from a topographic map, and are presented in Table 5.3, along with the physiographic characteristics of the channels. The only rainfall data available consists of the maximum daily rainfall at the city of Idfu, for different return periods. For this investigation the maximum daily rainfall with a return period of 100 years is used. No hyetographs

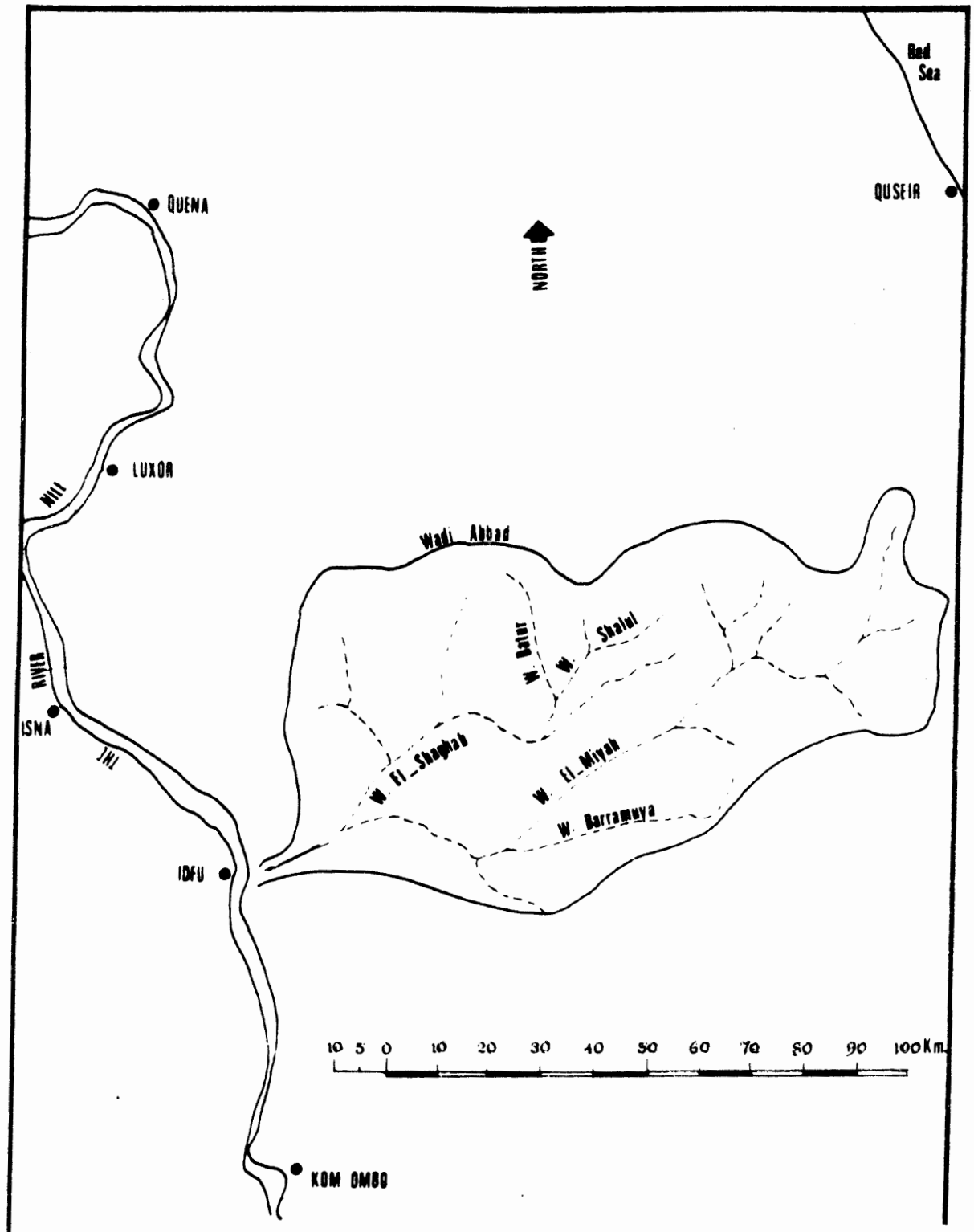

Figure 5.10: A map showing the location of Wadi Abbad (Aswan Governorate) (from Mabarek et al., March 1981).

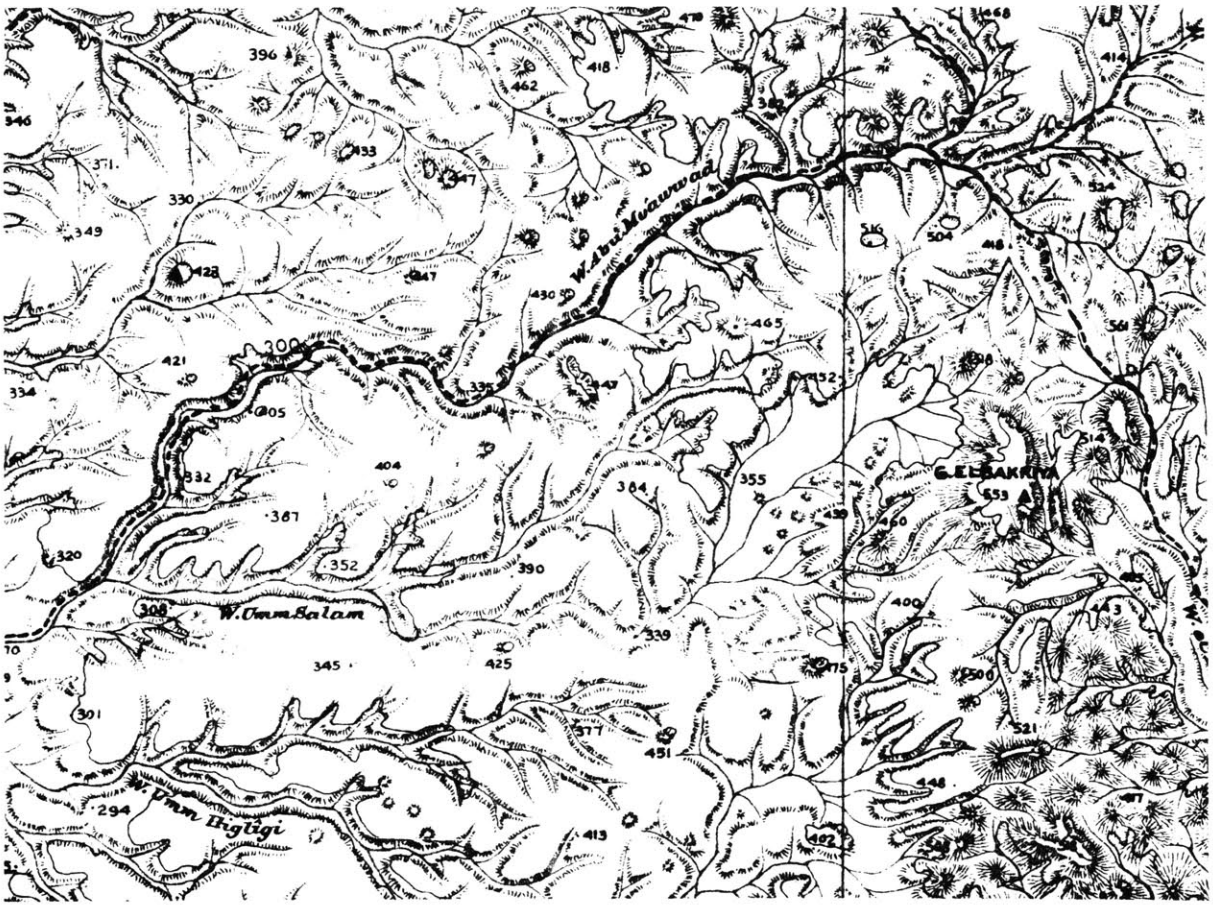

Figure 5.11: Wadi Umm Salam.

Table 5.3: Characteristics of Wadi Umm Salam

Stream Characteristics:

	y_o (m)	v_o (m/sec)	S_o (m/km)	L (km)	c_1 (m/sec)
1st order stream:	0.60	0.55	8.0	1.3	2.98
2nd order stream:	0.70	0.65	7.0	3.6	3.27
3rd order stream:	0.80	0.75	6.5	10.0	3.55

Geomorphologic Characteristics: $R_A = 3.1$; $R_B = 2.4$; $R_L = 2.8$

Initial Probabilities: $\theta_1(0) = 0.59$; $\theta_2(0) = 0.21$; $\theta 3(0) = 0.20$

Transition Probabilities:

$p_{r_1 r_2} = 0.105$ $p_{r_1 u_2} = 0.833$ $p_{r_1 r_3} = 0.061$ $p_{r_2 r_3} = 0.167$

$p_{r_2 u_3} = 0.833$ $p_{u_2 r_3} = 0.167$ $p_{u_2 u_3} = 0.833$

Path Probabilities:

$p(s_1) = 0.010$ $p(s_2) = 0.082$ $p(s_3) = 0.052$ $p(s_4) = 0.036$

$p(s_5) = 0.036$ $p(s_6) = 0.178$ $p(s_7) = 0.195$ $p(s_8) = 0.410$

are available and thus the rainfall intensity is assumed to be constant throughout the storm's duration.

The discharge hydrographs for storm durations of 2.0, 1.5, 1.0 and 0.5 hours are evaluated which for the total daily rainfall of 36.6 mm (from Mobarek et al., March 1981) yields the following storm intensities: 1.8, 2.4, 3.7 and 7.3 cm/hr, respectively. Only the average stream velocity of Wadi Umm Salam is available, and thus this velocity is used, instead of the peak velocity, to determine the required input parameters. The average velocity is determined from the estimated discharge to be 3.27 m/sec (from Mobarek et al., March 1981).

Using this average velocity, the total maximum rainfall with a 100 year return period, and the basin and channel characteristics, the discharge hydrographs for the different storm durations are determined. (See Table 3.3 for a summary of the input parameters.) The discharge hydrograph determined using the upstream and lateral inflow channel IUHs derived in this work, and the hydrograph determined using the exponential assumption for the channel response are both evaluated. The different geomorphologic IUHs and the associated discharge hydrographs are presented in Figures 5.12 to 5.16 and Figures 5.17 to 5.21, respectively. Comparing the two basin IUHs, Figures 5.12 and 5.17, the peaks are close, but the time to peaks differ significantly. Similarly, comparing the two types of discharge hydrographs for the same storm, the peaks are approximately equal, but the basin IUH using the channel IUHs derived in this work, produces hydrographs with significantly delayed time to peaks.

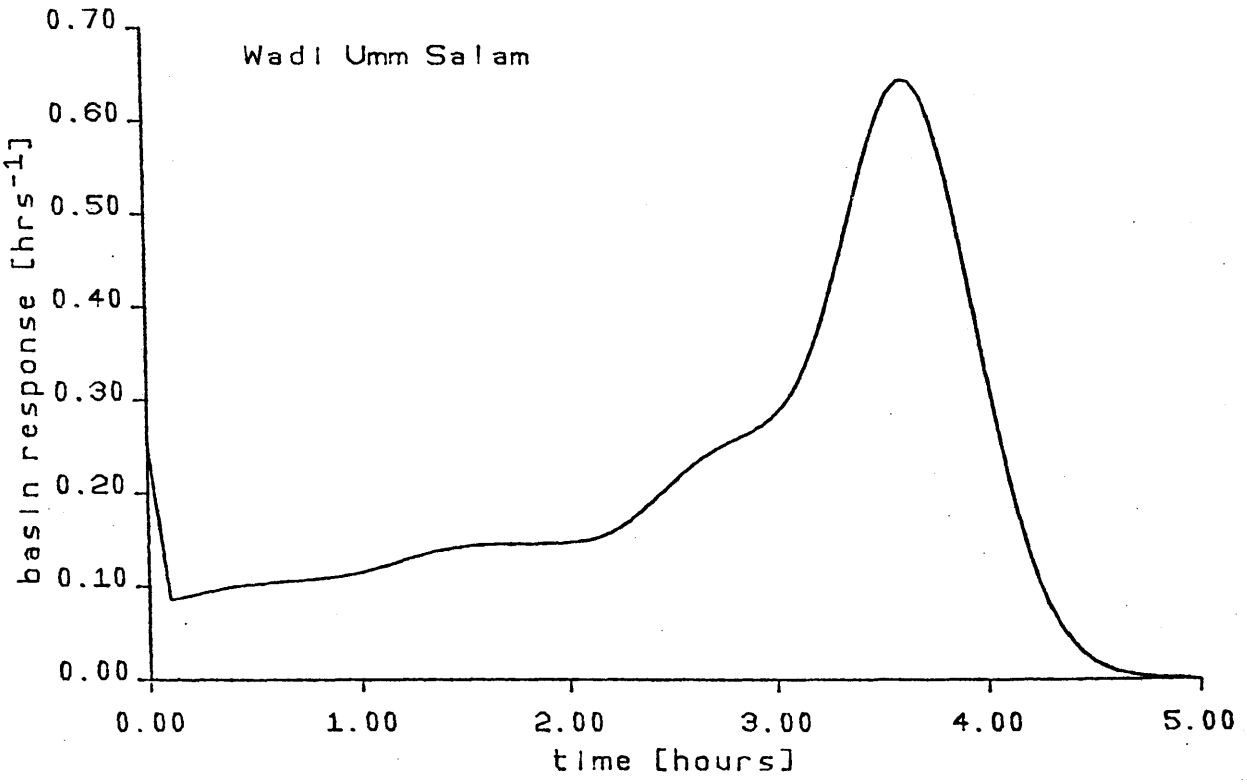

Figure 5.12: Geomorphologic IUH for Wadi Umm Salam.

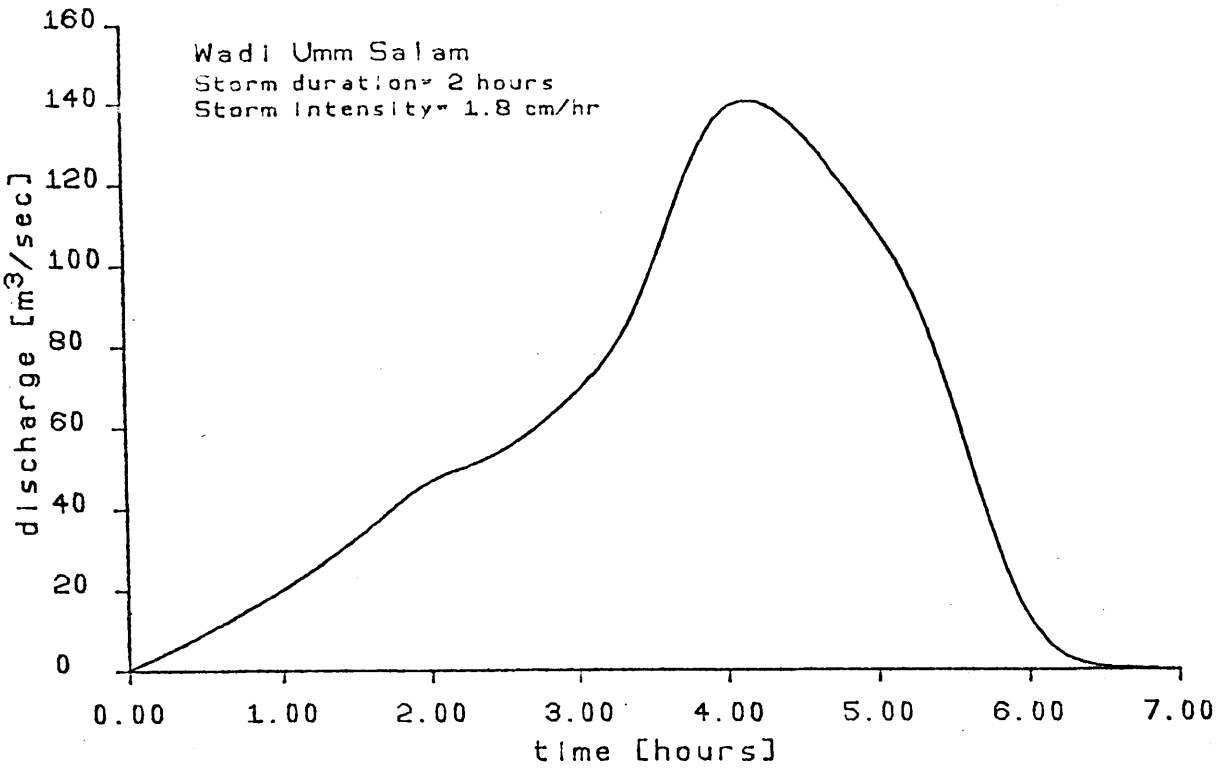

Figure 5.13: Discharge hydrograph for Wadi Umm Salam.

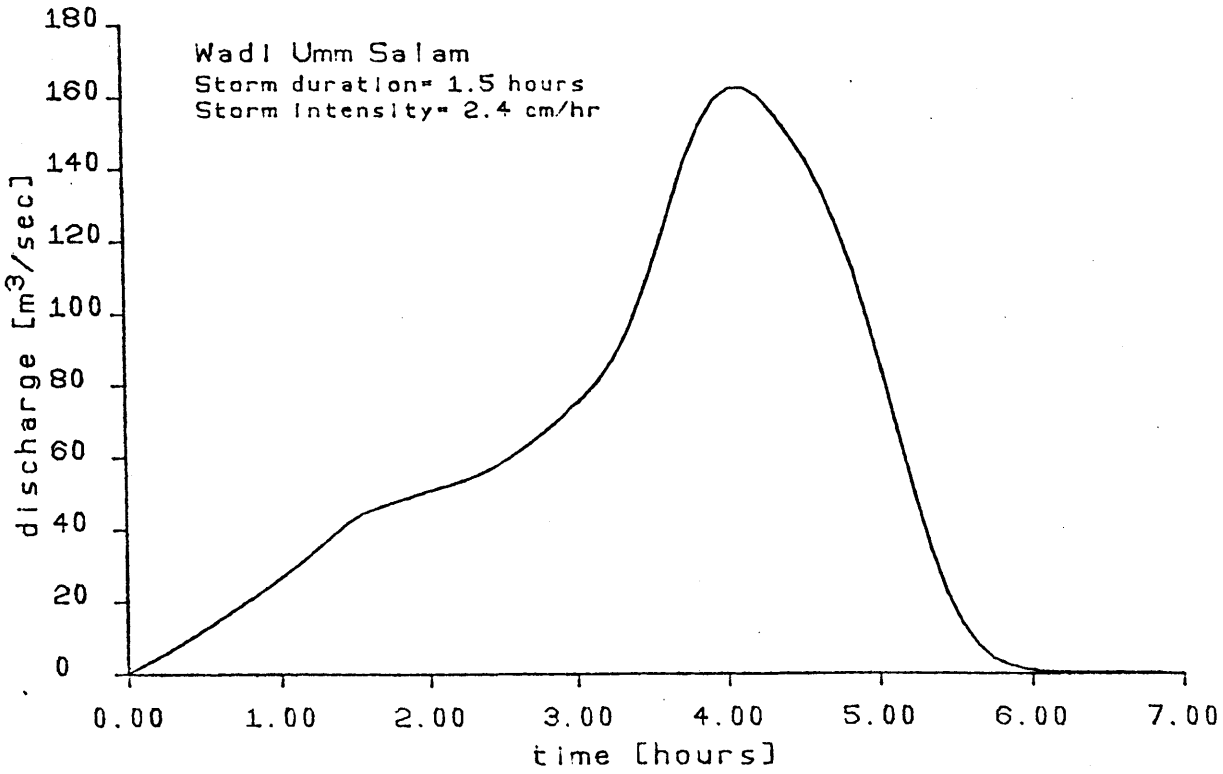

Figure 5.14: Discharge hydrograph for Wadi Umm Salam.

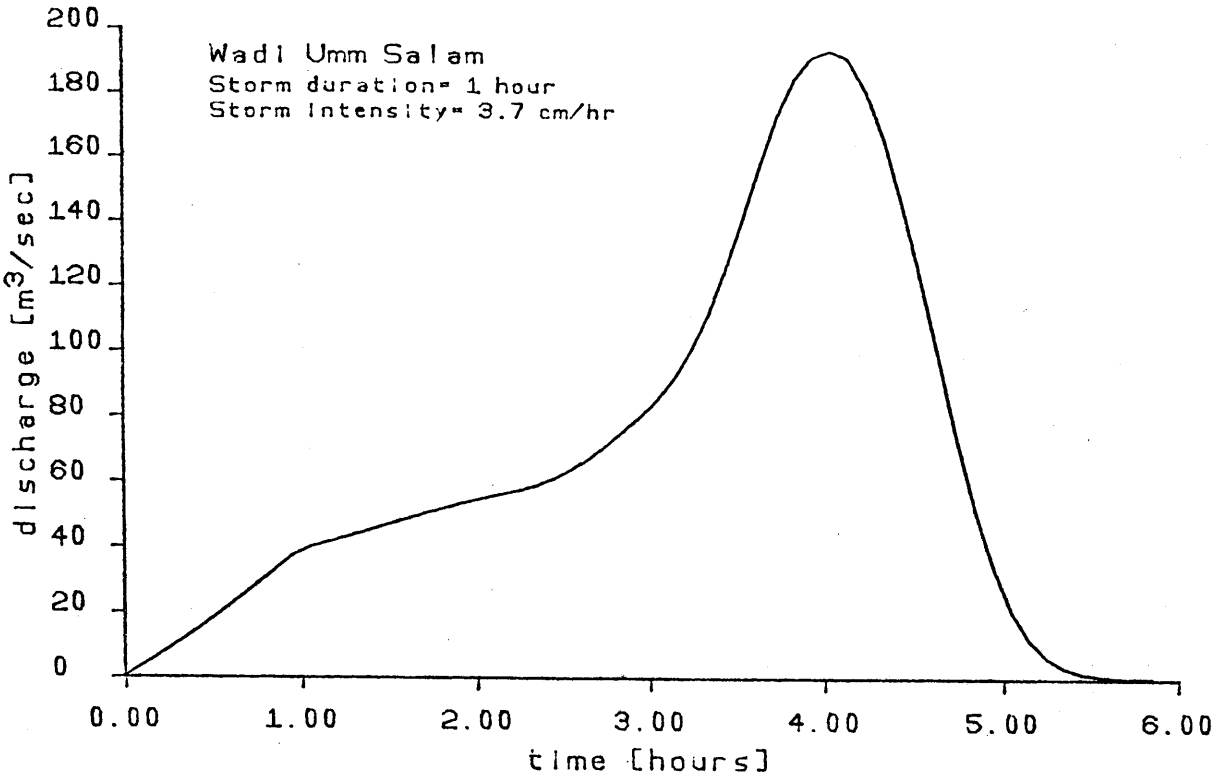

Figure 5.15: Discharge hydrograph for Wadi Umm Salam.

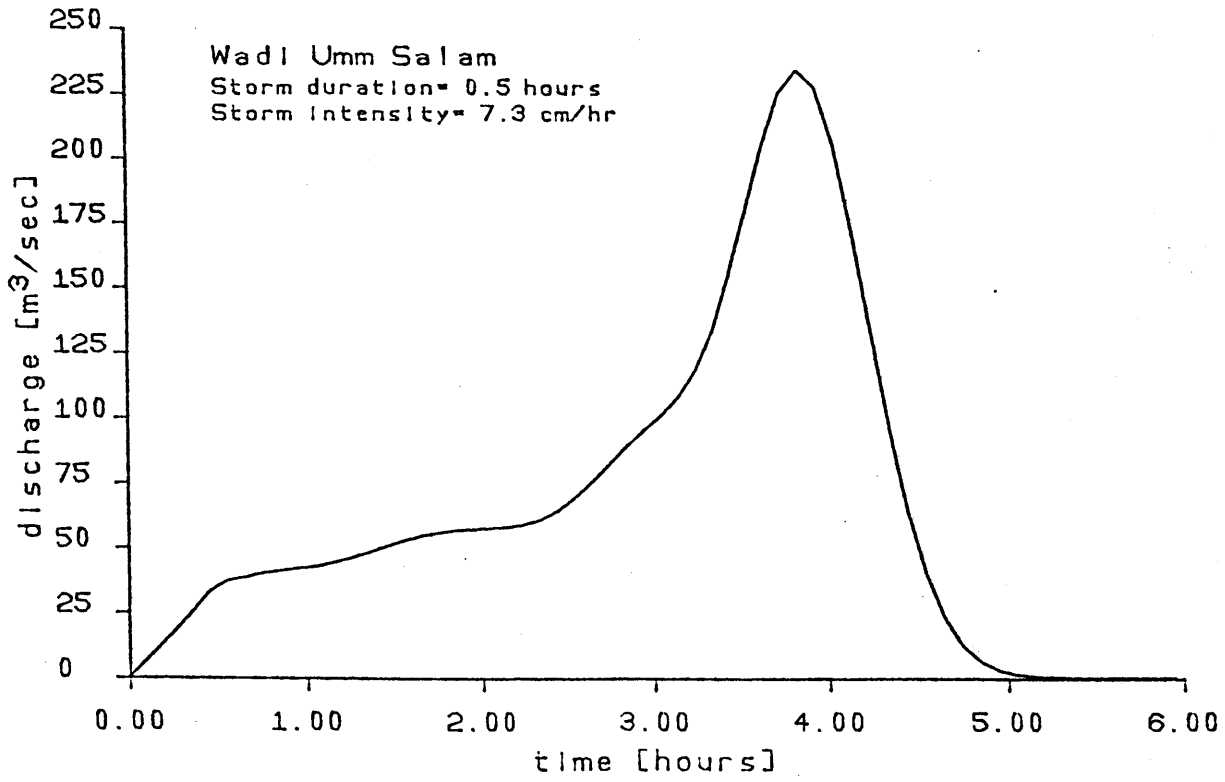

Figure 5.16: Discharge hydrograph for Wadi Umm Salam.

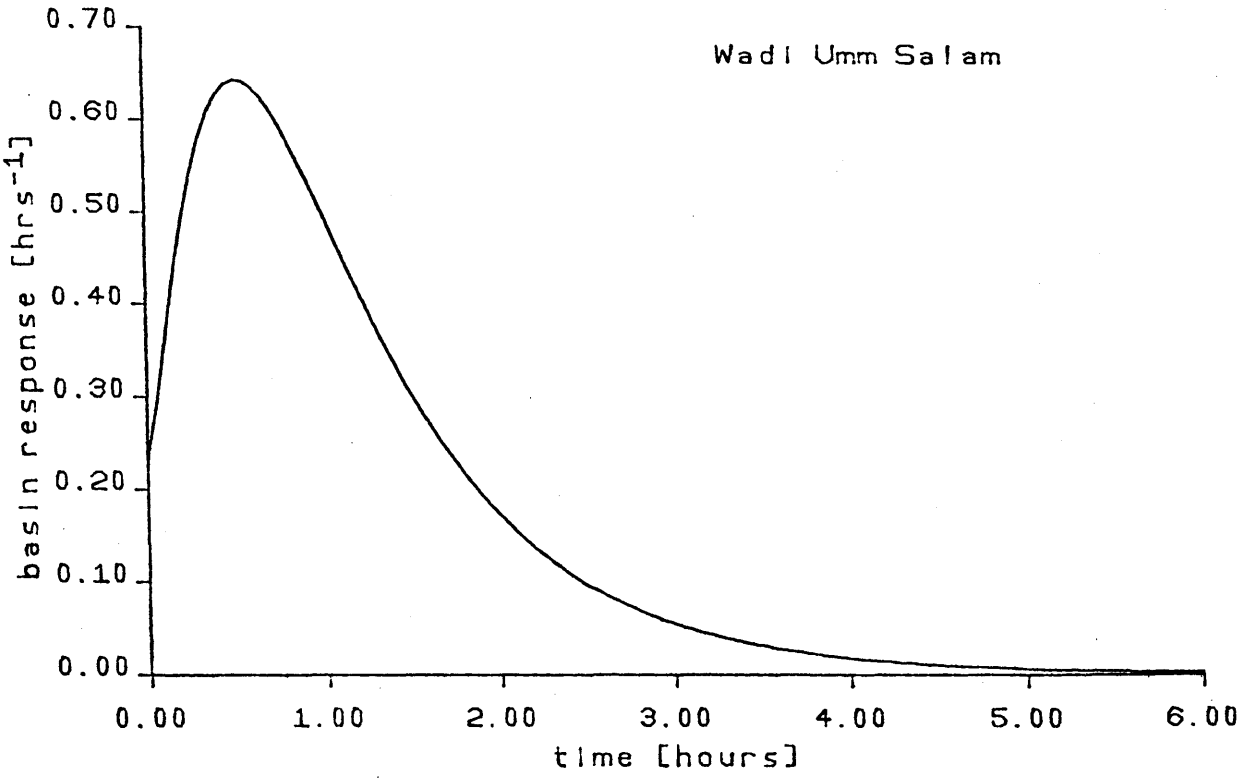

Figure 5.17: Geomorphologic IUH for Wadi Umm Salam using exponential assumption.

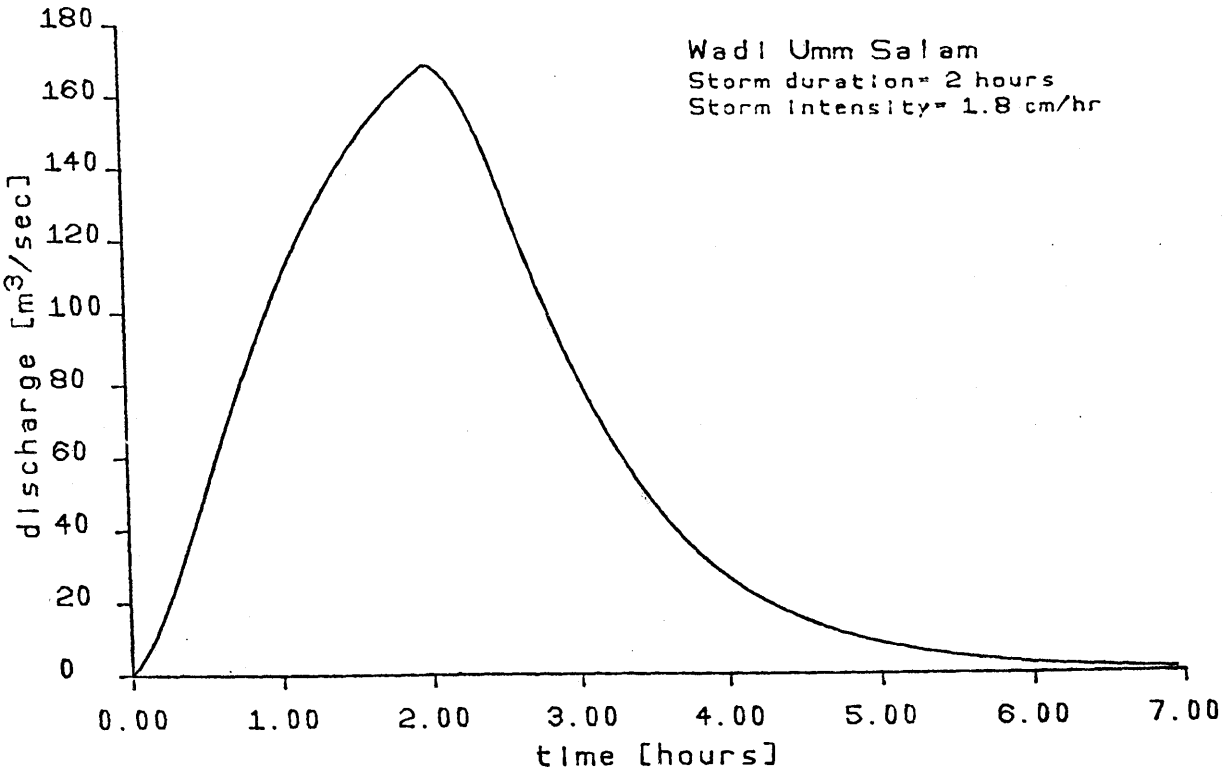

Figure 5.18: Discharge hydrograph for Wadi Umm Salam using exponential assumption.

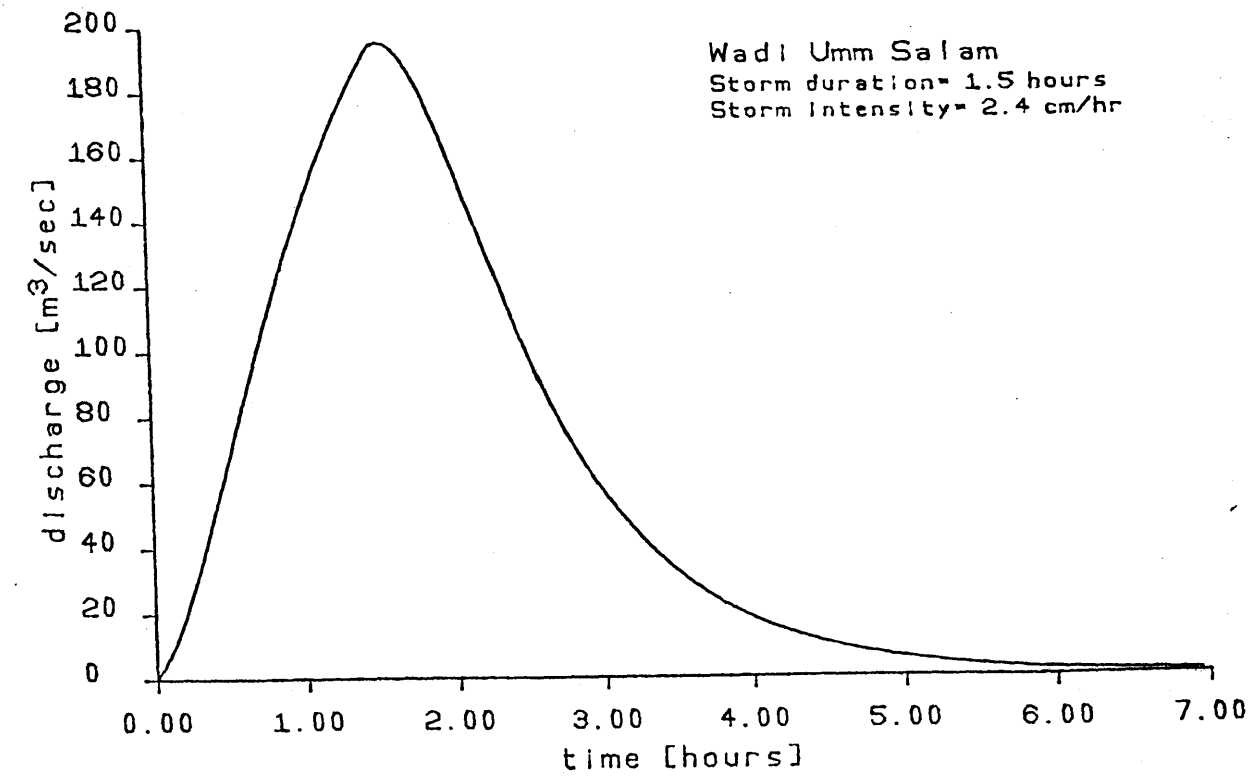

Figure 5.19: Discharge hydrograph for Wadi Umm Salam using exponential assumption.

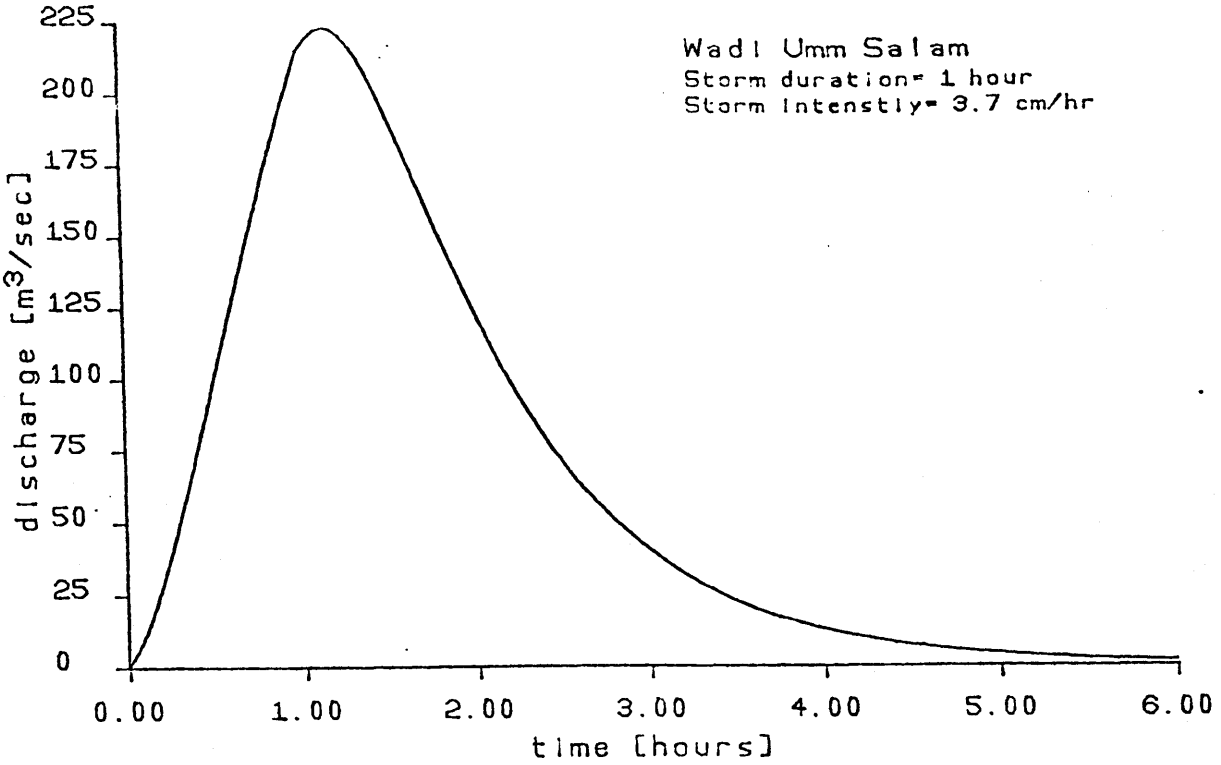

Figure 5.20: Discharge hydrograph for Wadi Umm Salam using exponential assumption.

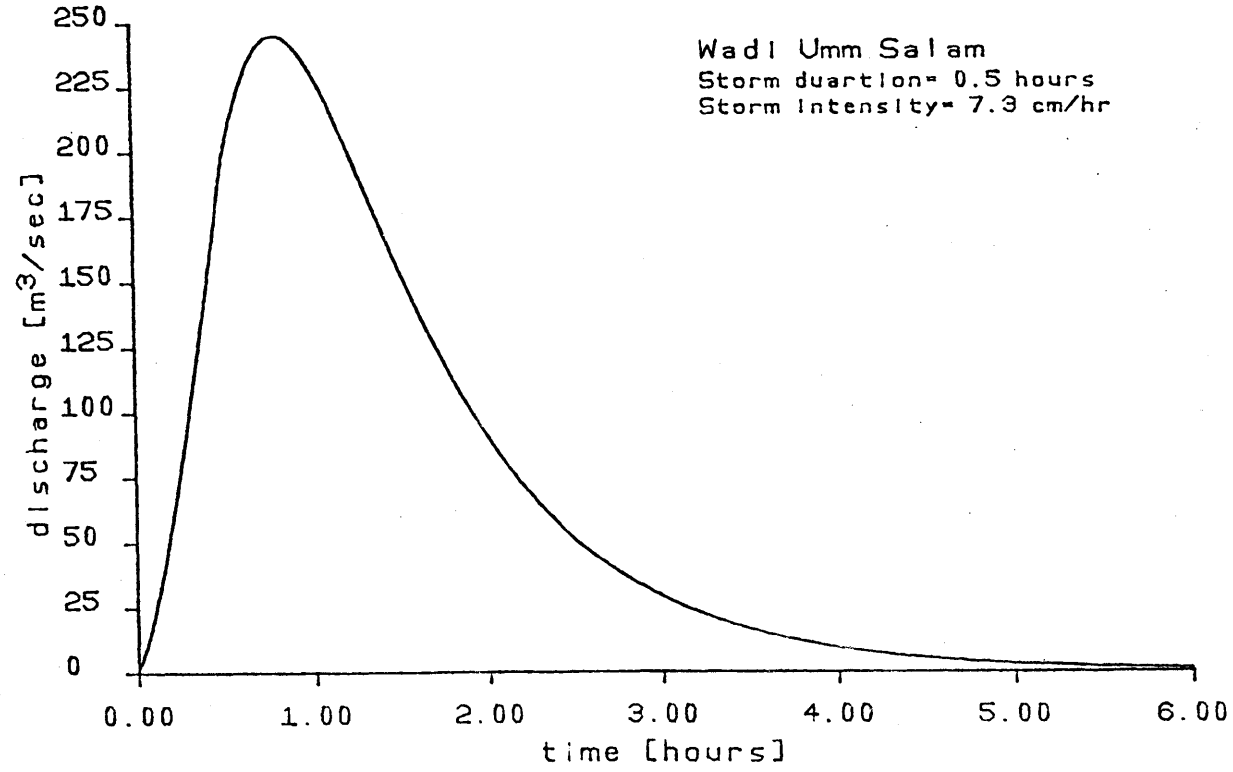

Figure 5.21: Discharge hydrograph for Wadi Umm Salam using exponential assumption.

Observing the overall shape of Wadi Umm Salam, shown in Figure 5.11, the basin is rather pear-shaped and one would expect that for a uniform rainfall over the whole basin, the initial response is due to the flow in the mainstream near the wadi's mouth. Then the flow from the lower order tributaries located in the upper regions of the basin begin to contribute to the discharge at the outlet, and thus the long delay for the peak. This type of behavior is also reflected in the low bifurcation ratio, R_B, of 2.4. For on the average there are less than 3 streams draining into the next higher order stream, but 2 of these 3 are required to form the stream of higher order. The transition probabilities, $p_{r_i u_{i+1}}$ and $p_{u_i u_{i+1}}$, are high and the upstream inflow channel IUH will contribute more to the overall basin IUH than the lateral inflow channel IUH.

This example illustrates the major contribution of the channel IUHs derived in this work to the geomorphologic IUH theory. The exponential assumption of the channel response only considers the average travel time of a drop along the channel, but the travel time for a drop traveling along the stream which forms the higher order stream, is a lot greater than the average. Due to the concept of random channel networks, the use of the exponential distribution to represent the flow from tributaries which enter laterally along the channel is reasonable as there is an equal probability of the tributary entering anywhere along the channel's length and thus the drop's travel time can be represented by the average. However, in cases where it is known that the tributary enters at a channel's most upstream point, a more representative channel IUH of the

actual travel time should be used. As presented in this work, the upstream and lateral inflow channel IUHs provide additional information such that the channel IUH can be chosen in accordance with the drop's path. Due to the lack of actual rainfall-runoff data, no conclusion can be made as to which model is more representative of the actual situation.

Chapter 6

CONCLUSIONS AND RECOMMENDATIONS

6.1 Conclusions

The discharge from river basins is a function of both the particular storm and basin characteristics. This work is based on the linear Instantaneous Unit Hydrograph theory and the theory of the geomorphologic IUH (Rodriguez et al., 1979). Modifications now make the response of channels of a given order dependent on the location of inputs. Responses are derived for inputs occurring at the stream's most upstream point and for inputs occurring anywhere along the channel's length. Both responses were determined by solving the linearized continuity and momentum equations for the corresponding boundary conditions. Inherent in these channel responses are the effects of the slope, length, and stream velocity.

The comparison of the hydrographs produced using the exponential assumption for the channel's response (Rodriguez et al., 1979) and those using both of the channel responses derived in this work, indicate significant differences in the overall shape of the hydrograph. Although for some cases the peaks and times to peak are approximately the same, the volume of water discharged before and after the peak differs. In other cases the peaks agree but the times to peak disagree. Due to the complex relationship between the variables which influence runoff, no general statement can be made concerning a relationship between the hydrographs

produced using the different channel responses. However, it is to be noted that the upstream and lateral inflow channel response functions are more representative of the actual flow situation.

This work is still fairly inconclusive since many experiments and attempts to calibrate known basin responses remains to be done. It is apparent, though, that a careful look at the assumed time distributions is required. The whole issue of calibration methods will have to be revisited if in fact the proposed methodology is believed adequate.

6.2 Recommendations

Given the results present in Chapter 5, of foremost importance is the estimation of the dynamic parameters which influence runoff. Using the exponential assumption, the dynamic effects are given by a peak stream velocity. For the upstream and lateral inflow IUHs, the dynamic effects are defined by the reference velocity, Froude number and dynamic wave speed, c_1; further research is needed to determine a relationship between these three variables and the climatic properties of the region such that the IUH is a function of both the physiographic and climatic characteristics of the area being investigated.

Further research on the influence of the overall drainage network on the hydraulic factors which determine runoff is suggested. In particular the effects of overland flow and infiltration should be investigated.

References

Crump, Kenny S., "Numerical Inversion of Laplace Transforms Using a Fourier Series Approximation," Journal of the Association for Computing Machinery, Vol. 23, No. 1, January 1976, pp. 89-96.

Doetsch, Gustav, Introduction to the Theory and Application of the Laplace Transformation. New York: Springer-Verlag, 1974.

Dooge, J. C. IU. and B. M. Harley, "Linear Routing in Uniform Open Channels," Proc. Int. Hydrology Symp., Fort Collins, Colorado, Vol. 1, paper 8, Sept. 1967.

Gupta, Vijay K., E. Waymire and C. T. Wang, "A Representation of an Instantaneous Unit Hydrograph From Geomorphology," Water Resources Research, 16 (5), 1980, pp. 855-862.

Harley, Brendan M., "Linear Routing in Uniform Open Channels," Master's Thesis, National University of Ireland, 1967.

Horton, Robert E., "Erosional Development of Streams and Their Drainage Basins, Hydrophysical Approach to Quantitative Morphology," Bulletin of the Geological Society of America, 56, 1945, pp. 275-370.

Leopold, Luna B. and Maddock, Thomas, Jr., "The Hydraulic Geometry of Stream Channels and Some Physiographic Implications," Geological Survey Professional Paper 252, 1953, pp. 1-57.

Mobarek, Ismail E., et al., "Flash Floods Hazard Prevention in Upper Egypt: Case Study of Aulad Salama Village (Sohag)," Cairo University-MIT Technological Planning Program, February 1981.

Mobarek, Ismail E., et al., "Flash Floods Hazard Prevention in Upper Egypt Villages: Case Study of El Edwa Village (Aswan)," Cairo University-MIT Technological Planning Program, March 1981.

Pilgrim, P. H., "Isochrones of Travel Time and Distribution of Flood Storage from a Tracer Study on a Small Watershed," Water Resources Research, 15(6), 1979, pp. 1409-1420.

Rodriguez-Iturbe, Ignacio and Rafael L. Bras, "A Geomorphoclimatic Theory of the Instantaneous Unit Hydrograph," Accepted for publication, Water Resources Research, 1981.

Rodriguez-Iturbe, I., G. Devoto, and J. B. Valdes, "Discharge Response Analysis and Hydrologic Similarity: The Interrelation Between the Geomorphologic IUH and the Storm Characteristics," Water Resources Research, 15(6), 1979, pp. 1435-1444.

Rodriguez-Iturbe, I., and J. B. Valdes, "The Geomorphlogic Structure of Hydrologic Response," Water Resources Research, 15(6), 1979, pp. 1409-1420.

Schumm, S. A., "Evolution of Drainage Systems and Slopes in Badlands at Perth Amboy, New Jersey," Geol. Soc. Amer. Bull., 67, 1956, pp. 597-646.

Shaake, J. C., "Deterministic Urban Runoff Model," Treatise on Urban Water Systems, ed. M. L. Albertson et al., Colorado State University, Fort Collins, 1971.

Shreve, Ronald L., "Stream Lengths and Basin Areas in Topologically Random Channel Networks," Journal of Geology, 77, 1969, pp. 397-414.

Shreve, Ronald L., "Infinite Topologically Random Channel Networks," Journal of Geology, 1967, pp. 178-186.

Shreve, Ronald L., "StatisticalLaw of Stream Numbers," Journal of Geology, 74, 1966, pp. 17-37.

Smart, J. S., "Statistical Properties of Stream Lengths," Water Resources Research, 4(5), 1968, pp. 1001-1013.

Smart, J. S., "Comparison of Smart and Scheidegger Stream Length Models," Water Resources Research, 5(6), 1969, pp. 1383-1387.

Smart, J. S., "Distribution of Interior Link Lengths in Natural Channel Networks," Water Resources Research, 5(6), 1969, pp. 1337-1342.

Smart, J. S., "Channel Networks," Advances in Hydroscience, ed. V. T. Chow, New York, Academic Press, 1972.

Strahler, Arthur N., "Quantitative Analysis of Watershed Geomorphology," Transactions, American Geophysical Union, 38(6), 1957, pp. 913-920.

Valdes, Juan B., Y. Fiallo, and I. Rodriguez-Iturbe, "Rainfall-Runoff Analysis of the Geomorphologic IUH," Water Resources Research, 15(6), 1979, pp. 1421-1434.

Appendix A

SUMMARY OF THE THEORETICAL DEVELOPMENT OF THE TRANSITION PROBABILITIES AND INITIAL PROBABILITIES

A.1 Transition Probabilities

The derivation of the transition probabilities, p_{ij}, uses results from Smart's(1968) random link length model. Referring back to Figure 2.1, an exterior link is a segment of channel network between a source and the first junction downstream, and an interior link is a segment of channel network between two successive junctions or between the outlet and the first junction upstream. Smart (1968) assumed that the lengths of interior links in a given network are independent random variables. The assumption implies that the distribution of interior link lengths is independent of order or any other topologic characteristic. Smart also used the assumption, originated by Shreve (1967), that all topologically distinct networks with a given number of sources are equally likely. An example of topologically distinct networks formed from 6 sources, is presented in Figure A.1. Using these two assumptions and the conditions imposed by Strahler's ordering scheme, Smart derived a general result for the mean number of interior links of order w in the complete network of order W:

$$E[w,W] = N_w \prod_{a=2}^{w} \frac{N_{a-1} - 1}{2N_a - 1} \qquad w=2,3,\ldots,W \tag{A.1}$$

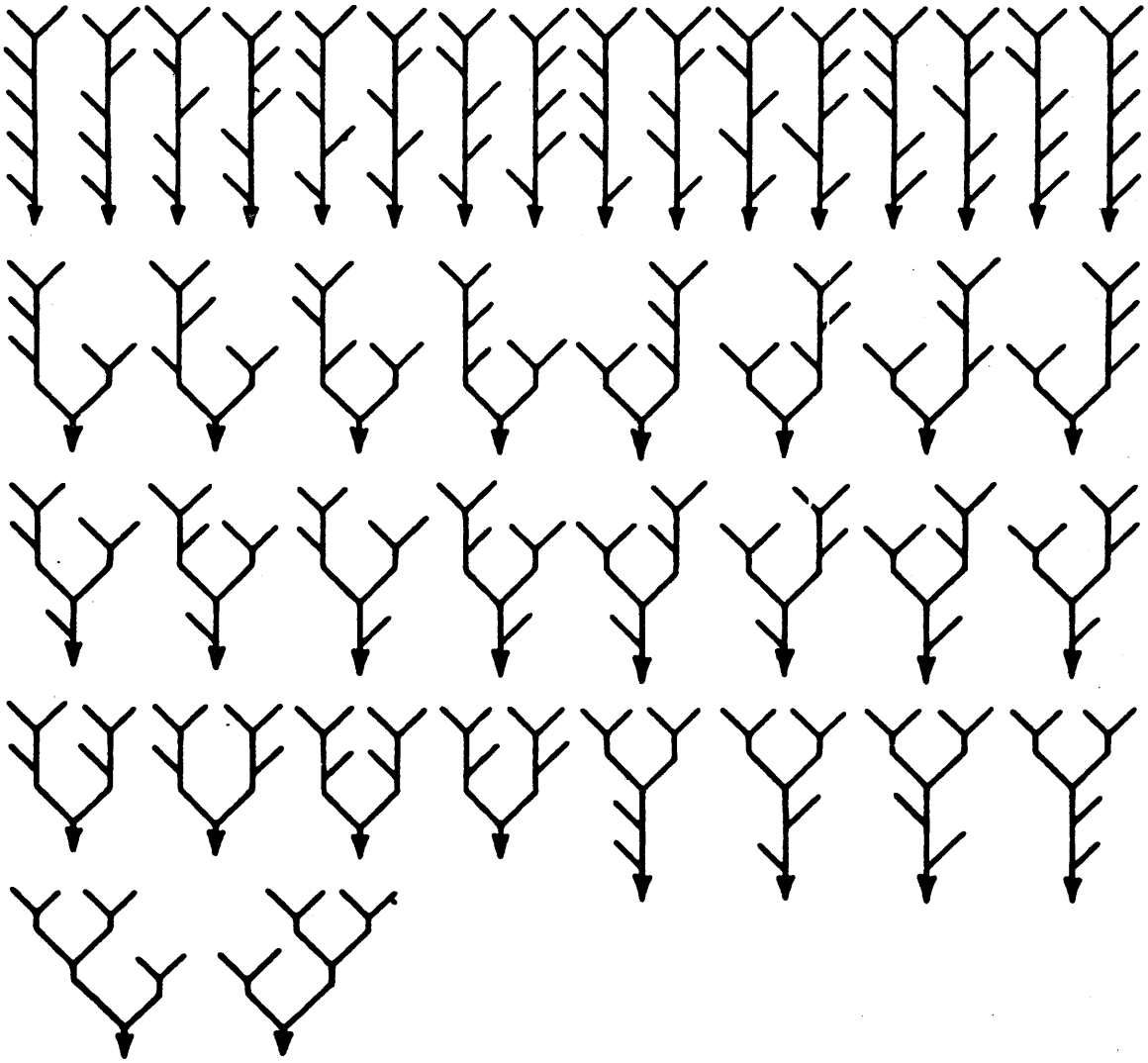

Figure A.1: Schematic diagrams of the 42 topologically distinct channel networks with 11 links and 6 first-order Strahler streams (from Shreve, 1966).

where the order of an interior link is given by the order of the channel of which the link is a segment. The mathematical development of Equation A.1 utilized concepts from probability theory and combinatorial mathematics (Smart 1968).

The transition probabilities are defined as follows:

$$p_{ij} = \frac{\text{number of streams of order i draining into order j}}{\text{total number of stream of order i}} \qquad \begin{matrix} i = 1,\ldots,W \\ j = i+1, \ldots, W+1 \end{matrix} \tag{A.2}$$

By Strahler's ordering scheme two streams of a lower order are required to form a stream of the next order, thus there exists $N_w - 2N_{w+1}$ streams remaining to be tributaries of streams of order w+1, ..., W. Since the interior link lengths are independent of order and any other topological characteristics the remaining $N_w - 2N_{w+1}$ streams join the higher order streams of w+1, ..., W according to

$$(N_w - 2N_{w+1}) \quad \frac{\text{number of links of order i}}{\text{total number of links of order w+1,...,W}} \qquad i=w+1,\ldots,W \tag{A.3}$$

Combining Equations A.1, A.2, and A.3 yields:

$$p_{ij} = \frac{(N_i - 2N_{i+1})\, E[j,W]}{\sum_{k=j}^{W} E[k,W] N_i} + \frac{2N_{i+1}}{N_i}\, \delta_{i+ij} \tag{A.4}$$

where δ_{i+1j} is 1 if i+1=j and 0 otherwise. As an example consider the transition probability p_{12} for a 3rd order basin.

Using Equation A.1

$$E[2,W] = N_2 \frac{(N_1 - 1)}{2N_2 - 1} \tag{A.5}$$

and

$$E[3,W] = N_3 \prod_{a=2}^{3} \frac{N_{a-1} - 1}{2N_a - 1} \tag{A.6}$$

$$= N_3 \left[\frac{N_1 - 1}{2N_2 - 1} \frac{N_2 - 1}{2N_3 - 1}\right]$$

Recalling that $N_3 = 1$ and substituting Equations A.5 and A.6 into A.4 yields:

$$p_{12} = \frac{(N_1 - 2N_2)N_2}{(2N_2 - 1)N_1} + \frac{2N_2}{N_1} \tag{A.7}$$

Substituting in the expression for R_B:

$$R_B = \frac{N_{w+1}}{N_w}$$

and rearranging yields:

$$p_{12} = \frac{R_B^2 + 2R_B - 2}{R_B(2R_B - 1)} \tag{A.8}$$

Thus p_{12} is only a function of the geomorphological parameter R_B.

A.2 Initial Probabilities

The derivation of the initial proabilities follows a similar procedure as the transition probabilities. The initial probability for a stream of order i is defined as

$$\theta_w(0) = \frac{\text{area draining directly into a stream of order w}}{\text{total area of the basin}} \qquad (A.9)$$

For w=1, the result is simply:

$$\theta_1(0) = \frac{N_1 \bar{A}_1}{\bar{A}_W} \qquad (A.10)$$

where $\bar{A}_1$ is the average area directly contributing to a stream of order 1, and $\bar{A}_W$ is the area of the basin. For a third order basin, the above is equivalent to

$$\theta_1(0) = R_B^2 R_A^{-2} \qquad (A.11)$$

where R_B and R_A are the bifurcation and area ratios. The derivation of $\theta_2(0)$ is a bit more complicated. Equation A.9 can also be interpreted as

$$\theta_w(0) = \frac{\text{area of order w minus area of order w contributing directly to lower order streams}}{\text{total area of the basin}} \qquad (A.12)$$

The area draining into the tributaries of the stream of order w is determined by evaluating the average number of links of order i, for

i=1,...,w-1, draining into streams of order w and then multiplying each value by its corresponding average area of order i. For example consider $\theta_2(0)$ for a third order basin. The number of streams of order 1 available to be tributaries of orders 2 and 3 is $N_1 - 2N_2$, and of these the number going into second-order streams is written as:

$$(N_1 - 2N_2) \frac{\text{number of links of order 2}}{\text{total number of links or orders 2 and 3}} \tag{A.13}$$

Substituting Equation A.1 and simplifying yields:

$$(N_1 - 2N_2) \frac{N_2}{2N_2 - 1} \tag{A.14}$$

Thus on the average a stream of order 2 has

$$(N_1 - 2N_2) \frac{1}{2N_2 - 1} + 2$$

streams of order 1 that drain into it, where the second term represents the two streams of order 1 which form this stream of order 2. The average area draining directly into a second order stream is then

$$\bar{A}_2 - \bar{A}_1 [\frac{N_1 - 2N_2}{2N_2 - 1} + 2]$$

and

$$\theta_2(0) = \frac{N_2}{\bar{A}_3} [\bar{A}_2 - \bar{A}_1 (\frac{N_1 - 2N_2}{2N_2 - 1} + 2)] \tag{A.15}$$

Rearranging the above equation and substituting in R_B and R_A yields:

$$\theta_2(0) = \frac{R_B}{R_A} - \frac{R_B^3 + 2R_B^2 - 2R_B}{R_A^2(2R_B - 1)} \tag{A.16}$$

Noticing that the second term of A.15 is $A_1 \frac{N_1}{N_2} p_{12}$, an equivalent expression for $\theta_2(0)$ is

$$\theta_2(0) = \frac{N_2}{\bar{A}_3} [\bar{A}_2 - \bar{A}_1 \frac{N_1 p_{12}}{N_2}] \tag{A.17}$$

Generalizing the above result for all initial probabilities yields:

$$\theta_w(0) = \frac{N_w}{\bar{A}_W} [\bar{A}_w - \sum_{j=1}^{w-1} \bar{A}_j (N_j p_{jw}/N_w)] \qquad w=2,\ldots,W \tag{A.18}$$

In summary, the following general results determine the initial and transition probabilities:

$$p_{ij} = \frac{(N_i - 2N_{i+1})E[j,W]}{\sum_{k=j}^{W} E[k,W]N_i} + \frac{2N_{i+j}}{N_i} \delta_{i+j} \qquad 1 \leq i < j \leq W$$

$$\theta_w(0) = \frac{N_1 \bar{A}_1}{\bar{A}_W}$$

$$\theta_w(0) = \frac{N_w}{\bar{A}_W} [\bar{A}_w - \sum_{j=1}^{w-1} \bar{A}_j (N_j p_{jw}/N_w)] \qquad w=2,\ldots,W$$

where

N_w = number of streams of order w

$\bar{A}_w$ = average area draining into streams of order w.

The general results can then be rearranged to yield expressions in terms of the bifurcation ratio, R_B and the area ratio, R_A.

Appendix B

MATHEMATICAL PROPERTIES OF THE UPSTREAM AND LATERAL INPUT CHANNEL IUHS

Appendix B is divided into three sections. The first section presents the solution of the linear partial differential equation given in Chapter 3. The second section presents the proof that the area under the upstream and lateral input response functions is one, the third section presents the derivation of the time lag expression for $\delta q(x,t)$, and the fourth section presents the evaluation of the first term of the lateral input channel IUH.

B.1 Analytical Solution of the Upstream Input IUH

The linear partial differential equation to be solved is, as presented in Chapter 3, Equation 3.7,

$$(gy_o - v_o^2)\frac{\partial^2 \delta q}{\partial x^2} - 2v_o \frac{\partial^2 \delta q}{\partial x \partial t} - \frac{\partial^2 \delta q}{\partial t^2} = 3gS_o \frac{\partial \delta q}{\partial x} + \frac{2gS_o}{v_o}\frac{\partial \delta q}{\partial t} \qquad (B.1)$$

Taking the Laplace transform of each term with respect to t and imposing the boundary conditions given in Chapter 3, yields

$$(gy_o - v_o^2)\frac{\partial^2 Q(x,s)}{\partial x^2} - 2v_o s \frac{\partial Q(x,s)}{\partial x} - s^2 Q(x,s) = 3gS_o \frac{\partial Q(x,s)}{\partial x} + \frac{2gSo}{v_o} sQ(x,s) \qquad (B.2)$$

where by definition

$$Q(x,s) = \int_0^\infty \exp(-st)\ \delta q(x,t)dt$$

is the Laplace transform of the output resulting from the unit impulse of the upstream input. Combining similar terms in Equation B.2 yields:

$$(gy_o - v_o^2)\frac{\partial^2 Q(x,s)}{\partial x^2} - (2v_o s + 3gS_o)\frac{\partial Q(x,s)}{\partial x} - (s^2 + \frac{2gS_o}{v_o}s)Q(x,s) = 0 \qquad (B.3)$$

The above equation is a second order homogeneous ordinary differential equation in x, whose solution is of the general form:

$$Q(x,s) = \beta(s)\exp[\lambda(s)x] \qquad (B.4)$$

where $\beta(s)$ and $\lambda(s)$ are unknown functions of s.

The expression for $\lambda(s)$ is given by the characteristic equation of B.3, which is:

$$\left[\lambda(s) - \frac{(2v_o s + 3gS_o) - \sqrt{(2v_o s + 3gS_o)^2 - 4(gy_o - v_o^2)(s^2 + \frac{2gS_o}{v_o} s)}}{2(gy_o - v_o^2)}\right].$$

$$\left[\lambda(s) - (2v_o s + 3gS_o) + \sqrt{(2v_o s + 3gS_o)^2 - 4(gy_o - v_o^2)(s^2 + \frac{2gS_o}{V_o} s)}\right]$$

$$= 0 \qquad \text{(B.5)}$$

Referring to Equation B.4, the general solution is:

$$Q(x,s) =$$

$$C_1 \exp\left\{\left[(2v_o s+3gS_o - \sqrt{(2v_o s + 3gS_o)^2 - 4(gy_o - v_o^2)(s^2 + \frac{2gS_o}{v_o} s)}\right]x\right\}$$

$$C_2 \exp\left\{\left[(2v_o s+3gS_o) + \sqrt{(2v_o + 3gS_o)^2 - 4(gy_o - v_o^2)(s^2 + \frac{2gS_o}{v_o} s)}\right]x\right\}$$

(B.6)

For any Laplace transform,

$$\lim_{s \to 0} Q(x,s) = 0$$

Thus $C_2 = 0$.

The value for C_1 is determined using the initial condition

$$\delta q(0,t) = \delta(t)$$

which in the transform space is

$$Q(0,s) = L[\delta(t)] = 1$$

Thus,

$$Q(0,s) = C_1 \exp(0) = C_1 = 1$$

and

$$Q(x,s) =$$

$$\exp\{(2v_o S + 3gS_o - \sqrt{(2v_o s + 3gS_o)^2 - 4(gy_o - v_o^2)(s^2 + \frac{2gS_o}{v_o} s)}\} \qquad \text{(B.7)}$$

The determination of $\delta q(x,t)$ requires the inversion of Equation B.7. In order to simplify notation, Equation B.7 will be rewritten as:

$$Q(x,s) = \exp\{- x \sqrt{as^2+bs+c} \quad +esx+fx \} \qquad \text{(B.8)}$$

where the expressions for the constants are given below:

$$a = \frac{1}{gy_o(1-F^2)^2}$$

$$b = \frac{S_o}{q_o}\ \frac{2 + F^2}{(1-F^2)^2}$$

$$c = \frac{9}{4}\left(\frac{S_o}{y_o}\right)^2\ \frac{1}{(1-F^2)^2}$$

$$e = \frac{v_o}{gy_o(1 - F^2)}$$

$$f = \frac{3}{2}\ \frac{S_o}{y_o}\ \frac{1}{(1 - F^2)}$$

$$F = \frac{v_o}{\sqrt{gy_o}}$$

Equation B.8 is now rewritten as a sum of Laplace transforms whose inverses can be obtained from tables of Laplace transforms. Q(x,s) is rewritten as:

$$\exp[-(\sqrt{a}\ -e)xs - (\frac{b}{2\sqrt{a}} - f)x] +$$

$$\exp[exs + fx]\ \{\exp(-x\sqrt{as^2+bs+c}\ ) - \exp(-\frac{b}{2\sqrt{a}}\ x - \sqrt{a}\ xs)\} \qquad (B.9)$$

The inversion of Equation B.9 requires the use of the shift formula:

$$L^{-1}\,[e^{-ms}\,f(s)] = u(t-m)\,F(t-m)$$

where

$$f(s) = \int_0^{\infty} e^{st}\,F(t-m)\,dt$$

$$u(t) = \begin{cases} 0 & t < 0 \\ 1 & t \geq 0 \end{cases}$$

To determine the inverse of the second term of B.9, we also use the fact that the expression

$$\exp(-x\sqrt{as^2+bs+c}\,) - \exp\left(\frac{-b}{2\sqrt{a}}\,x - \sqrt{a}\,xs\right) \tag{B.10}$$

is given as the Laplace transform of

$$\sqrt{d/a}\;x\;\exp\left(-\frac{b}{2a}\,t\right)\;\frac{I_1[\sqrt{d/a}\,\sqrt{t^2-ax^2}\,]}{\sqrt{t^2-ax^2}}\;u(t-\sqrt{a}\,x) \tag{B.11}$$

where

$$d = (b/2)^2 - ac$$

The inverse of each term is derived as follows:

$$\exp\left[-\left(\frac{b}{2\sqrt{a}} - f\right)x\right]\;L^{-1}[\exp(-(\sqrt{a} - e)xs)]$$

$$= \exp\left[-\left(\frac{b}{2\sqrt{a}} - f\right)x\right]\,u(t-(\sqrt{a}-e)x)\,F(t-(\sqrt{a}-e)x)$$

$$= \exp\left[-\left(\frac{b}{2\sqrt{a}} - f\right)x\right]u(t-(\sqrt{a}-e)x)\,\delta(t-(\sqrt{a}-e)x)$$

$$= \exp\left[-\left(\frac{b}{2\sqrt{a}} - f\right)x\right]\,\delta(t-(\sqrt{a}-e)x) \tag{B.12}$$

$$L^{-1}[\exp[exs+fx]\{\exp(-x\sqrt{as^2+bs+c}) - \exp(\frac{-b}{2\sqrt{a}}x - \sqrt{a}xs)\}]$$

$$= \exp(fx)\sqrt{d/a}\; x\; \exp(-\frac{b}{2a}(t+ex))\; \frac{I_1[\sqrt{d/a}\sqrt{(t+ex)^2 - ax^2}]}{\sqrt{(t+ex)^2 - ax^2}}\; u(t+ex-\sqrt{a}\,x) \tag{B.13}$$

The sum of the inverses can be rewritten as:

$$\delta(t - x/c_1)\exp(-px) +$$

$$\exp(-rt+zx)(x/c_1-x/c_2)h\,\frac{I_1[2h\sqrt{(t-x/c_1)(t-x/c_2)}]}{\sqrt{(t-x/c_1)(t-x/c_2)}}\; u(t-x/c_1) \tag{B.14}$$

where

$$c_1 = \frac{1}{\sqrt{a} - e} = v_o + \sqrt{gy_o}$$

$$c_2 = -\frac{1}{\sqrt{a} + e} = v_o - \sqrt{gy_o}$$

$$p = \frac{b}{2\sqrt{a}} - f = \frac{S_o}{2y_o}\,\frac{2-F}{F(1+F)}$$

$$r = \frac{b}{2a} = \frac{S_o v_o}{2y_o}\,\frac{2+F^2}{F^2}$$

$$z = f - \frac{be}{2a} = \frac{S_o}{2y_o}$$

$$h = \frac{\sqrt{d}}{2a} = \frac{S_o v_o}{2y_o} \quad \frac{\sqrt{(4-F^2)(1-F^2)}}{2F^2}$$

$$d = (\frac{b}{2})^2 - ac = (\frac{S_o}{g_o})^2 \frac{(1-F^2/4)(1-F^2)}{(1-F)^4}$$

$I_1[\cdot]$ = first order modified Bessel function of the first kind

$u(\cdot)$ = unit step function

B.2 Area of $\delta q(x,t)$ and $r_{a_i}(t)$

The following section presents analytical proofs that the area of the pdfs, $\delta q(x,t)$ and $r_{a_i}(t)$, are equal to 1.

B.2.1 Proof that the area of $\delta q(x,t)$ is 1

The area of $\delta q(x,t)$ equation B.13, is determined using the definition of the Laplace transform and its moments. $\delta q(x,t)$ is a function of x and t, where x is the distance the drop travelled. In this study x is the channel length, and the upstream response is written as a function of t only .

The nth moment of a function around the origin is given by:

$$m_n'(t) = \int_0^\infty f(t)t^n dt \qquad (B.15)$$

The nth derivative of the Laplace transform is given by

$$\frac{d^n Q(x,s)}{ds^n} = \int_0^\infty (-t)^n e^{-st} \delta q(x,t)dt$$

$$= (-1)^n \int_0^\infty t^n e^{-st} \delta q(x,t)dt \qquad (B.16)$$

From B.16, at s = 0,

$$\left.\frac{d^n Q(x,s)}{ds^n}\right|_{s=0} = (-1)^n \int_0^\infty t^n \delta q(x,t)dt$$

$$= (-1)^n m_n'(t) \qquad (B.17)$$

Thus the area under $\delta q(x,t)$ is given by:

$$m_0'(t) = Q(x,s)\Big|_{s=0}$$

Using Equation B.8,

$$m_0'(t) = \exp[x(-\sqrt{as^2+bs+c} + es + f)]\Big|_{s=0}$$

$$= \exp[x(-\sqrt{c} + f)]$$

$$= 1 \qquad (B.18)$$

as $f = \sqrt{c}$ (see Equation B.7).

B.2.2. Proof that the Area of $r_{a_i}(t)$ is 1

As in Section B.2.1, using the functional relationship between moments and Laplace transforms, the area of $r_{a_i}(t)$ is given by:

$$L[r_{a_i}(t)]\Big|_{s=0} \tag{B.19}$$

Substituting in Equation 3.15 into the above equation yields:

$$\frac{1}{\bar{L}_{a_i}(-\sqrt{as^2+bs+c}+es+f)}\left[\exp(\bar{L}_{a_i}(-\sqrt{as^2+bs+c}+es+f))-1\right]\Big|_{s=0} \tag{B.20}$$

Since the denominator equals zero at s=0, in order to evaluate B.20, L'Hopital's Rule is used, and the area of $r_{a_i}(t)$ is given by:

area of $r_{a_i}(t)$

$$= \lim_{s\to 0} \frac{\bar{L}_{a_i}[-\frac{1}{2}(as^2+bs+c)^{-\frac{1}{2}}(2as+b)+e]\exp(\bar{L}_{a_i}(-\sqrt{as^2+bs+c}+es+f))}{\bar{L}_{a_i}[-\frac{1}{2}(as^2+bs+c)^{-\frac{1}{2}}(2as+b)+e]}$$

$$= \lim_{s\to 0} e^{\bar{L}_{a_i}(-\sqrt{as^2+bs+c}+es+f} = 1$$

B.3 Time Lag for $\delta q(x,t)$

The time lag is the time between the centroid of the effective rainfall and that of the direct runoff. For rainfall which is symmetric with respect to time, the time lag, t_L, is given by:

$$t_L = \frac{\int_0^\infty t\ Q_B(t)dt}{\int_0^\infty Q_B(t)dt} - \frac{t_d}{2} \qquad (B.21)$$

where $Q_B(t)$ is the outflow hydrograph and t_d is the duration of the effective rainfall. The above expression can be shown to be equivalent to:

$$t_L = \int_0^\infty th(t)dt \qquad (B.22)$$

where h(t) is the IUH.

Using the relationship between moments and Laplace transforms:

$$t_L = m_1'(t) = \frac{dQ(x,s)}{ds}\bigg|_{s=0} (-1)^1 \qquad (B.23)$$

and substituting in the epxression for Q(x,s) (Equation B.8) yields:

$$m_1'(t) = x(-\tfrac{1}{2}(as^2+bs+c)^{-\frac{1}{2}}(2as+b)+e)\exp(x(-\sqrt{as^2+bs+c}+es+f))(-1)\Big|_{s=0}$$

$$= x(-\tfrac{1}{2}\frac{b}{\sqrt{c}} + e)e^{x(-\sqrt{c}+f)}(-1)$$

$$= x(\frac{b}{2\sqrt{c}} - e) \qquad \text{(B.24)}$$

Substituting in the expression for b, c, and e (Equation B.8) yields:

$$t_L = m_1'(t) = \frac{x}{1.5v_o} \qquad \text{(B.25)}$$

B.4 Evaluation of the First Term of Equation 3.10

The first term of Equation 3.10 is given by

$$\frac{1}{\bar{L}_{a_i}} \int_0^{\bar{L}_{a_i}} \delta(t-x/c_1)\exp(-px)dx \qquad \text{(B.26)}$$

Since $\delta(t-t/c_1)$ is non-zero only for $(t-x/c_1) > 0$, the upper limit of integration is $c_1 t$, and Equation B.26 is

$$\frac{1}{\bar{L}_{a_i}} \int_0^{c_1 t} \delta(t-x/c_1)\exp(-px)dx \qquad \text{(B.27)}$$

Upon a change of variables for $y=t-x/c_1$, $dy = -dx/c_1$, we obtain:

$$\frac{1}{\bar{L}_{a_i}} \int_t^0 \delta(y)\exp(-p(t-y)c_1)(-c_1)dy \tag{B.28}$$

Simplifying B. 28 yields:

$$\frac{1}{\bar{L}_{a_i}} \int_0^t \delta(y)\ \exp(-p(t-y)c_1)c_1 dy \tag{B.29}$$

Equation B.29 is only non-zero for y=0, yielding the following expression for Equation B.26:

$$\frac{c_1}{\bar{L}_{a_i}} \exp(-ptc_1) \tag{B.30}$$